Charles University in Prague
Second Faculty of Medicine

Program: **Postgraduate doctoral studies in biomedical fields**
Field: Biochemistry and Pathobiochemistry

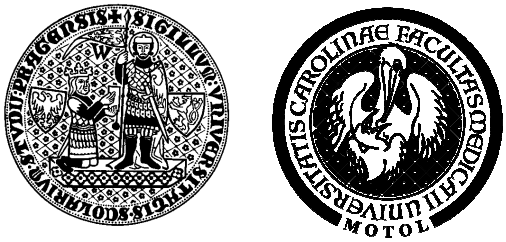

Mgr. Joško Ivica

The study of fluorescent products in the mitochondria after an attack by free radicals

Studium fluorescenčních produktů v mitochondriích po napadení volnými radikály

PhD thesis

Supervisor: prof. RNDr. Jiří Wilhelm, PhD.

Supervisor consultant: doc. RNDr. Jana Novotná, CSc.

Prague, 2012

Statement:

I declare that this PhD thesis has been written solely by me and that all of the sources and references have been properly cited. Furthermore, I declare that this thesis has not been used for the acquisition of the same or any other title.

I give my consent that the electronic version of my PhD thesis can be permanently saved in a system database of inter-university project Theses.cz for the systematic control of similarity of doctoral theses.

In Prague, 16 November, 2012

Mgr. JOŠKO IVICA

Signature:

Identification record:

IVICA, JOŠKO. *Studium fluorescenčních produktů v mitochondriích po napadení volnými radikály [The study of fluorescent products in the mitochondria after an attack by free radicals]*. Prague, 2012. Pages: 112, appendices: 3. PhD thesis. Charles University, Second Faculty of Medicine, Department of Medical Chemistry and Clinical Biochemistry, 2012. Supervisor: prof. RNDr. Jiří Wilhelm, PhD.

ACKNOWLEDGEMENTS

I would like to thank my supervisor prof. RNDr. Jiří Wilhelm, PhD for his help, support and advice and for directing me in my work. Furthermore, I would like to thank all my colleagues from the Department of Medical Chemistry and Clinical Biochemistry at Second Faculty of Medicine, Charles University, especially, my supervisor consultant doc. RNDr. Jana Novotná, CSc., MUDr. Alice Skoumalová, PhD and Pavlína Šantorová for their professional help, advice and kindness. I would like to thank my wife Mgr. Bsc. Nataša Lekić for being supportive and encouraging during my entire studies. I would also like to thank foundation 'Nadání Josefa, Marie a Zdeňky Hlávkových' for their financial support. This work was supported by grant No. P303/11/0298 of Grant Agency of Czech Republic (GAČR)

TABLE OF CONTENTS

LIST OF ABBREVIATIONS

3D - tridimensional

ACN - acetonitrile

AD - Alzheimer's disease

ATP - adenosine triphosphate

CHD - coronary heart disease

CuZn-SOD - copper & zinc-containing superoxide dismutation

DNA - deoxyribonucleic acid

ETC - electron transport chain

Fe-S - iron-sulphur centre

FMN - flavinmononucleotide

GPX - glutathione peroxidase

GPX-1 - mitochondrial matrix glutathione peroxidase

Grx - glutaredoxin

GSH - reduced glutathione

GSSG - glutathione disulfide

GST - glutathione-S-transferase

h - hour

HHE - 4-hydroxy-2-hexenal

HNE - 4-hydroxy-2-nonenal

H_2O_2 - hydrogen peroxide

$HO_2^{\cdot -}$ - hydroperoxyl radical

HPLC - high performance liquid chromatography

LC-MS - liquid chromatography – mass spectrometry

LFP - lipofuscin-like pigments

MDA - malondialdehyde

MeOH - methanol

µL – microlitre

µm - micrometre

mg – milligram

mL - millilitre

mM - millimolar, millimole per litre

min - minute

Mn-SOD - manganese-containing superoxide dismutase

MS/MS - tandem mass spectrometry

mtDNA - mitochondrial deoxyribonucleic acid

NAD^+ - oxidized nicotinamide adenine dinucleotide

NADH - reduced nicotinamide adenine dinucleotide

$NADP^+$- oxidized nicotinamide adenine dinucleotide phosphate

NADPH - reduced nicotinamide adenine dinucleotide phosphate

nm - nanometre

$NO^{\cdot}$ - nitric oxide

$NO_2^{\cdot}$ - nitrogen dioxide

NOS - nitric oxide synthase

$^1O_2$ - singlet oxygen

$O_2^{\cdot -}$ - superoxide anion

$OH^{\cdot}$ - hydroxyl radical

$ONOO^-$ - peroxynitrite

PE - dipalmitoyl phosphatidyl etahanolamine

PHGPX - phospholipid-hydroperoxide glutathione peroxidase

PM - pyridoxamine

PRX-3 - peroxiredoxin-3

PUFA - polyunsaturated fatty acid

RET - reverse electron transfer

RNS - reactive nitrogen species

ROS - reactive oxygen species

SOD - superoxide dismutase

tert-BuOOH – tert-butylperoxide

TBARS - thiobarbituric acid-reactive substances

Trx-2 - thioredoxin-2

UQ - ubiquinone

$UQ^{\cdot -}$ - semiubiquinone radical

UQH_2 - ubiquinol

UV - ultraviolet

1. INTRODUCTION

1.1 Mitochondrial production of reactive species

Mitochondria are renowned for being a major production site of reactive oxygen species (ROS). Free radicals of oxygen (superoxide anion, $O_2^{\cdot -}$; hydroxyl, $OH^{\cdot}$) as well as species that do not have an unpaired electron (hydrogen peroxide, H_2O_2) belong to the group of ROS. The main ROS produced within mitochondria is $O_2^{\cdot -}$ and its formation occurs as a consequence of one-electron reduction of O_2 in electron transport chain (ETC) (Fig.1) (Turrens J. F., 2003). It has been frequently stated in literature that as much as 2 % of O_2, consumed by mitochondria, fails to be converted to water and that is, consequently, reduced by single electron giving $O_2^{\cdot -}$ (Boveris A and Chance B., 1973). However, it appears that in reality much less of O_2 diverts from the full reduction in ETC and this amount is approximately 0.2 % of mitochondrial O_2 (St-Pierre J. et al., 2002; Brand M. D., 2010). Approximately 1 % of $O_2^{\cdot -}$ is protonated to hydroperoxyl radical ($HO_2^{\cdot}$), which is a conjugated acid of $O_2^{\cdot -}$. $HO_2^{\cdot}$ is a very reactive radical species (De Grey A. D., 2002; Jezek P and Hlavata L., 2005). A substantial amount of $O_2^{\cdot -}$ is generated by Complex I (NADH-ubiquinone oxidoreductase), where the radical is released exclusively into mitochondrial matrix. It is believed that iron-sulphur centres (Fe-S), ubiquinone (UQ) and flavin mononucleotide (FMN) cofactor take part in production of radicals that can partially reduce molecular oxygen into $O_2^{\cdot -}$. Fully reduced FMN is found to participate in these events mainly during forward electron transport, while the dominant site for ROS production in reverse electron transfer (RET), in which electrons flow from reduced ubiquinone – ubiquinol (UQH_2) back to NAD^+, is UQ-binding site. This is particularly encouraged by high membrane potential, which allows this reaction to happen from thermodynamic point of view (Chen Y. R. et al., 2005; Grivennikova V. G and Vinogradov A. D., 2006; Kussmaul L and Hirst J.,

2006; Judge S and Leeuwenburgh C., 2007; Kowaltowski A. J. et al., 2009). If we consider $O_2^{\cdot -}$ production by RET as a mere result of single-electron reduction of O_2 by Complex I components, then in that case we can say that Complex II (succinate dehydrogenase) does not generate this radical in a relevant quantity (Liu Y. et al., 2002; Grivennikova V. G and Vinogradov A. D., 2006). Another significant source of free radicals within ETC is Complex III (ubiquinone-cytochrome c oxidoreductase) where semiubiquinone radical ($UQ^{\cdot -}$) is formed during electron transport through this complex. It is generally accepted that $UQ^{\cdot -}$ may be produced on both sides of the inner mitochondrial membrane (St-Pierre J. et al., 2002; Quinlan C. L. et al., 2011). As for Complex IV (cytochrome c oxidase), it is well-known that four-electron reduction of O_2 to H_2O occurs in a stepwise fashion thus producing radical intermediates. However, it does not deliver them to its surroundings in a measurable amount (Miwa S. et al., 2003). Apart from the complexes of ETC, other mitochondrial enzymes that participate in donating electrons to ETC are also capable of producing ROS. Such enzymes are glycerol 3-phosphate dehydrogenase and electron transferring flavoprotein-ubiquinone oxidoreductase (St-Pierre J. et al., 2002). Mitochondrial glycerol 3-phosphate dehydrogenase is also a part of electron transport in the inner membrane and it is a source of superoxide at least in brown adipose tissue (Drahota Z. et al., 2002). Furthermore, enzymes of citric acid cycle pyruvate dehydrogenase and α-ketoglutarate dehydrogenase are also recognized as sources of mitochondrial ROS, where dihydrolipoyl dehydrogenase subunit of the enzyme is responsible for ROS production (Gazaryan I. G. et al., 2002; Starkov A. A. et al., 2004; Tretter L and Adam-Vizi V., 2004). Monoamine oxidase, an outer mitochondrial membrane enzyme that catalyses oxidative deamination of monoamines (Cadenas E and Davies K. J., 2000) and dihydroorotate dehydrogenase, located in the inner mitochondrial membrane and a component of pyrimidine de novo synthesis (Lenaz G., 2001), are able to produce ROS as well. As far as the fate of mitochondrial $O_2^{\cdot -}$ is concerned, it usually becomes a subject of

dismutatation with a subsequent production of H_2O_2. This may be followed, if transition metals are present, by further reduction of H_2O_2 to a potent oxidant hydroxyl radical ($OH^{\cdot}$). H_2O_2 reacts with $O_2^{\cdot -}$ in Haber-Weiss reaction to produce $OH^{\cdot}$ along with hydroxide anion and molecular oxygen. The first step of this reaction is, however, reduction of ferric ions to ferrous ($Fe^{3+} + O_2^{\cdot -} \rightarrow Fe^{2+} + O_2$). Ferrous ions are further re-oxidized in the second step, which is named Fenton reaction ($Fe^{2+} + H_2O_2 \rightarrow Fe^{3+} + OH^- + OH^{\cdot}$). Dismutation of $O_2^{\cdot -}$ may occur spontaneously or it can be catalysed by the action of a specific enzyme - superoxide dismutase (SOD), which occurs in mitochondria in two forms, a manganese containing matrix isoenzyme (Mn-SOD) and a copper-zinc containing isoenzyme from intermembrane space (CuZn-SOD) (Buettner G. R. et al., 2006).

It has been reported that singlet oxygen ($^1O_2$) is also generated in vivo, for example during decomposition of lipid hydroperoxides. These particularly unstable early products of lipid peroxidation easily decompose in the presence of metal ions to peroxyl or alkoxyl radicals, which in turn in a so-called self-reaction give rise to $^1O_2$. Whether $^1O_2$ can be generated in this manner directly by mitochondria is debatable and the stronger evidence is still needed to confirm that. Nonetheless, this cannot be excluded since lipid peroxidation, which normally takes place in PUFA enriched mitochondria, is regarded as a source of $^1O_2$ (Miyamoto S. et al., 2003).

Another group of reactive species that is as important in biology as ROS is called reactive nitrogen species (RNS). The most prominent member of this group is nitric oxide ($NO^{\cdot}$), which is a free radical itself. $NO^{\cdot}$ arises in the reaction between arginine and O_2 that is catalysed by nitric oxide synthase (NOS). There are three isoforms of NOS: neuronal, inducible and endothelial. It is presumed that NOS are localized in every cell compartment (Castro L. et al., 2011; Del Rio L. A., 2011; Robinson M. A. et al., 2011; Forstermann U and Sessa W. C., 2012). Considering that $NO^{\cdot}$ is a gaseous molecule that can pass through lipid

bilayer with little difficulty, it can diffuse into mitochondria from cytosol or other sites where it is produced (Habib S and Ali A., 2011). Bates et al. were first to prove the existence of mitochondrial NOS using immunocytochemical techniques in rat brain and liver mitochondria (Bates T. E. et al., 1995). Mitochondrial NOS was shown to be present in cardiac mitochondria as well (Kanai A. J. et al., 2001). Additional oxide of nitrogen regarded as RNS is nitrogen dioxide ($NO_2^{\cdot}$). $NO_2^{\cdot}$ is generated in reaction between $NO^{\cdot}$ and O_2 or when nitrite is oxidized by $OH^{\cdot}$. If $NO_2^{\cdot}$ reacts with $NO^{\cdot}$, nitrous anhydride (N_2O_3) is produced (Lancaster J. R., 2006; Silkstone R. S. et al., 2012). $NO^{\cdot}$ can further react with $O_2^{\cdot -}$ to give another highly reactive nitrogen species, peroxynitrite ($ONOO^-$), which is in equilibrium with its conjugated acid ONOOH (Balazy M and Nigam S., 2003; Habib S and Ali A., 2011).

It is noteworthy that mitochondria not only produce ROS at the highest rate in many cells and tissues, but they can also stimulate production of ROS by other cellular sources like NADPH oxidase, xanthine oxidase or NOS (Dikalov S., 2011).

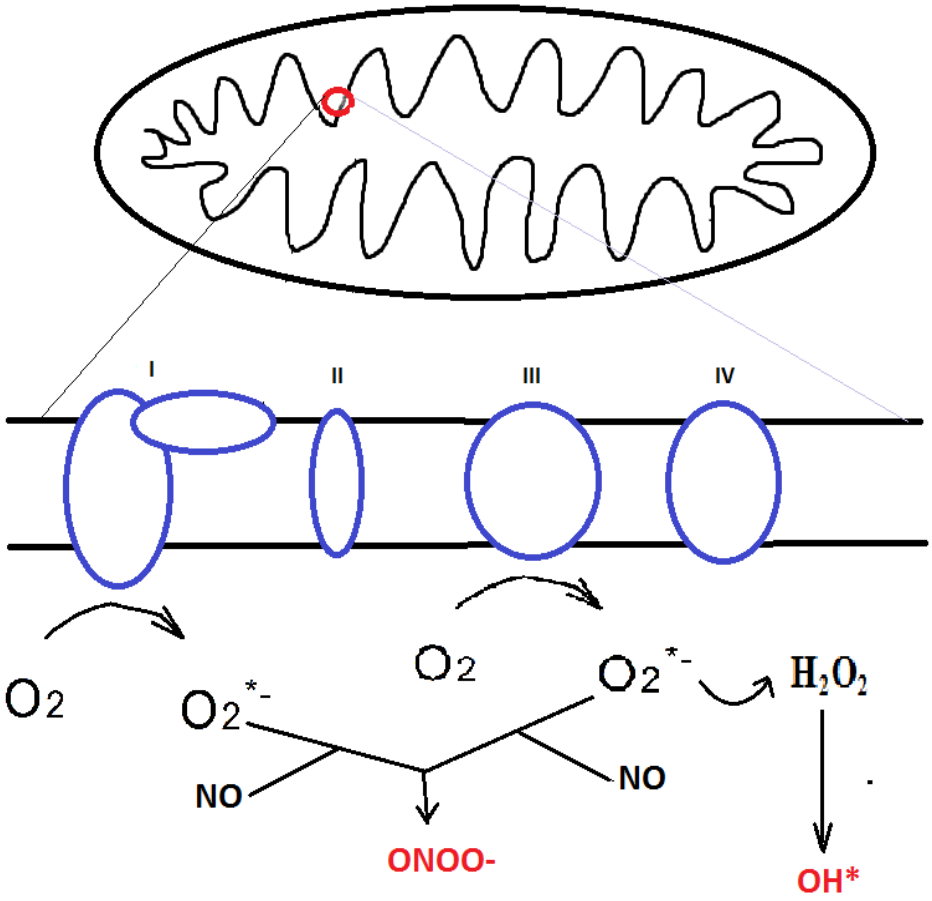

Figure 1. *Mitochondrial production of free radicals*

1.2 Mitochondrial antioxidant defence

Mitochondria are a major source of ROS/RNS in the cell, hence it is not surprising they have so powerful and developed an antioxidant defence (Weisiger R. A and Fridovich I., 1973; Halliwell B., 1997; Limon-Pacheco J and Gonsebatt M. E., 2009; Cardoso A. R. et al., 2012). Several enzyme systems exist within mitochondria responsible for converting ROS into harmless species. At the first line of mitochondrial antioxidant defence stand Mn-SOD in the matrix and CuZn-SOD in the intermembrane space. Nuclear gene *sod2* encodes for Mn-SOD. Mn-SOD is found in the mitochondrial matrix in fairly high concentrations. The

enzyme scavenges $O_2^{-\cdot}$ arisen from one-electron reduction of O_2 in the reaction $2O_2^{-\cdot} + 2H^+ \rightarrow H_2O_2 + O_2$ (Weisiger R. A and Fridovich I., 1973; Weisiger R. A and Fridovich I., 1973; Okado-Matsumoto A and Fridovich I., 2001). H_2O_2 is also ROS, which is capable of damaging extramitochondrial material along with mitochondrial components. Owing to an uncharged character of the molecule, H_2O_2 can diffuse through biological membranes, which is most likely aided by a transporter aquaporin. Therefore mitochondrial H_2O_2 can freely act upon various extramitochondrial biomolecules (Boveris A and Cadenas E., 2000; Han D. et al., 2003). In recent years, however, the evidence has been rising regarding a new role of H_2O_2 as a signalling molecule. It can thus participate as a mediator of cell growth and apoptosis (Giorgio M. et al., 2007), in stress response, energy metabolism, redox balance (Droge W., 2002; Kowaltowski A. J. et al., 2009) and muscle differentiation (Lee S. et al., 2011).

H_2O_2 concentration in mitochondria is normally regulated by several enzymes, namely, catalase, glutathione peroxidase (GPX) and thioredoxin peroxidase also called peroxiredoxin. Catalase converts H_2O_2 to water and molecular oxygen. Catalase has been so far confirmed only in heart (Radi R. et al., 1991), brain (Drechsel D. A and Patel M., 2010) and liver mitochondria (Salvi M. et al., 2007). On the contrary, mitochondrial glutathione peroxidase is widespread among different tissues. There are two forms of mitochondrial GPX: matrix GPX-1 (Esworthy R.S. et al., 1997) and phospholipid-hydroperoxide GPX (PHGPX, GPX-4) situated in the inner mitochondrial membrane (Panfili E. et al., 1991; Maiorino M. et al., 2003; Holley A. K. et al., 2010). Both GPXs use reduced glutathione (GSH) as a reductant of H_2O_2. PHGPX is mainly engaged in detoxification of phospholipid-hydroperoxides that arise in the membrane during lipid peroxidation. Another GSH dependent enzyme participating in lipid-peroxide detoxification in mitochondrial membrane is glutathione-S-transferase (GST). This enzyme is also very important in metabolism of xenobiotics and in

this regard it is GSH that, by the action of GST, convert the reactive species derived from exogenous compounds to the harmless ones (Mari M. et al., 2009). It is important to stress the central role of GSH in mitochondrial antioxidant defence. GSH is a tripeptide (γ-glutamyl-cysteinyl-glycine) having a thiol-group when reduced, and which is able to give electrons to ROS thus becoming oxidized. The oxidized form of glutathione is glutathione disulfide (GSSG) (Fig. 2). GSH is synthesized in cytosol and it is transported across the outer mitochondrial membrane easily through porins, whereas at least two inner mitochondrial carriers, dicarboxylate and α-ketoglutarate enable its transport into matrix (Mari M. et al., 2009). Mitochondrial H_2O_2 can be further removed by mitochondria-specific peroxiredoxin-3 (PRX-3) that utilizes electrons from thioredoxin-2 (Trx-2), which in turn becomes oxidized. Reduced Trx-2 is a low molecular weight thiol-disulfide oxidoreductase and has two sulfhydryl groups in the active site. It also takes part in reducing oxidized cysteine groups in proteins directly (Stanley B. A. et al., 2011; Kudin A. P. et al., 2012). Another thiol-disulfide oxidoreductase present in mitochondria is glutaredoxin (Grx). Grx system is responsible for reducing mixed disulfides arisen from protein glutathionylation. In this case there is a disulfide bond between protein cysteine residue and GSH (Herrero E and de la Torre-Ruiz M. A., 2007). GSSG and oxidized Grx are reduced by GSH-reductase, while oxidized Trx-2 is reduced by thioredoxin reductase-2. Both reductases use NADPH as a donor of reducing equivalents (Patenaude A. et al., 2004; Lowes D. A. and Galley H. F., 2011). Mitochondrial NADPH level is maintained constant mainly by three enzymes involved in its production. These are NADP-isocitrate dehydrogenase, malic enzyme and NADH/NADPH transhydrogenase. NADP-isocitrate dehydrogenase regenerates NADPH by catalysing oxidation of isocitrate to α-ketoglutarate using $NADP^+$ (Dukhande V. V. et al., 2009; Yu W. et al., 2012). Malic enzyme, which catalyses oxidative decarboxylation of malate to pyruvate, is $NADP^+$-dependant and contributes to NADPH production within mitochondria (Greco T. et

al., 2011). NADH/NADPH transhydrogenase is the inner mitochondrial membrane-bound protein that works as a proton pump. Electrochemical proton gradient (Δp) causes proton translocation from intermembrane space into mitochondrial matrix, which drives reduction of $NADP^+$ to NADPH (Mather O. C. et al., 2004). The complete reaction catalysed by the enzyme is: $H^+_{out} + NADH + NADP^+ \leftrightarrow H^+_{in} + NAD^+ + NADPH$. Mitochondrial transhydrogenase is, however, strongly product inhibited. It is estimated that at least 45% of all NADPH generated in this organelle originates from this enzyme. Therefore it is a crucial enzyme for maintaining high $NADPH/NADP^+$ ratio and consequently GSH/GSSG ratio in mitochondria. GSH/GSSG ratio is an excellent measure of oxidative stress. Furthermore, it is important for keeping protein thiols in reduced form. This implies its leading role for proper functioning of mitochondrial antioxidant defence (Rydstrom J., 2006). It is noteworthy the fact that mitochondrial GSH and NADPH concentrations are high, with NADPH concentration being approximately 3-5 mM and that of GSH 2-14 mM (Adam-Vizi V and Starkov A. A., 2010). Although NADPH is established mainly as indirect antioxidant, there is a possibility that itself can react with free radicals and thus be a direct antioxidant. De Groot and colleagues suggest that NADPH as well as NADH react with $ONOO^-$, in fact with two radicals derived from $ONOO^-$ - carbonate radical ($CO_3^{\cdot-}$), which actually arises as a product of reaction of $ONOO^-$ and CO_2, and nitrogen dioxide ($NO_2^{\cdot}$). The authors propose that NAD(P)H can react with further free radical species (Kirsch M and De Groot H., 2001). In the experiment conducted with cultured hepatocytes the production of $^1O_2$ was induced, which readily reacted with NAD(P)H and oxidized it to $NAD(P)^+$ (Petrat F et al., 2003).

Apart from GSH and NADPH-dependent antioxidants, mitochondria contain some other ROS scavengers. These may not be as important for normal function of the organelle as GSH-NADPH-linked systems, but they are certainly indispensable for thorough antioxidant protection. Cytochrome c, situated on the outer side of the inner mitochondrial membrane and

a key-component of ETC, is also considered to be a free radical scavenger. The oxidized form of cytochrome c can be reduced by $O_2^{\cdot -}$ giving molecular oxygen. In this manner, a reactive radical is removed and the electrons from reduced cytochrome c can be passed further to cytochrome c oxidase. Likewise, UQH_2 can scavenge a variety of ROS within membrane; although in its seminquinone form ($UQ^{\cdot}$) it is well established as a pro-oxidant species. Another well-known antioxidant compound – vitamin E (α-tocopherol), which is normally present in cellular membranes, hence in mitochondrial membranes as well, contributes to neutralizing lipid peroxides and other intermediates of lipid peroxidation process occurring in the membranes (Turrens J. F., 2003). Peroxyl-radicals react 1 000 times faster with α-tocopherol than with polyunsaturated fatty acid side-chains. Thus α-tocopherol terminates chain reaction of lipid peroxidation (Lauridsen C. and Jensen S. K., 2012).

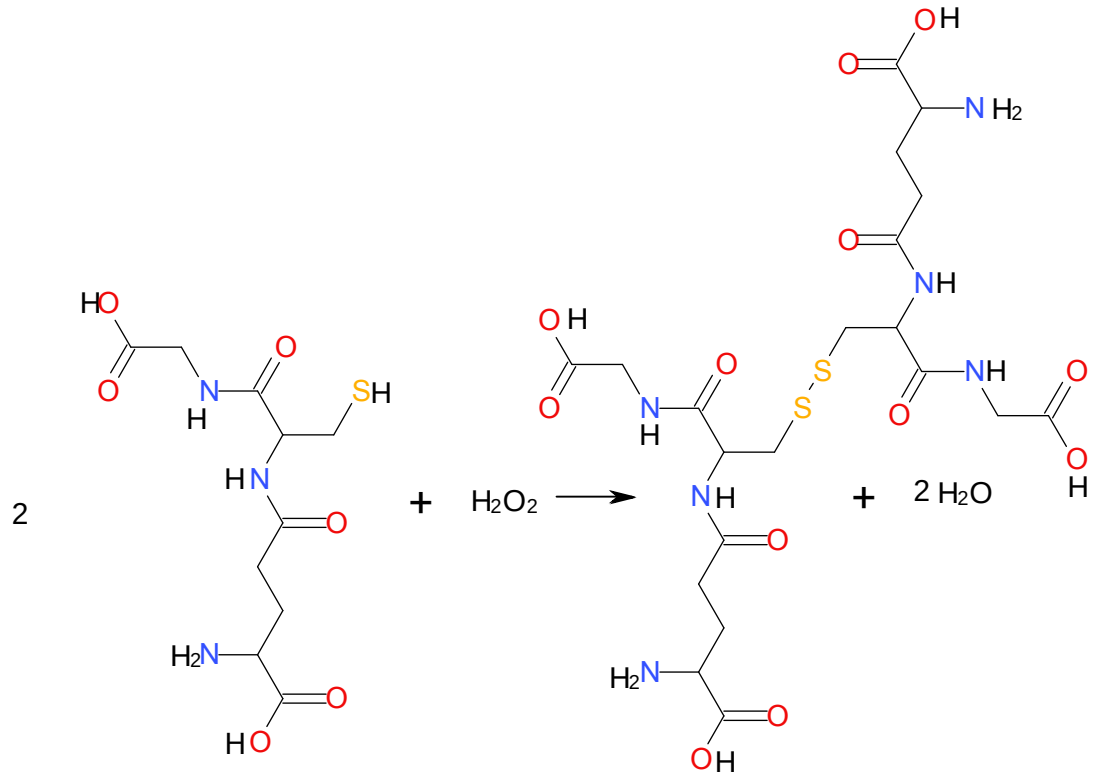

Figure 2. *Reaction catalysed by glutathione peroxidase*

1.3 Mitochondrial targets of reactive species

Since mitochondria are major cellular source of ROS, it is logical that their own molecules become a target for ROS. ROS along with RNS can interact, causing most often impairment, with virtually all macromolecules. Thus mitochondrial lipids, proteins and DNA are particularly susceptible to modification by ROS/RNS. One such class of lipids that are especially prone to oxidation by ROS is polyunsaturated fatty acids found in phospholipids. Mitochondrial inner membrane contains specific diphospholipid – cardiolipin (Fig. 3), which is an easy target of ROS caused by its unsaturated acyl chains (mostly linoleic acid) and its localization in the vicinity of ROS production sites (Gonzalvez F. and Gottlieb E., 2007). It is believed that the unaltered molecule of cardiolipin is required for the normal function of Complexes I and IV. Therefore, ROS can peroxidize cardiolipin, which subsequently leads to a decrease in the activities of these two complexes (Paradies G. et al., 2002).

$O_2^{\cdot -}$ can reversibly inactivate aconitase by oxidizing iron in iron-sulphur cluster. This leads to a release of Fe^{2+} and H_2O_2 that can step into reaction and generate $OH^{\cdot -}$ (Chandel N. S and Budinger G. R., 2007). It can also oxidize iron of [4Fe-4S] clusters in other dehydratases, such as fumarase (Fridovich I., 1995). ROS is found to inhibit a few other citric acid cycle enzymes along with aconitase, but in somewhat different fashion. Such enzymes are for example succinate-dehydrogenase and α-ketoglutarate dehydrogenase. It is thought that ROS do not inactivate these two enzymes in a direct interaction with them, but via reversible glutathionylation (Nulton-Persson A. C and Szweda L. I., 2001). Complex I can promote the self-inactivation by $O_2^{\cdot -}$ produced by this enzyme complex, which then in turn reacts with cystein thiol residue forming cysteinyl radical. Cysteinyl radical can react with tyrosine residue and thus oxidize it (Chen Y. R. et al., 2005). All these reversible inhibitions of

mitochondrial proteins, constituents of important biochemical pathways – citric acid cycle and ETC, are form of their regulation.

Even more interesting is the interaction of RNS, namely $NO^{\cdot}$ and $ONOO^{-}$, with certain mitochondrial components. $NO^{\cdot}$ is a reversible inhibitor of cytochrome c oxidase (Complex IV) and in this manner it plays certain role in ETC regulation. It binds to Cu^{2+}-B centre of the enzyme. Other heme- and metal-containing proteins are also susceptible to nitrosylation by $NO^{\cdot}$ (Cleeter M. W. et al., 1994; Kowaltowski A. J. et al., 2009). Furthermore, Complex I is the target of reversible inhibition by $NO^{\cdot}$ that most likely happens via S-nitrosylation of a protein thiol-residue (Davis C. W. et al., 2010). On the other hand, $ONOO^{-}$ is a potent oxidant and nitrating agent that can cause irreversible damage to mitochondrial proteins. It can oxidize and generate nitro-derivatives of particular amino acids, for example, cysteine, tryptophan, methionine, and tyrosine (Wang Y. et al., 2010). $ONOO^{-}$ can oxidize and nitrate mitochondrial phospholipids i.e. start lipid peroxidation. Particular mitochondrial proteins inhibited by $ONOO^{-}$ are Complexes I, II and IV, ATP synthase, aconitase, creatine kinase and Mn-SOD (Starkov A. A. et al., 2004; Jezek P and Hlavata L., 2005).

Finally, ROS and RNS, especially very reactive and harmful $OH^{\cdot}$ and $ONOO^{-}$, can cause damage to mitochondrial DNA (mtDNA) and, consequently, mtDNA mutations. This can provoke a vicious cycle, in which mtDNA mutations induce production of more ROS by distorted ETC that leads, eventually, to more extensive mtDNA damage. The higher vulnerability of mtDNA is also due in part to its location near the inner mitochondrial membrane, where ROS are formed. Moreover, it lacks protective histones and DNA repair activity (Shigenaga M. K. et al., 1994; Judge S and Leeuwenburgh C., 2007).

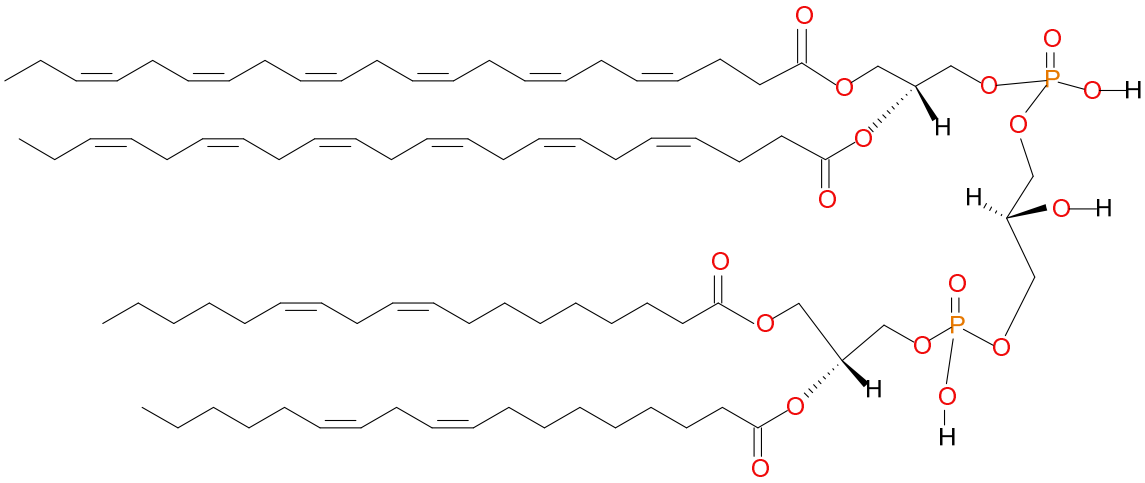

Figure 3. *Cardiolipin*

1.4 Lipid peroxidation

ROS generated in the mitochondria and extramitochondrial sites react with various biological targets. Such target molecules highly sensitive to oxidative alterations by ROS are polyunsaturated fatty acids (PUFA) found in complex lipids e.g. phospholipids in cellular membranes and lipoproteins. The process where PUFA are chemically modified by various ROS, which leads to their degradation, is called lipid peroxidation (Girotti A. W., 1985; van Kuijk F. J and Dratz E. A., 1987). Lipid peroxidation has been identified as a basic deteriorative process in cellular membranes (Trombly R and Tappel A., 1975). PUFA present in human lipids are, for example, essential linoleic (18:2 ω-6) and α-linolenic (18:3 ω-3) fatty acids (Catala A., 2010). PUFA are also long-chain fatty acids belonging to ω-3 group, such as eicosapentaenoic (EPA) (20:5 ω-3), docosapentaenoic (clupanodonic, DPA) (22:5 ω-3) and docosahexaenoic acid (DHA) (22:6 ω-3). In ω-6 group of fatty acids are also γ-linolenic (18:3 ω-6), eicostetraenoic (arachidonic, AA) (20:4 ω-6) and

docosatetraenoic acid (adrenic) (22:4 ω-6) (Russo G. L., 2009; Mozaffarian D and Wu J. H., 2011).

Lipid peroxidation (Fig. 4) in cellular membranes is initiated by either addition of ROS or by hydrogen atom (allylic hydrogen) abstraction by ROS from methylene group between two double bonds in PUFA chain. These reactions yield a carbon-centred radical of PUFA. Unpaired electron can migrate between carbon atoms and it causes formation of conjugated dienes. Inside the membranes the concentration of oxygen is rather high so that the conjugated dienes of PUFA most often react with it and a peroxyl radical is produced. Peroxyl radicals are particularly reactive, especially towards neighbouring PUFA chains, and can remove hydrogen from them. Thus, the lipid peroxidation process is propagated. In this reaction a lipid hydroperoxide and carbon-centred radical are formed. Cyclic lipid endoperoxides may be also formed instead of lipid hydroperoxide. In the presence of transition metal ions (ferrous, cuprous ions) lipid peroxides can react with them yielding alkoxyl radicals (Halliwell B and Gutteridge J. M. C., 2007; Reed T. T., 2011). Moreover, the metal ions can promote destabilization of lipid peroxide molecule causing its decomposition to smaller products. These products are diverse, ranging from simple hydrocarbons to various ketones and saturated and unsaturated aldehydes. Hydrocarbons produced during lipid peroxidation are minor end-products and the most commonly measured are gaseous pentane and ethane. Pentane can result, for example, from β-scission reaction of alkoxyl radical. Further decomposition products of lipid peroxides, renowned for their reactivity and toxicity, are aldehydes such as acrolein, malondialdehyde (MDA), 4-hydroxy-2-nonenal (HNE) (Esterbauer H. et al., 1991) and 4-hydroxy-2-hexenal (HHE) (Fig. 6) (Van Kuijk F. J. et al., 1990). MDA and HNE are widely used markers of lipid peroxidation. HNE is formed as a peroxidation product of ω-6 PUFA, such as linoleic acid, whereas MDA arises mainly as a product of peroxidation of PUFA with more than two

double bonds, such as arachidonic acid (Esterbauer H. et al., 1990; Slatter D. A. et al., 2000 Halliwell B and Gutteridge J. M. C., 2007).

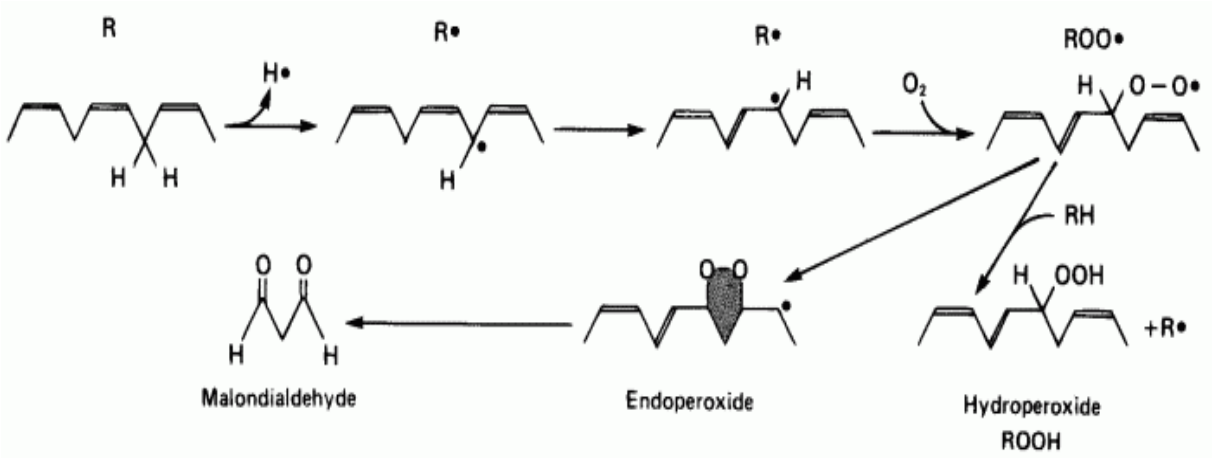

Figure 4. *Peroxidation of polyunsaturated fatty acids*

1.5 Lipophilic fluorescent end-products of free radical reactions

The α, β – unsaturated aldehydes readily react with many biomolecules (proteins, amino acids, DNA, phospholipids), which results in damage of biological material. Carbonyl groups of aldehydes react with amino groups of the biomolecules forming Schiff bases (Niki E., 2009). Finally, relatively stable chloroform extractable lipophilic fluorescent end-products are formed (Chio K. S and Tappel A. L., 1969; Yin D, 1995). Tappel and colleagues (Chio K. S and Tappel A. L., 1969) were first to demonstrate that lipid peroxidation product – malondialdehyde (MDA), in reaction with free amino groups, produces the fluorescent pigments. The end-products were initially named lipofuscin-like pigments (LFP) on the basis of the similarity of their fluorescence properties with those of lipofuscin - the pigment of old age (Chio K. S. et al., 1969). The most studied aldehydes participating in fluorescent end-

product formation are HNE and MDA (Del Rio D. et al., 2005; Catala A., 2009). Fluorophores, produced by cross-linking amino groups with carbonyl moieties of reactive aldehydes, represent a mixture of numerous compounds of known and unknown chemical structure. The fluorescent pigments showing representative lipofuscin-like fluorescence of known structure or at least of known origin have been best characterized and described in experiments where they were formed in vitro by incubating aldehydes derived from lipid oxidation (MDA, HNE) with compounds having a free amino group (Fig. 5). Similarly, compounds with primary amino group can be incubated with PUFA itself or PUFA containing phospholipids in order to analyse arising fluorophores (Wang J. Y. et al., 1996). Fluorescent compounds produced in model reactions in vitro with known and unknown chemical structure have been analysed in order to gain an insight into mechanism of their formation. Trombly and Tappel prepared such fluorescent products in reaction between arachidonic acid and synthetic phospholipid - dipalmitoyl phosphatidyl etahanolamine (PE), being irradiated with UV light to initiate free radical formation, as well as by mixing MDA and PE. They determined excitation maxima of the products, which were at wavelengths 260 nm and 365 nm, and one emission maximum at 430 nm. The fluorescence observed here lies within interval typical for lipid peroxidation end-products (Trombly R and Tappel A., 1975). In similar in vitro experiments Deng and colleagues synthesized fluorescent products in direct reaction of MDA with biological amines e.g. gamma-aminobutyric acid and taurine. In addition, they confirmed a structure of lipofuscin-like fluorescent product – 1,4-dihydropyridine, which was detected by means of HPLC. Besides that, these findings also show the scavenging properties of various biological amines on reactive aldehydes formed during lipid peroxidation. The amines can attenuate reactive aldehydes' harmful effect as they are able to compete for aldehyde carbonyl groups with amino groups of important

macromolecules, thus preventing protein adduct and cross-link formation (Deng Y. et al., 2011; Deng Y. et al., 2012).

In another experiment MDA was incubated with pyridoxamine (PM), which yielded three different products analysed by HPLC and LC-MS: 1-amino-3-iminopropene, 1-pyridoxamino-propenal and a dihydropyridine-pyridinium complex. Dihydropyridine-pyridinium derivative and dihydropyridine are end-products showing typical lipofuscin-like fluorescence. The same authors incubated bovine serum albumin with MDA, which resulted in formation of fluorescent products with fluorescence similar to dihydropyridines, and whose intensity was decreased when PM was added, clearly indicating that PM can inhibit, to some extent, the reaction of MDA with proteins (Kang Z. et al., 2006).

Slatter et al. found that the principal product of the reaction of MDA and propylamine is a stable dihydropyridine derivative, namely *N*-propyl-4-methyl 2,6-dihydropyridine 3,5-dicarbaldehyde. Likewise, if protein lysine residue, whose amino group is most reactive towards aldehydes, reacts with MDA the product is *N*-lysyl-4-methyl 2,6-dihydropyridine 3,5-dicarbaldehyde. Additionally, the aldehyde side-chains on the dihydropyridine ring can further react with other amino groups to form protein cross-links. Similarly, protein amino groups other than those of lysine can directly react with MDA to form adducts (Slatter D.A. et al., 1998; Slatter D.A. et al., 2000).

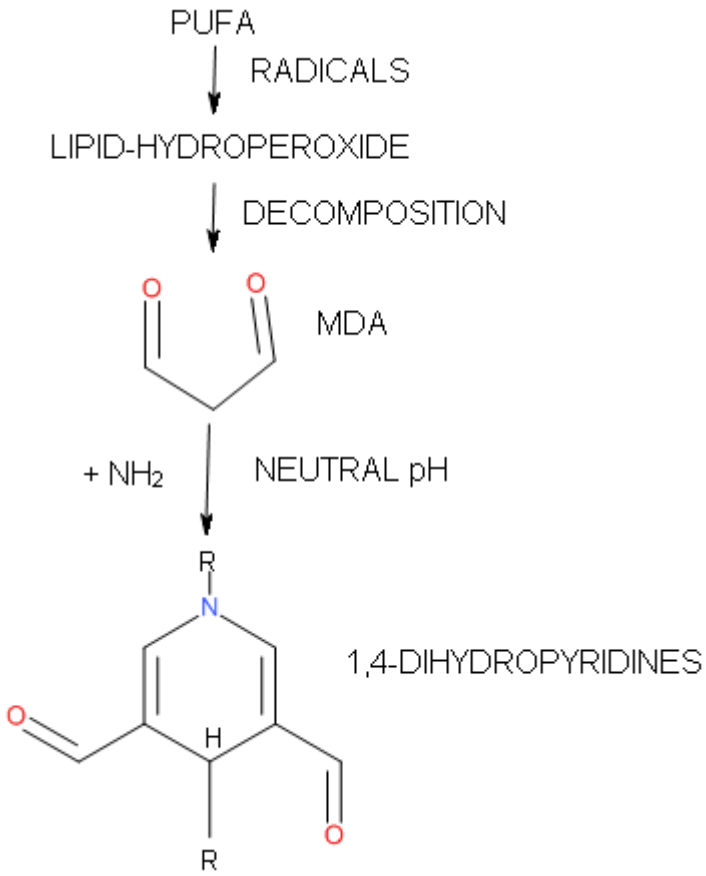

Figure 5. *The production of fluorescent LFP*

Another reactive aldehyde formed during lipid peroxidation, HNE, is also responsible for production of fluorescent compounds in reactions with amino groups. It has been found that HNE forms a fluorescent hydroxyiminodihydropyrrole derivative with the amino group of lysine residue in oxidized low-density lipoprotein (Itakura K. et al., 2000). In another study, where in a model reaction lysine derivative was exposed to autoxidation of linoleic acid, a fluorophore with hydroxyiminodihydropyrrole structure was produced. The fluorophore was analysed by HPLC with fluorescence detection (360/430 nm excitation/emission). HPLC analysis revealed two different products, one being lysine derivative-HNE adduct, while the second adduct was made of another lipid peroxidation product, 9-hydroxy-12-oxo-10-dodecanoic acid, and the lysine derivative. This finding was

confirmed by LC-MS analysis (Itakura K and Uchida K., 2003). Riazy et al. described lipid peroxidation end-products formed by addition of unfragmented oxidation products of arachidonic and linoleic acid, probably being unfragmented aldehydic products, hydroperoxides or endoperoxides, onto amino groups of proteins and phospholipids. On analysing these adducts by MS/MS the authors found that some of the arachidonic acid-derived lysine-adducts were isolevuglandins containing lactam and hydroxylactam rings. The fluorescence maxima for these products were 360 nm for excitation and 430 nm for emission (Riazy M. et al., 2011). These findings point out that not only decomposition products of lipid-hydroperoxides (mainly aldehydes), but also unfragmented oxidized lipids, can form LFP fluorophores.

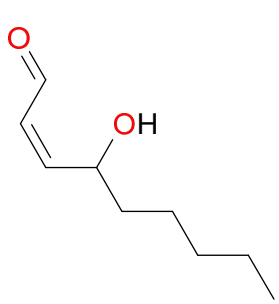

4-hydroxy-2-nonenal

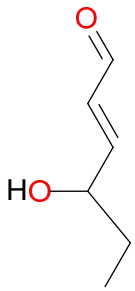

4-hydroxy-2-hexenal

Figure 6. *α,β - hydroxyalkenals*

1.6 LFP as markers of oxidative stress in model systems

LFP are nowadays mainly used as indicators of oxidative stress. As relatively stable end-products of lipid peroxidation, LFP are good markers of a free radical production and of consequent damage of lipids. Moreover, they are used not only as markers of lipid degradation but also to estimate amino acid or protein loss due to cross-linking. So far, LFP have been mostly used as robust markers of oxidative damage without defining specific chemical identity of compounds representing these pigments. In such cases, the fluorescent pigments are simply markers of free radical production under different circumstances.

Free radical production and oxidative damage in biological systems, caused by various triggers, were assayed by measuring LFP in many studies. Hypoxia, hyperoxia and ischemia/reperfusion are accompanied with increased production of free radicals and LFP were used as markers of oxidative damage (Wihlmark U. et al., 1996; Wilhelm J and Herget J., 1999; Siskova A and Wilhelm J., 2001; Ostadalova I. et al., 2007). Elevated LFP concentrations were found in erythrocytes and spleen from rats exposed to hypoxia for different time periods when compared with animals that had been kept at normoxic conditions (Wilhelm J and Herget J., 1999). Measurement of LFP concentration proved to be useful when assessing antioxidative property of different potential antioxidants (Ostadalova I. et al., 2007; Skoumalova A. et al., 2008). Furthermore, LFP were used as indicators of oxidative stress induced by physical activity (Vasankari T. et al., 1995), phagocytosis of oxidized proteins (Shimasaki H. et al., 1995) and ionizing radiation (Wilhelm J and Sonka J., 1980; Wilhelm J and Sonka J., 1980; Wilhelm J and Sonka J., 1981; Wilhelm J and Sonka J., 1981; Wilhelm J and Sonka J., 1982; Rejholcova M and Wilhelm J., 1986; Rejholcova M and Wilhelm J., 1989; Wilhelm J. et al., 1989). LFP were analysed in various tissues and cell compartments of rats exposed to radiation such as liver homogenates and mitochondria

(Wilhelm J and Sonka J., 1981), (Wilhelm J and Sonka J., 1980; Wilhelm J and Sonka J., 1982), skeletal muscles (Wilhelm J and Sonka J., 1980), erythrocytes (Wilhelm J. et al., 1989), spleen (Wilhelm J. et al., 1989) and adipose tissue (Rejholcova M and Wilhelm J., 1986; Rejholcova M and Wilhelm J., 1989). There are also studies where, for example, erythrocyte ghosts or mitochondria were peroxidized in vitro using different triggers of free radical production (ferrous ions and ascorbic acid) or incubated with lipid peroxidation intermediates (MDA), in order to study the mechanisms of LFP formation or to assess the extent of radical-mediated damage (Wilhelm J. et al., 2005; Skoumalova A. et al., 2008; Ivica J. et al., 2011; Skoumalova A. et al., 2012). Low-density lipoprotein, which plays undoubtedly a very important role in atherosclerotic lesion formation, has been also extensively studied as a model protein, with regard to its oxidation and forming fluorescent adduct on the protein amino groups (Itakura K et al., 2000; Riazy M. et al., 2011). As it has been mentioned before, lipofuscin is the ageing pigment and it accumulates as a normal part of senescence. On the other hand, LFP are produced as a result of oxidative stress, which is connected with pathological processes. LFP are known to be involved in ageing and diseases related to it e.g. neurodegenerative and heart diseases. Hence, LFP are a potential marker of oxidative damage to biological material due to increased ROS production in aged subjects. In one such study, LFP were used as a tool to assess the extent of ROS formation in brain cortex of rats during early postnatal development. The highest accumulation was found immediately after birth and the levels were falling until three months from birth, which is believed to be a period when ageing starts in rats (Wilhelm J. et al., 2011). LFP were also used in an experiment conducted on dogs diagnosed with canine counterpart of senile dementia of Alzheimer's type as one of the markers of lipid peroxidation, which has been proposed to take part in pathogenesis of this condition (Skoumalova A. et al., 2003). Sen et al. measured fluorescent lipid peroxidation end-products as markers of ageing in rat brains. Aged rat brains

had considerably increased accumulation of end-products compared to those from young animals (Sen T et al., 2007). Davydov and Shvets analysed lipid peroxidation products, with LFP being one of them, in the heart of adult and old rats exposed to stress to assess whether myocardium becomes less resistant against stress at old age (Davydov V. V and Shvets V. N., 2001). LFP were also measured in brain of rats exposed to lead in order to investigate possible mechanism of lead toxicity and its role in oxidative stress in brain (Patkova J. et al., 2012).

1.7 Application of LFP analysis in biomedicine

Since LFP are markers of oxidative damage of lipids and other molecules caused by ROS, their measurement may be a useful tool for monitoring pathological processes linked with oxidative stress. ROS overproduction, which leads to impairment of biological molecules, underlies the pathophysiological mechanism of many diseases. The most common disorders, whose developments ROS contribute to, are neurodegenerative diseases e.g. Alzheimer's disease (Lassmann H., 2011), Parkinson's disease (Schapira A.H., 1995) and multiple sclerosis (Lassmann H., 2011), atherosclerosis and other vascular diseases (Sugamura K and Keaney J.F., 2011), cancer (Klaunig J.E. et al., 2011) and diabetes (Victor V.M. et al., 2011).

The role of ROS in pathogenesis of Alzheimer's disease (AD) has been widely accepted as there is a strong evidence for it in scientific literature. ROS production exceeding their removal by antioxidant mechanisms leads to oxidative injury in AD brain. PUFA from brain phospholipids are notably prone to oxidation and there are several studies pointing that lipid peroxidation is increased in AD patient compared with healthy subjects (Montine T. J. et al., 1999; McGrath L.T. et al., 2001). There have been described fluorophores, identified as HNE-adducts with pyrrole structure, in neurons and lesions of AD subjects (Zhu X. et al.,

2012). Inasmuch as LFP are end-products of lipid peroxidation, they might be used as specific markers of AD. In a study by Skoumalova and colleagues, LFP extracted from red blood cells of patient with AD and their age-matched controls were analysed in order to find a diagnostic marker easy to measure since blood samples can be routinely taken. There was found an increase in LFP formation, measured by means of fluorescence, in patients diagnosed with AD when compared with controls. As particular fluorophores, obtained by fluorescence measurements, represent a mixture of different compounds they were subsequently resolved into distinctive fractions by HPLC. Chromatograms from these two groups revealed a difference in LFP composition between them (Skoumalova A. et al., 2011). Another neurodegenerative disease linked with oxidative stress is multiple sclerosis. Yet the relation between oxidative stress and progression of disability in multiple sclerosis is still unclear. Therefore, Koch and colleagues attempted to assess this relation using LFP as a marker of oxidative stress. LFP was measured in plasma from patients with different disease course of multiple sclerosis and healthy controls. LFP levels were increased in patients with multiple sclerosis, comparing to controls, but the authors failed to prove the relation between oxidative stress and disease course and progression (Koch M. et al., 2007).

Vascular diseases characterized by formation of atherosclerotic lesions are associated with oxidative stress. ROS overproduction leads to increased oxidation of low-density lipoprotein, endothelial dysfunction and vascular smooth muscle cell proliferation, which promotes progression of atherosclerotic events (Madamanchi N.R and Runge M. S., 2007; Puddu P et al., 2009). Coronary heart disease (CHD) is featured by accumulation of atherosclerotic plaques and their subsequent rupture in coronary arteries that supply myocardium with oxygen and nutrients. Among other parameters that predict disease development and progression, lipid peroxidation products malondialdehyde and fluorescent end-products are ones that are frequently utilized (Rao V and Kiran R., 2011). Wu et al.

carried out clinical studies using fluorescent LFP as potential markers of oxidative stress. LFP were measured in plasma from individuals participating in the epidemiological studies to evaluate their ability to predict development of CHD as well as to assess their potential as a global marker of oxidative stress in this type of studies. It was found that high levels of fluorescent products were significantly associated with incidence of CHD among individuals without previous cardiovascular events. Furthermore, these markers were found to be an independent risk factor for CHD. The same authors concluded that LFP measured in plasma could be a useful marker of oxidative stress for large epidemiological studies (Wu T. et al., 2007; Wu T.et al., 2007). Tertov et al. measured LFP in normal and atherosclerotic areas of human aorta to deepen the knowledge about atherogenesis and the development of advanced lesions in arterial walls. The level of fluorescent LFP, measured at 360/430 nm (excitation/emission), did not differ remarkably between normal intima and initial lesions. Nevertheless, there was a significant rise in LFP level from atherosclerotic plaques compared to unaffected intima. In addition, it was found that LFP content in lipid extracts from the media underlying normal intima and initial lesions was similar, whereas it was significantly higher in extracts from the media underlying advanced atherosclerothic lesions (Tertov V.V. et al., 2001). Gu and colleagues reported a potential usefulness of a specific lipid peroxidation product, omega-(2-carboxyethyl) pyrrole, as a marker for prediction of development of age-related macular degeneration. This protein adduct is formed from product of free-radical induced oxidation of docosahexaenoic acid (Gu X. et al., 2003) .

2. DESIGN OF STUDY

The aim of this study was to test the hypothesis that fluorescent end-products of free radical reactions, the so called lipofuscin-like pigments (LFP), might represent a new metabolome with medically important properties.

For that purpose we studied in a great detail the kinetics of formation of lipofuscin-like pigments in beef heart mitochondria exposed in vitro to various reactive oxygen and reactive nitrogen species. LFP were characterized by spectrofluorometric techniques and we developed new HPLC separation procedures to resolve individual fluorescent species.

As the next step of this study we evaluated the potential of LFP as markers of oxidative damage in various cells and tissues. LFP were analysed during early development of rat brain and in erythrocytes from patients with Alzheimer's disease.

As a result, we were able to resolve several tens of individual fluorescent species and confirmed the existence of a new metabolome of related compounds that participate in the development of oxidative damage accompanying several pathological states.

3. MATERIALS AND METHODS

3.1 Experimental material

3.1.1 Isolation of mitochondria

Mitochondria from beef heart were isolated according to the procedure described by (Haas D. W and Elliott W. B., 1963) with some modifications. Throughout the whole experiment all the materials used for isolation were kept on ice. The preparation of mitochondria was carried out within few of the hours after slaughter of cow. Firstly, beef heart was cut into smaller pieces, which were ground and homogenized. For homogenization, buffer solution consisting of 0.05 M Tris, 0.9 % NaCl and 0.001 M EDTA, pH 7.4 adjusted with HCl was used. Homogenized heart was then filtered through cheesecloth and the filtrate was collected for mitochondria isolation. Mitochondria were isolated by differential centrifugation. Homogenate was centrifuged twice at 2000 × g for 10 min and the precipitate was thrown away. Supernatant, which was being collected, was centrifuged at 16 000 × g for 10 min and mitochondria were precipitated. Mitochondrial sediment was again dissolved in Tris buffer. Reconstituted mitochondria were once more centrifuged at 16 000 × g for 10 min and the sediment dissolved in Tris buffer. Mitochondria were then frozen and kept at -20°C. Small amount of mitochondria was taken for protein assay by Lowry's method (Lowry O. H. et al., 1951).

3.1.2 Rat brain homogenates

A total of 70 pregnant female Wistar rats were used throughout the experiments. They had free access to water and standard laboratory diet. The offspring of both sexes were divided into 10 groups. Group A (110 fetuses) was sampled 7 days before birth, group B (110 fetuses) 1 day before birth, group C (50 animals) on postnatal day 1, group D (50 animals) on postnatal day 2, group E (50 animals) on postnatal day 5, group F (50 animals) on postnatal day 10, group G (50 animals) on postnatal day 15, group H (30 animals) on postnatal day 25, group I (30 animals) on postnatal day 35, and group J (20 animals) 3 months after birth. The animals were euthanized by decapitation in ether narcosis. The frontal brain was rapidly removed, separated from white matter if possible, snap-frozen in liquid nitrogen, and stored at $-70\ ^{\circ}C$ until use.

3.1.3 Patients

Male and female subjects with established clinical diagnosis of “probable Alzheimer's disease” according to NINCDS-ADRDA criteria (McKhann G. et al., 1984), and with history of symptoms of Alzheimer’s disease for at least 6 months, and with Mini Mental State Examination (MMSE) (Folstein M. F. et al., 1975) score $\leq$ 24/30 points (N=44) and age-matched controls (N = 16) from out-patient memory clinic and in-patient of the Department of Geriatric Medicine, the General Faculty Hospital and First Faculty of Medicine of the Charles University in Prague were selected. For the study, 5 mL of heparinized blood samples were obtained centrifuged, and the erythrocyte sediment was used for analysis. All samples were anonymously coded. The Ethics Committee of the General Faculty Hospital in Prague approved the study.

3.2 In vitro peroxidation of mitochondria

3.2.1 In vitro peroxidation with iron – ascorbic acid system

Mitochondria were incubated with $FeSO_4$, ascorbic acid and EDTA for up to 48 h. Incubation mixture consisted of mitochondria at protein concentration 1.5 mg/mL, 0.1 M phosphate buffer pH 5.5, 0.33 mM $FeSO_4$, 3.33 mM ascorbic acid and 1.7 mM EDTA (Wilhelm J., 1983). Once the incubation mixture had been made, aliquots were taken exactly after 0, 1, 2, 4, 6, 24 and 48 h for TBARS and lipofuscin-like pigments measurements. In vitro incubations were performed at 25 ºC and 37 ºC.

3.2.2 In vitro peroxidation with malondialdehyde

Mitochondria were incubated with MDA (Fig. 7) for up to 48 h. Each incubation mixture consisted of mitochondria at protein concentration 1.5 mg/mL, 0.1 M phosphate buffer pH 5.5 and lipid peroxidation product MDA at the concentration 100 μM. Once the incubation mixture had been made, aliquots were taken exactly after 0, 1, 2, 4, 6, 24 and 48 h for lipofuscin-like pigments measurements. In vitro incubations were performed at three temperatures: 25 ºC, 37 °C and 50 °C.

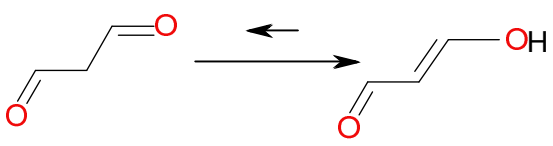

Figure 7. *Tautomerization of malondialdehyde*

3.2.3 In vitro peroxidation with tert-butylperoxide

Mitochondria were incubated with tert-BuOOH (Fig 8.) for up to 48 h. Each incubation mixture consisted of mitochondria at protein concentration 1.5 mg/mL, 0.1 M phosphate buffer pH 5.5 and generator of free radicals tert-BuOOH at the concentration 100 µM. Once the incubation mixture had been made, aliquots were taken exactly after 0, 1, 2, 4, 6, 24 and 48 h for lipofuscin-like pigments measurements. In another experiment mitochondria were incubated in 0.1 M phosphate buffer, pH 7.4 with higher concentrations of tert-BuOOH that were 200 µM and 1 mM for 24 h. The mitochondrial protein concentration was 10 mg/mL. The aliquots were taken exactly after 0, 1 and 24 h for lipofuscin-like pigments measurements.

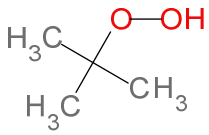

Figure 8. *Tert-butylhydroperoxide*

3.2.4 In vitro peroxidation with peroxynitrite

Mitochondria were incubated in 0.1 M phosphate buffer, pH 7.8 with two different concentrations of $ONOO^-$ for 24 h. The concentrations of $ONOO^-$ in incubation mixtures were 2 mM and 4 mM and the mitochondrial protein concentration was 10 mg/mL. The aliquots were taken exactly after 0, 1 and 24 h for lipofuscin-like pigments measurements.

3.3 Fluorescence measurement of lipofuscin-like pigments

LFP from mitochondria incubated with iron – ascorbic acid system, tert-BuOOH, 4-HNE, MDA and $ONOO^-$ were measured according to the modified method described by Goldstein B. D and McDonagh E. M., 1976 and Wilhelm J and Herget J., 1999. 4 mL of chloroform-methanol mixture (2:1, v/v) was added to 0.5 mL of mitochondrial suspension and let for extraction of lipophilic LFP on a motor-driven shaker for one hour. After that, 2 mL of distilled water was added and the samples were vigorously mixed. The mixture was subsequently centrifuged for 10 min at 2000 × g and the lower chloroform phase was separated from aqueous phase and used for measurements. The same procedure for lipophilic LFP extraction was used in the experiment with rat brain homogenates. Approximately 30 mg of frozen brain sample was weighed, chopped to fine pieces, and transferred into a glass-stoppered test tube containing 6 mL of chloroform – methanol mixture (2:1, v/v). For the extraction of LFP from red blood cells chloroform – isopropanol mixture (3:2, v/v) was used.

LFP fluorescence was measured on Aminco-Bowman Series 2 spectrofluorometer. Tridimensional excitation spectra and synchronous excitation spectra were measured using AB-2 computer program. Tridimensional excitation spectra were measured in the range of 250-400 nm for emission set between 320 and 510 nm with a step of 10 nm. As for synchronous spectra from mitochondrial extracts, the excitation wavelengths were measured in the range 300-500 nm and the difference between excitation and emission was set 50 nm, so that emission was measured in the range 350-550 nm. Synchronous spectra from erythrocyte extracts were measured in the excitation range 250-500 nm with the constant difference of 25 nm. The second derivatives of synchronous spectra were obtained using AB-2 software.

The spectrofluorometer was calibrated with 130 μM quinine hemisulfate in 0.05 M H_2SO_4 and fluorescence was expressed in relative units (RFU) per mg of protein. The fluorescence maxima were always read from tridimensional spectral arrays.

3.4 TBARS measurement

Thiobarbituric acid-reactive substances (TBARS) were measured using the method described by Vazquez-Memije et al. (2008). 500 μL of 40 % trichloracetic acid was added into suspension containing 500 μL of mitochondria and it was centrifuged at 4000 × g for 10 min. Afterwards, 300 μL of supernatant was mixed with 750 μL of 1 % thiobarbituric acid dissolved in 50 mM NaOH and let stand at 90 °C in a bath for 30 min. After cooling, 2 mL of butanol was added into a test-tube, centrifuged at 2000 × g for 10 min and the extracted TBARS were measured in upper butanol phase at 532 nm on spectrophotometer (Helios λ, Thermo Electron Corporation). Concentrations were calculated using calibration curve made with malondialdehyde standard.

3.5 LFP analysis by reverse phase high-performance liquid chromatography (RP-HPLC)

Specific fluorophores obtained by tridimensional and synchronous excitation spectral measurements were further analysed by RP-HPLC with isocratic or gradient elution. The separation of fluorophores was carried out on HPLC instrument equipped with pump (PU-2080, Jasco), auto-sampler (AS-2055, Jasco) and fluorescence detector (FP-2020, Jasco). When gradient elution was used another pump (PU-2080, Jasco) and mixer (MX-2080-32)

were applied in analysis. The columns used in the experiments were C18 columns typical for reverse phase HPLC: TC-C18(2) column (4.6 x 250 mm, 5 µm) Agilent, USA; Separon C18 column (4 x 250 mm, 5 µm), Tessek, Czech Republic. Fluorescence wavelengths set on the detector were actually fluorescence maxima obtained from 3D and synchronous spectra.

3.5.1 HPLC analysis of LFP from rat brain

Firstly, LFP were extracted from samples of frontal part of rat brains previously removed from either animal fetuses or born animals. The samples were collected seven days, and one day before birth, and on day 1, 2, 5, 10, 15, 25, 25 and 90 after birth. Extracted LFP (Wilhelm J. et al., 2011) were measured by means of spectrofluorometry. Fluorescence maxima of particular fluorophores analysed by HPLC were obtained from 3D and synchronous spectral arrays.

Brain chloroform extracts were evaporated under vacuum and the samples were re-dissolved in approximately 1 mL of mobile phase. For isocratic separation C18 column (4 × 250 mm, 5 µm) was used. Mobile phase consisted of acetonitrile (ACN) – methanol (MeOH) – water mixture in different volume ratios. Several different mixtures with different polarities were used as mobile phases to test which would give the most satisfactory resolution. Mobile phases examined in the experiment were ACN – MeOH – H_2O (50:10:40, v/v), ACN – MeOH – H_2O (30:10:60, v/v), ACN – MeOH – H_2O (50:10:50, v/v) and ACN – MeOH – H_2O (50:10:60, v/v). Three major fluorophores (F325/380, F335/410 and F355/440) were resolved into fractions by HPLC with corresponding excitation/emission values set on detector. Sample volume injected in the analyses was 10 µL and the optimal separation was achieved with 0.2 mL/min flow rate. Analysis was performed at 25 °C.

3.5.2 HPLC analysis of LFP from erythrocytes

Erythrocytes were isolated from blood withdrawn from patients with Alzheimer's disease and subjects with normal cognitive functions labelled as controls. LFP from erythrocytes were extracted according to the method of Goldstein and McDonagh (1976) and measured spectrofluorimetrically using 3D and synchronous spectral analysis. Chloroform extracts were evaporated under vacuum and the samples were re-dissolved in approximately 1 mL of mobile phase that consisted of a mixture of ACN – MeOH – H_2O (50:10:40, v/v). The analysis was performed in isocratic mode. Four distinctive fluorophores (F350/440, F285/310, F330/380 and F335/360) were analysed and resolved into fractions. The C18 column (4 × 250 mm, 5 μm) was used and the flow rate was 0.2 mL/min. Additionally, F285/310 was also resolved with 0.4 mL/min flow rate. 20 μL of each sample was injected for analysis, which was performed at 25 °C.

3.5.3 HPLC analysis of LFP from mitochondria

3.5.3.1 Isocratic HPLC

LFP from mitochondria incubated with tert-BuOOH were analysed by isocratic chromatographic technique. Many different mobile phases, composed of various volume ratios of ACN – MeOH – H_2O mixture, had been tested before the optimal solvent mixture was found. The percentage of water in mobile phase ranged from 20 - 70 % as well as various ratios of organic solvents were tested. Furthermore, different mobile phases that contained only ACN/water or MeOH/water mixtures were also tried out when optimal solvent

composition for LFP separation was sought. In this case percentage of water in mobile phase was from 50 – 70 %. We also employed a test of how an acidic mobile phase would affect separation of the complex mixture of lipophilic pigments by adding 1 % acetic acid to aqueous phase. It did not show any improvement on separation. Different flow rates were also examined (0.3 – 0.6 mL/min) in order to find the most appropriate one. Eventually, mobile phase ACN – MeOH – H_2O (20:40:40, v/v) and the flow rate 0.4 mL/min were chosen for the analysis as they gave the most acceptable separation of individual peaks. Four major fluorophores (F350/440, F310/440, F340/390, F360/410), found as maxima in fluorescence spectra, were resolved into fractions on C18 column (4 × 250 mm, 5 μm) using 30 μL of samples. All analyses were performed at 25 °C. Furthermore, F350/440, which had maximal fluorescence in 3D spectra, was analysed by mobile phase ACN – H_2O (60:40, v/v) on TC-C18(2) column (250 × 4.6 mm, 5 μm). In this analysis we tested how the amount of sample injected affects separation of individual peaks. After testing several different injection volumes (1 – 30 μL) we chose 3 μL of sample to apply in the analysis. The flow rate was 0.5 mL/min. All analyses were performed at 35 °C.

LFP from mitochondria incubated with MDA were analysed by isocratic chromatographic technique. LFP obtained by incubating mitochondria with MDA were resolved with several mobile phases. In search for good separation conditions we again tested several different running phases. Thus, ACN – MeOH – H_2O (20:40:40, v/v) was used, as it proved to be rather good in previous experiments. In addition, mobile phase composed of ACN and distilled water mixed in different ratios was tested and the ACN volume fraction used for the analysis was 30 - 80 %. The most satisfactory separation was obtained with 40 % and 60 % ACN, with respect to analysed samples. Separation was done on TC-C18(2) column (250 × 4.6 mm, 5 μm), but apart from the standard C18 column used in our measurements C8 (4 × 250 mm, 5 μm) column was also tested. A different separation pattern and improvement

were not observed when this type of column was used. Regarding the injection volume, the low ones (1-10 µL) were tried out and the volume of 5 µL was accepted for analysis. The flow rate of mobile phase was 0.5 mL/min and one fluorophore (F350/440) was measured. This was found as maximal fluorescence in 3D spectra. All measurements were performed at 30 °C.

3.5.3.2 Gradient HPLC

LFP extracted from beef heart mitochondria as well as from peroxidized mitochondria with tert-BuOOH or $ONOO^-$ were analysed by means of chromatography with gradient elution. To develop a good method for separation of complex mixture of different compounds comprising individual fluorophores found in 3D and differential spectra, it was necessary to find appropriate solvents and to establish their optimal mixing throughout analysis. Polar solvent used in the analyses was ACN/water, MeOH/water or isopropanol/water mixture, while the non-polar solvent was pure ACN, MeOH or isopropanol. Organic solvent was mixed with distilled water in various ratios, which ranged from 5 – 40 % of the solvent in the mixture. Analysis was started with 10 % of non-polar solvent, running for 5 min in isocratic mode, and then it continued to run in gradient mode until 100 % non-polar solvent was achieved. Duration of analysis, which was subject to change, determined the rate of solvent composition change from 10 % to the final 100 % of non-polar solvent. Several flow rates had been considered before one was chosen for analysis of all samples. I tested 0.4 mL/min, 0.7 mL/min and 1 mL/min flow rates. Similarly, injection volumes 0.5 µL, 1 µL, 5 µL, 10 µL and 20 µL were tested. All analyses were performed at 30 °C. After various combinations had been tested during the search for optimal separation conditions, one method that proved to be the most convenient was chosen for analysis of the samples. In both experiments, i.e. with

tert-BuOOH and $ONOO^-$ the same methods were used. The difference was in excitation and emission wavelengths set at the detector, since the fluorescence maxima were different. In the experiment with tert-BuOOH the fluorescence was set at 360/430 nm, 380/460 nm and 460/517 nm. In the experiment with $ONOO^-$ the excitation/emission wavelengths adjusted on detector were: 355/430 nm, 358/500 nm and 360/450 nm. The separation conditions were as follows: polar solvent (A) was 8 % ACN in water and non-polar solvent (B) was 100 % ACN. The analysis time was 25 min. The chromatographic analysis began with the following solvent composition: 90 % A, 10 % B. This solvent composition ran in isocratic mode for 5 min. After fifth minute gradient mode was used, in which composition of solvent B changed from 10 % to 75 % until 25 min when the analysis was ended. Between two analyses the column was equilibrated with the starting mobile phase (10 % B) for 10 min. The chosen flow rate was 0.7 mL/min and the injection volume was 20 µL. Inasmuch as the fraction of interest eluted from the column when the percentage of solvent B was in the range 40 – 50 %, further analysis was performed with this particular solvent composition in order to seek better separation. Therefore, the chromatographic analysis was running for 5 min in isocratic mode with 40 % B mobile phase and further continued from the fifth minute to 25^{th} minute in gradient mode. During the gradient chromatographic analysis the mobile phase composition was changing from 40 % B (5^{th} min) to 50 % B (25^{th} min).

4. RESULTS

4.1 In vitro lipid peroxidation of mitochondria with iron – ascorbate system

4.1.1 LFP fluorescence measurements

In this experiment the kinetics of in vitro lipid peroxidation of isolated beef heart mitochondria with iron – ascorbate system and its dependence on temperature were studied. The kinetics of lipid peroxidation was assessed by analysing fluorescent end-products of the process. The measurements were performed at 25 °C and 37 °C. The mitochondria were incubated with generators of free radicals for 48 h.

The pronounced production of LFP from mitochondria incubated with iron – ascorbic acid system at 25 °C, which was assessed by 3D excitation spectra, was observed in samples taken from incubation mixture after 24 h and 48 h from the beginning of the experiment (Fig. 9). The 3D spectral arrays reveal fluorescence maximum at 350/470 nm (excitation/emission) in the sample incubated for 24 h, whereas after 48 h a shift in fluorescence maximum was observed as the emission maximum observed here was 420 nm. Other peak excitation wavelengths were found at 308 nm and 305 nm in 24 h and 48 h incubation samples, respectively.

In the experiment carried out at 37 °C the increased production of LFP was seen in the samples incubated for 24 h and 48 h (Fig. 10). 3D spectral array shows that the maximum excitation wavelength is within interval 305-310 nm for 24 h sample, with another excitation maximum in the range 350-360 nm. For both excitation ranges the maximum emission observed is 460 nm. 3D spectral array of the 48 h sample reveals two excitation maxima, one of them being again in the range 305-310 nm and the other at 340-360 nm. However, the

emission maxima for these excitation wavelengths are shifted to 430 nm, when compared with 24 h sample.

The synchronous excitation spectra of the two samples have the shape that is changed when compared with the control sample (0 h) in the both experiments, where the fluorescence maxima are shifted towards lower emission wavelengths. In the course of in vitro peroxidation of mitochondria for up to 48 h, there is not only a higher production of LFP, but there is also a change in composition and the ratio of individual fluorophores.

In both experiments there was a measurable increase in LFP concentration after 24 h of incubation. After 48 h there was even greater increase observed. From the shapes of 3D spectral arrays it is apparent that during the time course of lipid peroxidation the composition of fluorescent LFP changes. In both experiments synchronous spectra show the alteration in relative composition of fluorophores in samples 24 h and 48 h when compared to 0 h. In the experiment carried out at 37 °C (Fig. 11) a slight increase in fluorescence in sample 48 h is evident when compared to the sample from the experiment performed at 25 °C (Fig. 12).

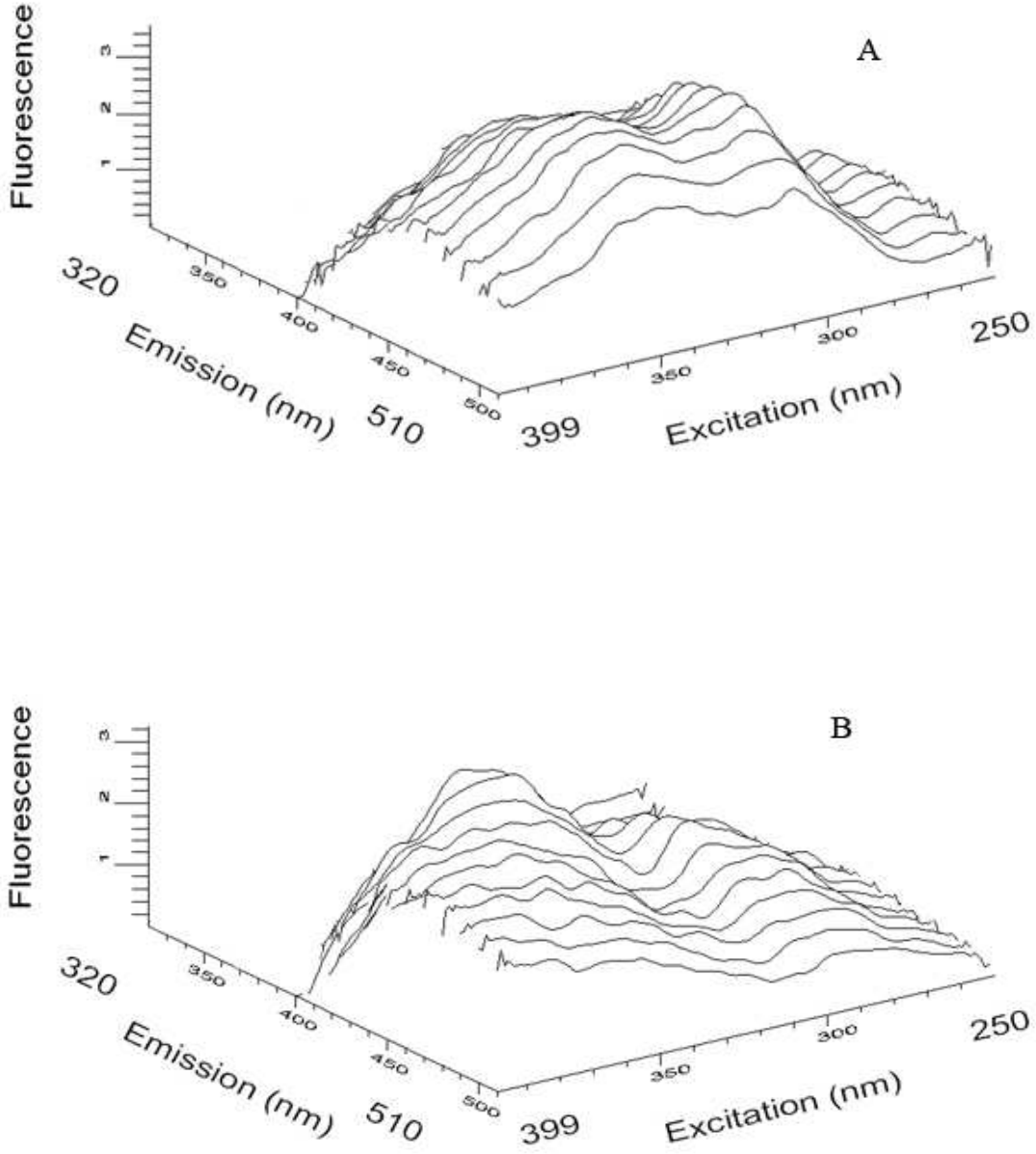

Fig. 9. Tridimensional fluorescence spectral arrays of extracts of beef heart mitochondria incubated with 0.33 mM $FeSO_4$ and 3.33 mM ascorbic acid at 25 °C. The panel A represents the sample obtained after 24 h of incubation and the panel B represents the sample obtained after 48 h of incubation. Fluorescence intensity is expressed in relative fluorescence units.

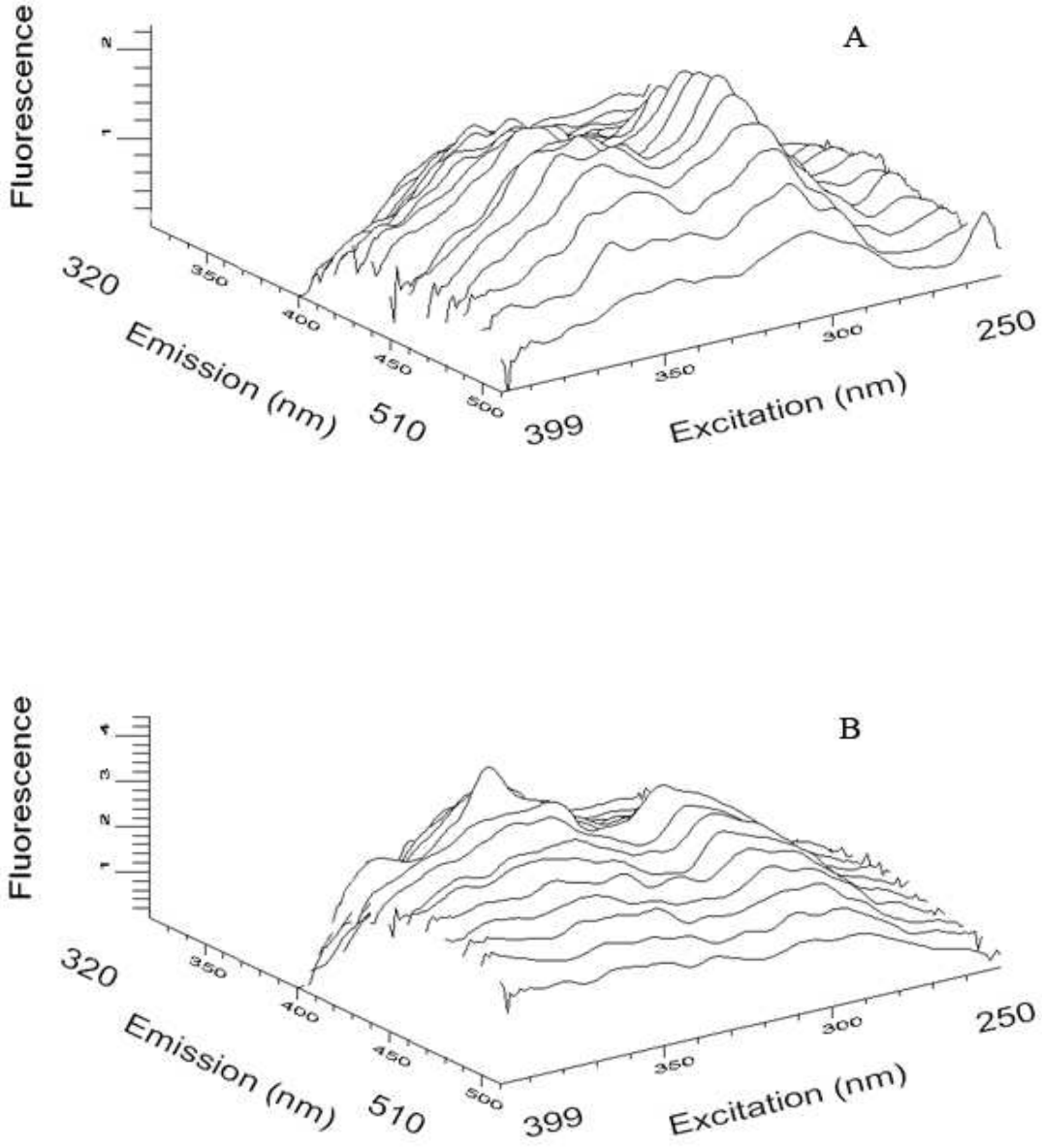

Fig. 10. Tridimensional fluorescence spectral arrays of extracts of beef heart mitochondria incubated with 0.33 mM $FeSO_4$ and 3.33 mM ascorbic acid at 37 °C. The panel A represents the sample obtained after 24 h of incubation and the panel B represents the sample obtained after 48 h of incubation. Fluorescence intensity is expressed in relative fluorescence units.

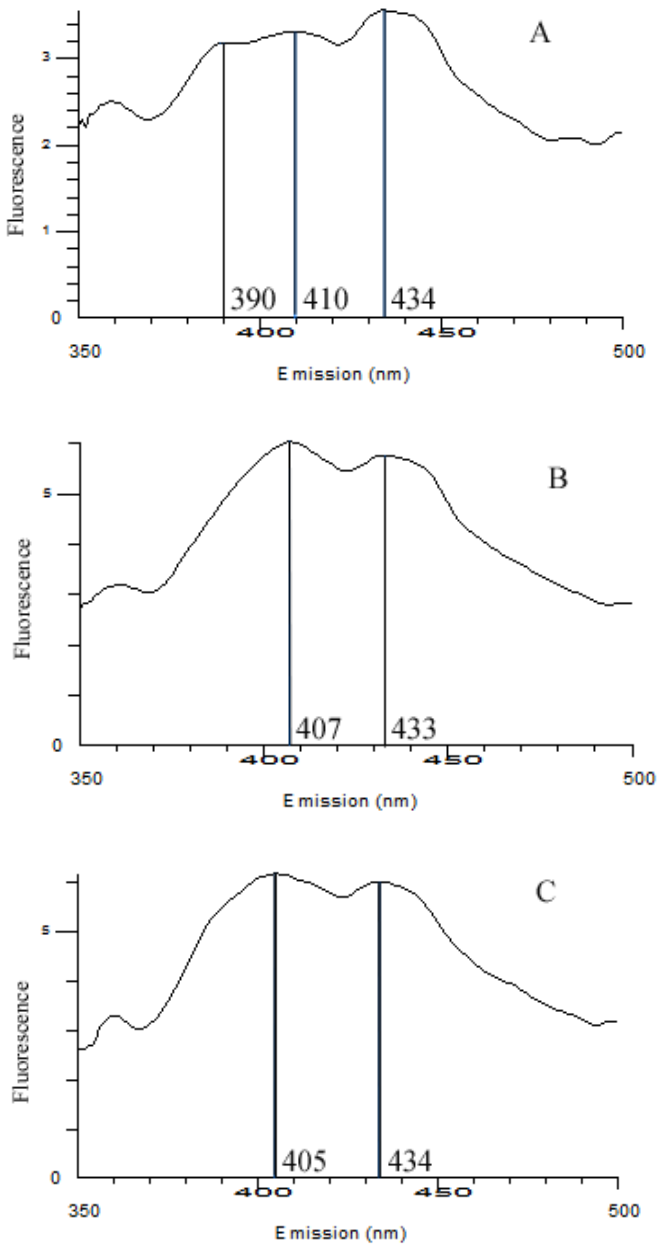

Fig. 11. Synchronous excitation spectral arrays of extracts of beef heart mitochondria incubated with 0.33 mM $FeSO_4$ and 3.33 mM ascorbic acid at 25 °C. The panel A represents the sample obtained after 0 h of incubation, the panel B represents the sample obtained after 24 h of incubation and the panel C represents the sample obtained after 48 h of incubation. Fluorescence intensity is expressed in relative fluorescence units.

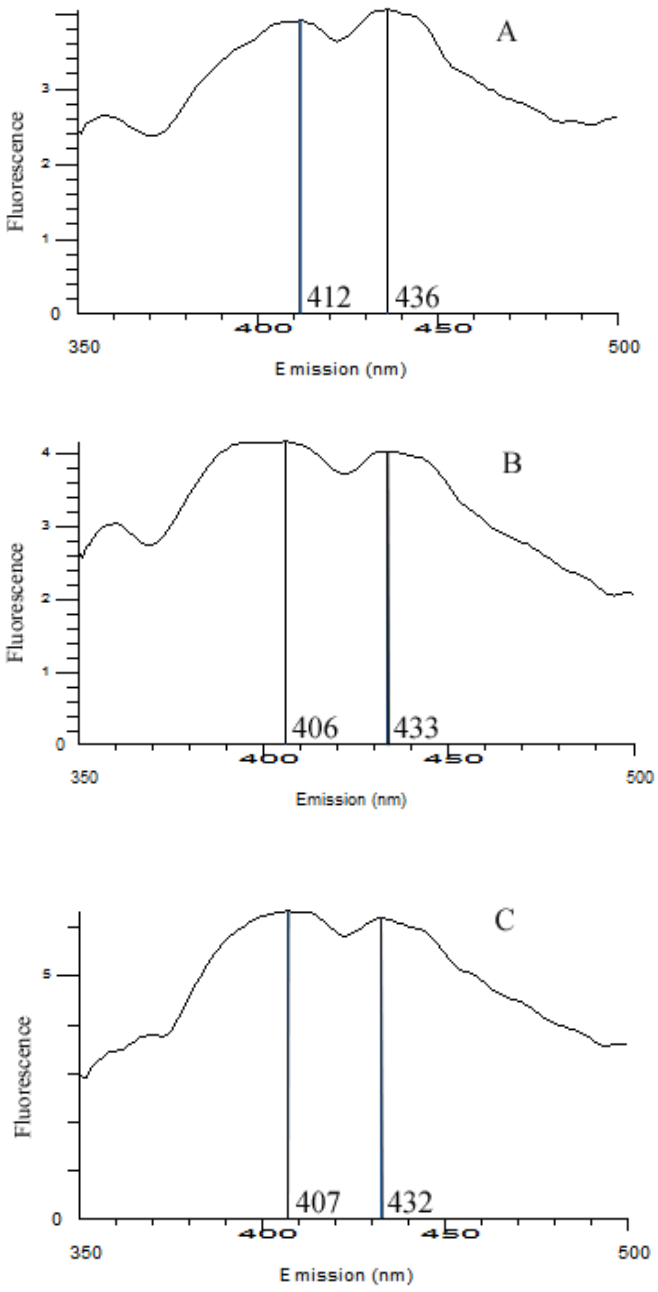

Fig. 12. Synchronous excitation spectral arrays of extracts of beef heart mitochondria incubated with 0.33 mM $FeSO_4$ and 3.33 mM ascorbic acid at 37 °C. The panel A represents the sample obtained after 0 h of incubation, the panel B represents the sample obtained after 24 h of incubation and the panel C represents the sample obtained after 48 h of incubation. Fluorescence intensity is expressed in relative fluorescence units.

4.2 Incubation of mitochondria with lipid peroxidation product malondialdehyde

4.2.1 LFP fluorescence measurements

The kinetics of LFP formation in isolated beef heart mitochondria incubated with MDA and its dependence on temperature were studied in this experiment. The measurements were performed at 25 °C, 37 °C and 50 °C. The mitochondria were incubated with MDA for 48 h.

In the experiment performed at 25 °C 3D spectra revealed the production of LFP only after 48 h of incubation. In other samples LFP production was not observed. Maximum fluorescence in 48 h sample was found at 350/440 nm (excitation/emission). When the mitochondria were incubated with MDA at 37 °C, LFP production was already seen after 24 h of incubation, although it was very low. In 48 h sample there was a pronounced increase in LFP formation. In both samples the fluorescence maximum, found from 3D spectra, was at 365/440 nm (excitation/emission). When mitochondria were exposed to MDA at higher temperature, that is 50 °C, free radical reactions producing fluorescent LFP were even more accelerated. A slight production of LFP was observed in the sample of 4 h incubation. Well defined 3D fluorescence spectra were present in samples of 24 h and 48 h incubation. In the sample 24 h incubation we found the absolute fluorescence maximum at 355/430 nm (excitation/emission). From the 3D spectral array it was observed an increase of fluorescence in another area with the maximum at 290/390 nm. Similarly, 48 h incubation sample shows the maximum in that area at 310/420 nm. The absolute maximum in this sample was found at 340/410 nm, which indicates a shift to lower excitation/emission wavelengths when compared with 25 °C and 37 °C (Fig. 13).

Synchronous excitation spectra confirm the rise of LFP production after 48 h of incubation, with the most obvious increase in the experiment carried out at 50 °C. Interestingly, the shape of synchronous spectra of 48 h samples obtained from incubation at 37 °C and 50 °C did not differ remarkably from 0 h. Nevertheless, the 48 h sample from the experiment performed at 25 °C, although with lower LFP fluorescence when compared with higher temperatures, showed the difference in shape of synchronous spectra if compared with 0 h (Fig. 14).

The incubation of mitochondria with MDA at 25 °C, 37 °C and 50 °C showed that this reactive aldehyde reacted with mitochondrial components yielding fluorescent products at fastest rate at the highest temperature, where the LFP production was observed as early as four hours from the beginning of incubation. On the other hand, when the mitochondria were incubated with MDA at 25 °C the LFP production was not observed before 48 h. It is noteworthy that different temperature not only affects the amount of LFP produced, but also fluorophores composition that is evident from differing fluorescence maxima.

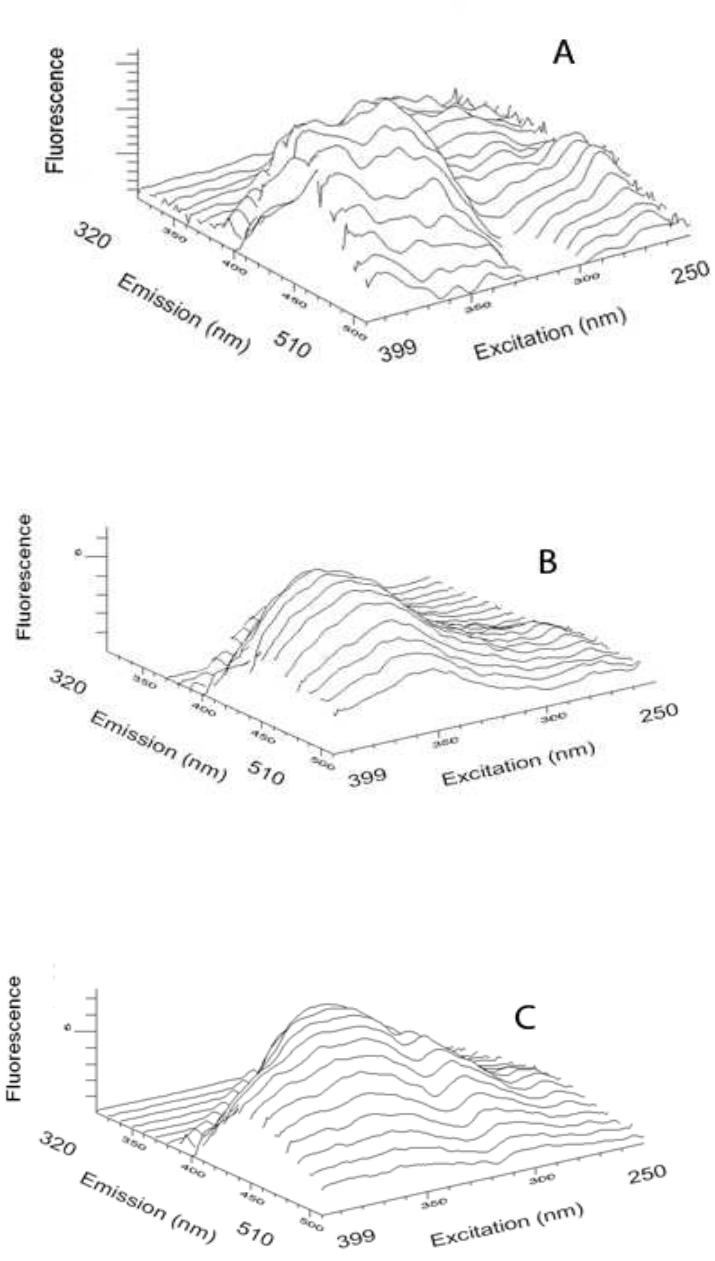

Fig. 13. Tridimensional fluorescence spectral arrays of extracts of beef heart mitochondria incubated with 100 μM MDA for 48 h. Panels A, B and C represent samples incubated at 25 °C, 37 °C and 50 °C, respectively. Fluorescence intensity is expressed in relative fluorescence units.

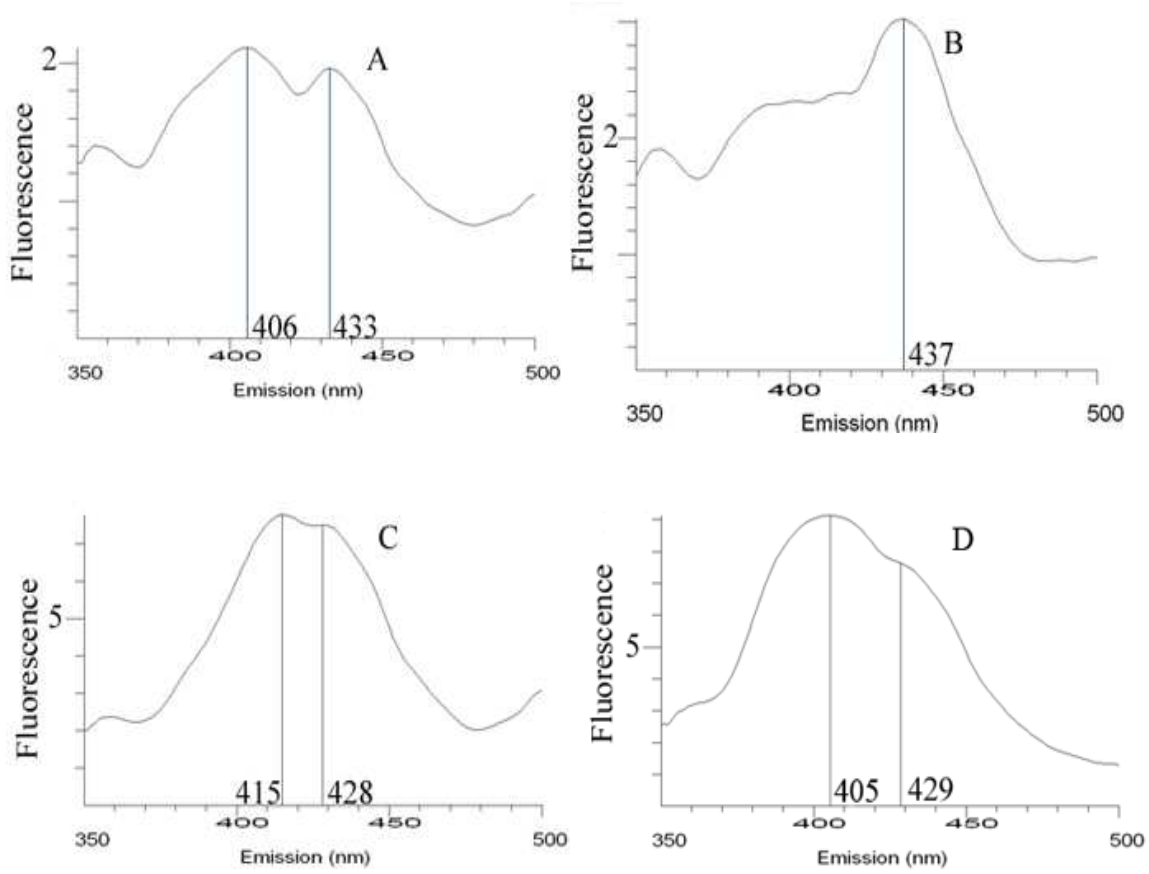

Fig. 14. Synchronous excitation spectra of extracts of beef heart mitochondria incubated with 100 μM MDA. The panel A represents control sample (0 h) and the panels B, C and D represent samples incubated for 48 h at 25 °C, 37 °C and 50 °C, respectively. Fluorescence intensity is expressed in relative fluorescence units.

4.2.2 Qualitative HPLC analysis

Chloroform extracts were analysed by HPLC with fluorescence detector in order to resolve particular fluorophores into distinctive fractions. The extracts were obtained from the experiment in which the kinetics of LFP production in mitochondria incubated with MDA at 25 °C and 50 °C was followed. Fluorophore 350/440 nm (excitation/emission), found as maximum fluorescence in 3D spectra, was chosen for HPLC analysis.

From the chromatographic analysis of lipophilic extracts of mitochondria incubated with MDA at 25 °C (Fig. 15) it is apparent that specific fluorophore arose significantly only after 48 h of incubation. The fluorophore is represented by fraction 3 in the chromatogram. However, it is necessary to note that the peak can be observed even after 6 h from the beginning of incubation, although it is much smaller. It was not present at the onset of the experiment. The chromatographic analysis of lipophilic extracts of mitochondria incubated with MDA at 50 °C (Fig. 16) revealed that fluorophore assigned as F350/440 consisted of a few fractions. After 6 h of incubation there was a well-defined peak, lacking in previous samples, and which was present in the following samples. The analysis of 48 h sample revealed the production of two completely new fractions (2 and 4).

By increasing the temperature the LFP production was accelerated, as it is seen from the appearance of a new peak (fraction 3) 6 h from the start of incubation. In previous samples there is only a small rise of the baseline observed. Furthermore, 48 h incubation at 50 °C yielded two more fractions, confirming that fluorophores produced in the experiment are complex mixtures composed of several different molecular species.

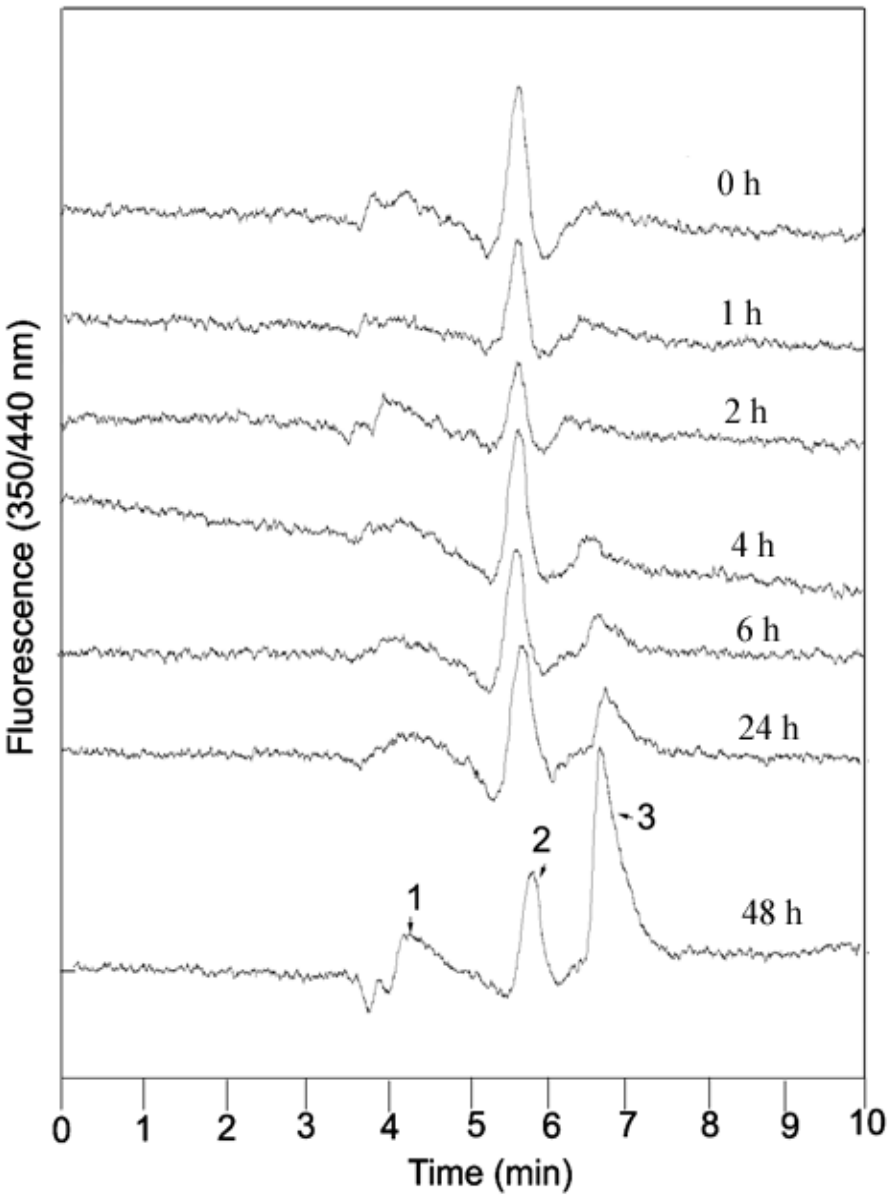

Fig. 15. The chromatograms obtained by HPLC analysis of lipophilic extracts of beef heart mitochondria incubated with 100 μM MDA at 25 °C. The ordinate indicates fluorescence intensity at 350/440 nm and the abscissa indicates the time of chromatographic analysis.

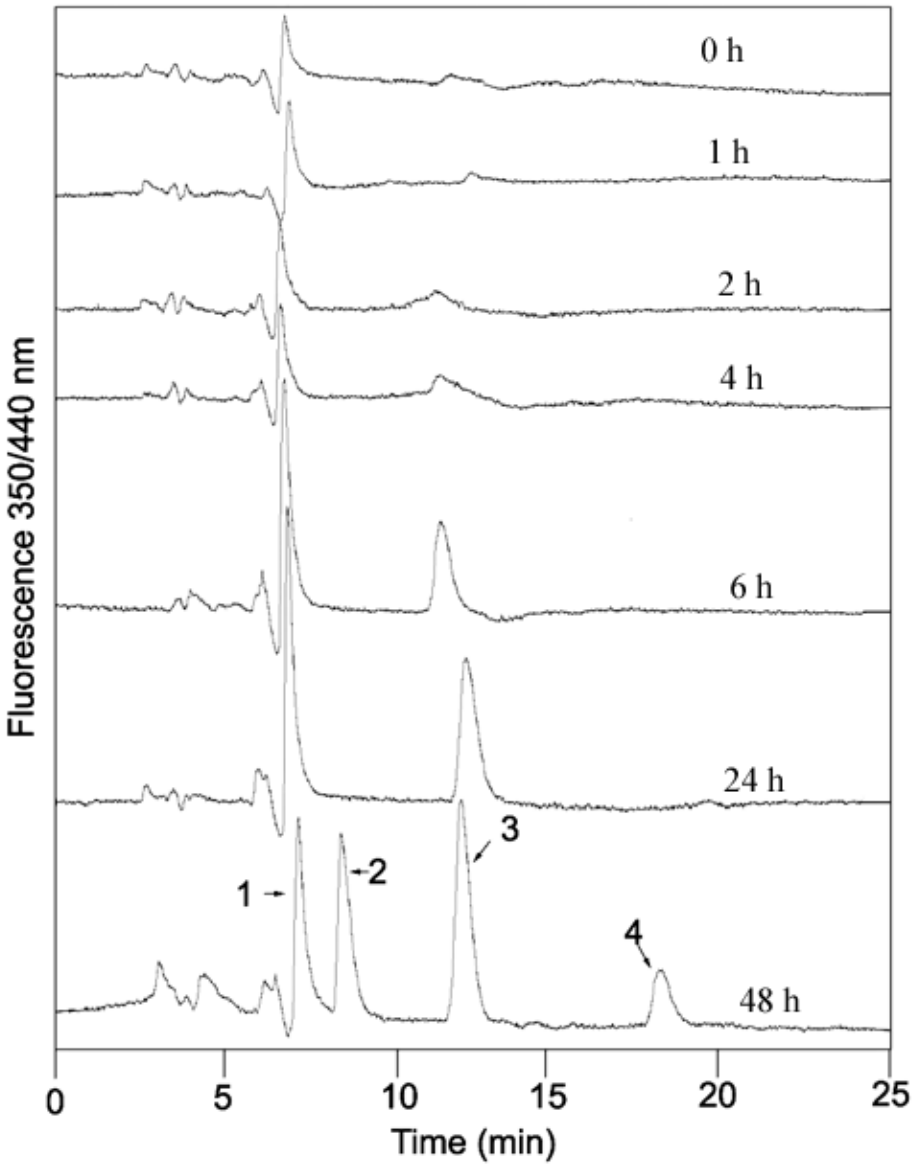

Fig. 16. The chromatograms obtained by HPLC analysis of lipophilic extracts of beef heart mitochondria incubated with 100 μM MDA at 50 °C. The ordinate indicates fluorescence intensity at 350/440 nm and the abscissa indicates the time of chromatographic analysis.

4.3 In vitro lipid peroxidation of mitochondria with tert-butylperoxide and peroxynitrite

4.3.1 Incubation with 100 μM tert-BuOOH

4.3.1.1 LFP fluorescence measurements

In this experiment the kinetics of in vitro lipid peroxidation of isolated beef heart mitochondria with tert-BuOOH and its dependence on concentration of the generator of free radicals were studied. The kinetics of lipid peroxidation was assessed by analysing fluorescent end-products of the process. In the experiment with 100 μM tert-BuOOH, which was the lowest concentration of this lipid peroxidation initiator used in the experiments, incubation was carried out for up to 48 h.

It was only in the 48 h sample that the LFP production occurred, according to the results obtained after the control 3D spectrum (0 h) had been subtracted from all the samples (Fig. 17). The fluorescence maximum found from 3D spectrum was 350/440 nm. The synchronous excitation spectra also revealed qualitative as well as quantitative changes occurred during in vitro peroxidation, with regard to fluorescence maxima found in these spectra. Comparing the control sample with 48 h sample, there is an evident increase in emission around 400 nm with the peak emission at 394 nm (Fig. 18). In the region of blue emission there is a shift in maximum emission wavelength to a lower value in peroxidized sample. The second derivatives of synchronous spectra give much finer resolution of emission maxima in a particular sample and nicely depict qualitative changes (Fig. 19). It shows that fluorescence pattern is different between non-peroxidized and peroxidized mitochondria.

According to spectrofluorometric measurements of lipophilic extracts of mitochondria incubated with 100 µM tert-BuOOH, it seems that only after long period of incubation with the generator of free radicals (48 h) end-products of lipid peroxidation are formed. In addition, basic fluorescence of non-peroxidized mitochondria differs from those exposed to in vitro peroxidation by fluorophores' composition and relative abundance.

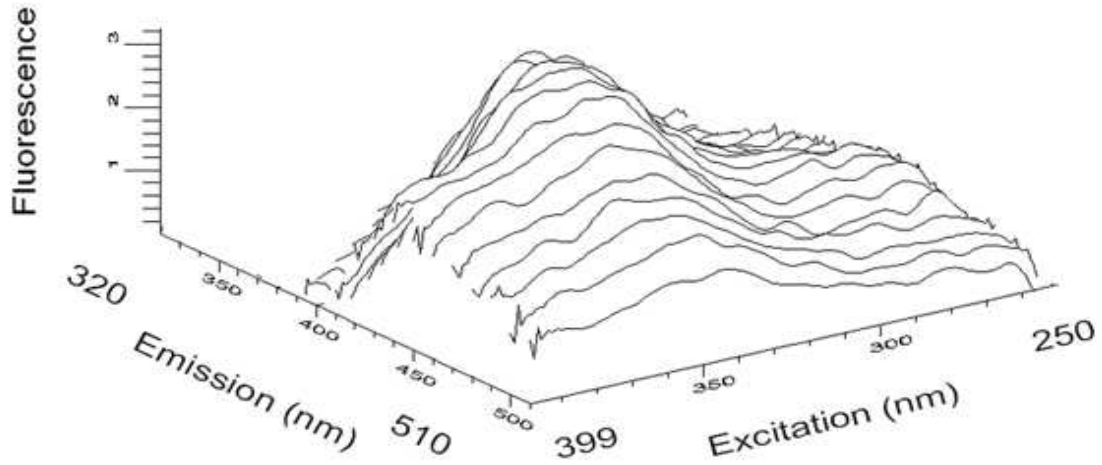

Fig. 17. Tridimensional fluorescence spectral array of extract of beef heart mitochondria incubated with 100 µM tert-BuOOH for 48 h. It is obtained after being subtracted from the control (0 h). Fluorescence intensity is expressed in relative fluorescence units.

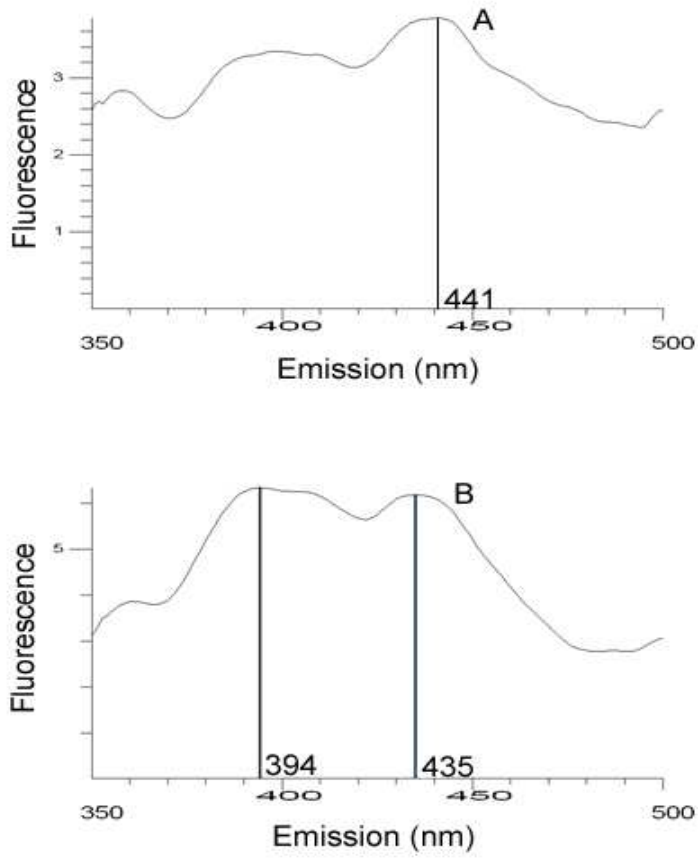

Fig. 18. Synchronous excitation spectral arrays of extracts of beef heart mitochondria incubated with 100 µM tert-BuOOH at 25 °C. The panel A represents the sample obtained after 0 h of incubation, the panel B represents the sample obtained after 48 h of incubation. Fluorescence intensity is expressed in relative fluorescence units.

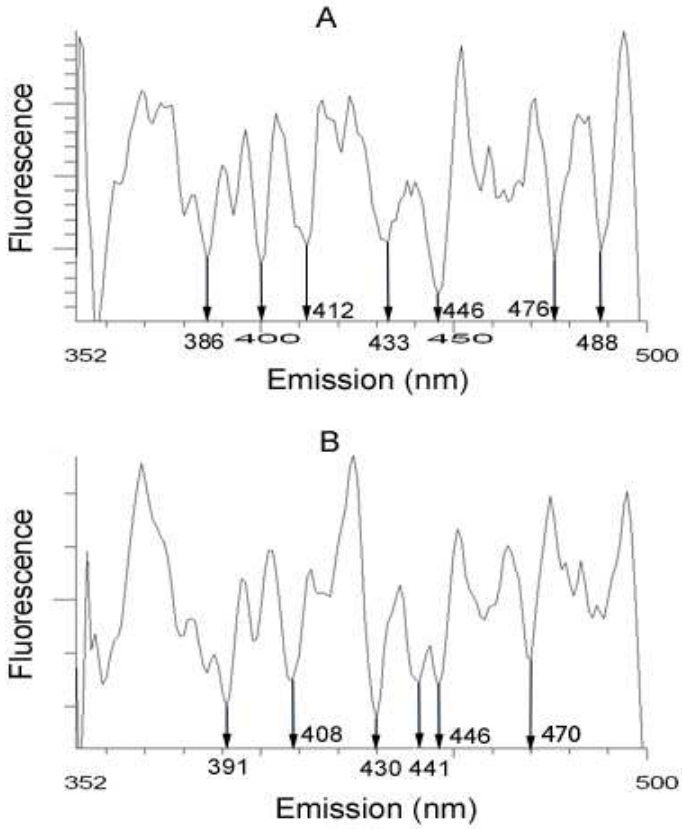

Fig. 19. Second derivatives of synchronous excitation spectral arrays of extracts of beef heart mitochondria incubated with 100 µM tert-BuOOH at 25 °C. The panel A represents the sample obtained after 0 h of incubation, the panel B represents the sample obtained after 48 h of incubation. Fluorescence intensity is expressed in relative fluorescence units.

4.3.1.2 Qualitative HPLC analysis

Chloroform extracts were analysed by isocratic HPLC with fluorescence detector set at 350/440 nm (excitation/emission), after the fluorescence maximum had been found at these wavelengths (Fig. 20). The analysis was performed in order to resolve this fluorophore (F350/440) into fractions.

Upon resolving the samples it was found that the relative abundance of one of the fractions (fraction 1), which elutes from the column around minute 9, changed during the time course of peroxidation. Its relative abundance became lower after 4 h and 6 h of incubation, when compared to time 0 h. At time 24 h it was slightly higher. This corresponds to the findings from fluorimetric measurements. In the sample obtained after 48 h of incubation, which showed the relevant increase in total LFP level visible from 3D spectra, the fraction 9 was also increased. Another fraction (fraction 2) that elutes from the column after 15^{th} minute did not change during the time course of incubation.

Isocratic HPLC analysis of F350/440 successfully resolved it into two significant fractions. The fraction 1 showed the changes in its amount, whereas fraction 2 remained constant during lipid peroxidation. Fraction 1, which had been already present in the control sample, was produced also by in vitro peroxidation of mitochondria with 100 µM tert-BuOOH.

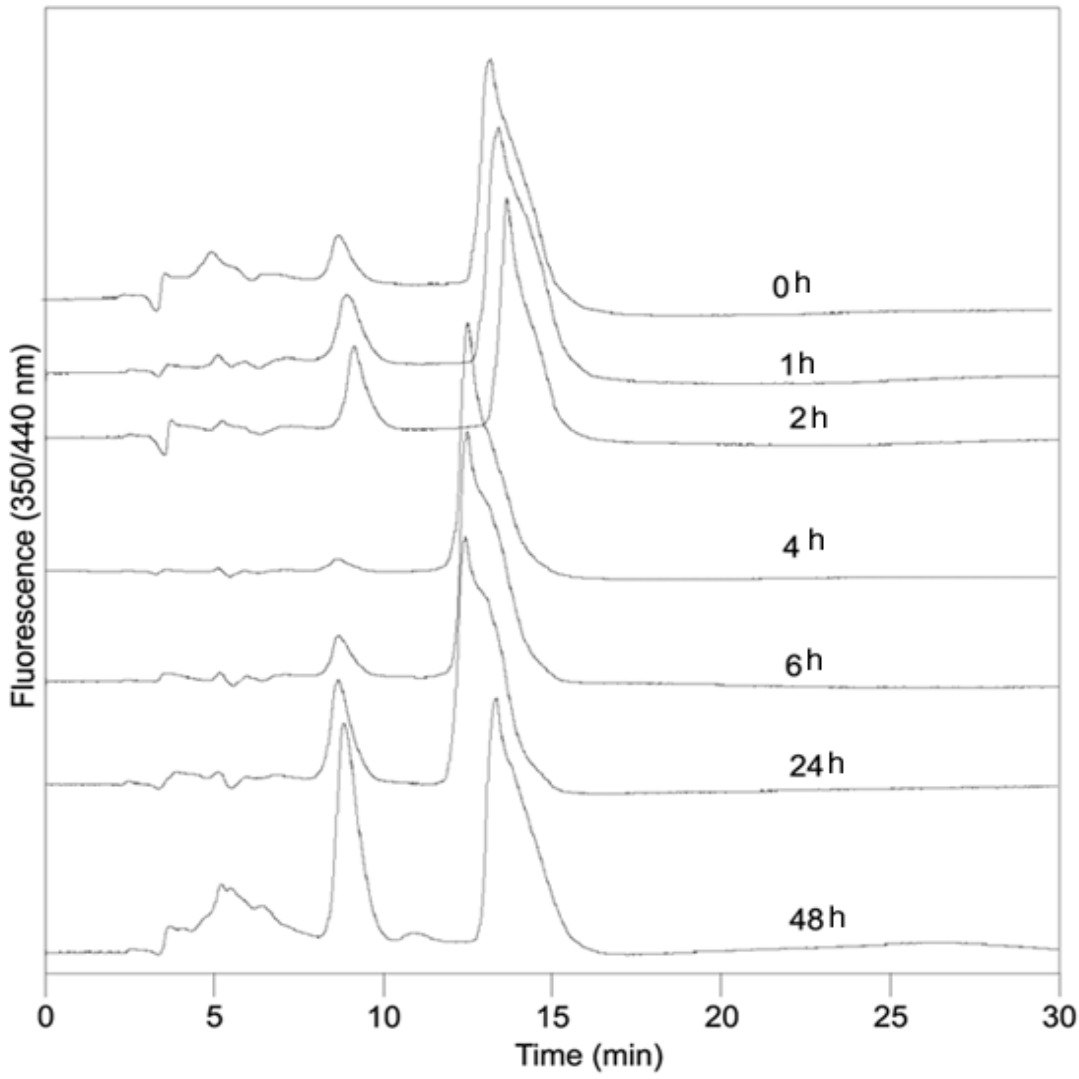

Fig. 20. The chromatograms obtained by HPLC analysis of lipophilic extracts of beef heart mitochondria incubated with 100 μM tert-BuOOH at 25 °C. The ordinate indicates fluorescence intensity at 350/440 nm and the abscissa indicates time of chromatographic analysis.

4.3.2 Incubation with 200 μM and 1 mM tert-BuOOH

4.3.2.1 LFP fluorescence measurements

The kinetics of in vitro lipid peroxidation, assessed by measurement of lipophilic fluorescent end-products, was further studied with higher tert-BuOOH concentrations and the results were also compared with autooxidation of mitochondria. Lipid peroxidation was followed until 24 h from the beginning. Tridimensional excitation spectra were measured in order to find fluorescence maxima at time 0h (Fig. 21) and 24 h (Fig. 22).

The fluorescence maximum was found at excitation/emission 357/440 nm. Furthermore, there were two additional fluorescence peaks at higher emission wavelengths: 380/460 nm and 460/517 nm and these fluorophores were resolved by HPLC.

As it was expected, the kinetics of production of fluorescent lipid peroxidation end-products was affected by the concentration of tert-BuOOH. The higher concentration (1 mM) caused a rapider increase in LFP. What is also noteworthy is that mitochondria incubated in buffer without an oxidizing agent showed an increase in fluorescence at the end of incubation period (24 h). Thus, LFP formation is also partially due to autooxidation process.

4.3.2.2 Qualitative HPLC analysis

Fluorophores found as fluorescence maxima in 3D spectra of lipophilic extracts were subjected to HPLC analysis with gradient elution in order to resolve them into fractions. Chloroform extracts were first analysed by gradient HPLC, in which mobile phase composition ranged from 10 % of organic solvent at the beginning of the analysis up to 75 % at the end (Fig. 23). The organic solvent used in the analysis was acetonitrile.

The fluorophores were successfully resolved into several fractions. However, one fraction was of a particular interest. The retention time of this fraction was around 16th minute. There were remarkable changes in size of this peak among different samples. For example, when compared to autooxidation samples of the same duration of incubation, in the samples with tert-BuOOH the peak is larger. This is particularly the case with 1 mM tert-BuOOH. Additionally, it becomes larger as duration of incubation increases within one incubation group. Since one fluorophore is actually a mixture of various chemical species, which may be much alike in terms of their chemical structure, I tried to resolve this peak with a different mobile phase. The peak eluted when the solvent composition was between 40 % and 50 % of solvent B (pure acetonitrile) (Fig. 24). By using this mobile phase composition this fraction was resolved, as I expected, into a few more fractions. However, the largest peak eluted shortly after the start of analysis. Other peaks in the chromatograms were much smaller and they did not show a substantial change in size.

The chromatographic methods used for the analysis of lipophilic extracts efficiently resolved the fluorophore mixture into a few fractions. Both methods, however, gave only one fraction which seemed to be interesting from lipid peroxidation point of view.

4.3.3 Incubation with 2 mM and 4 mM $ONOO^-$

4.3.3.1 LFP fluorescence measurements

The impact of different concentrations of $ONOO^-$ on production of lipid peroxidation fluorescent products and the kinetics of the production was studied in this experiment. Lipid peroxidation was followed until 24 h from the beginning. The results were compared with spectra obtained from mitochondrial autooxidation experiment. Tridimensional excitation

spectra were measured in order to find fluorescence maxima at time 0h (Fig. 21) and 24 h (Fig. 22).

The fluorescence maximum was found at excitation/emission 355/430 nm. Furthermore, there were two additional fluorescence peaks: 358/500 nm and 360/450 nm and all these fluorophores were resolved by HPLC. In the samples with 2 mM $ONOO^-$ the fluorescence rose immediately (0 h) and yet it was much higher as the incubation proceeded. On the other hand, when the concentration of $ONOO^-$ was 4 mM, the LFP fluorescence was lower with the maximum at 358/500 nm (excitation/emission) at time 0 h. Moreover, 3D fluorescence spectral arrays showed the almost complete loss of fluorescence in the sample of mitochondria incubated for 24 h.

The fluorescence measurement of lipophilic extracts revealed that the impact of $ONOO^-$ is concentration-dependent. While 2 mM concentration caused a significant fluorophores production, 4 mM $ONOO^-$ did not. It even caused a decrease in fluorescence during the time course of incubation.

4.3.3.2 Qualitative HPLC analysis

Fluorophores found as fluorescence maxima in 3D spectra of lipophilic extracts were subjected to HPLC analysis with gradient elution in order to resolve them into fractions. The same methods used in the experiments with tert-BuOOH were applied in the experiments with $ONOO^-$.

The most dramatic results were obtained when fluorophore F358/500 was resolved into fractions. Unlike other fluorophores, chromatographically analysed in this experiment, F358/500 from extracts with 2 mM $ONOO^-$ was resolved into two dominant fractions. The first fraction eluted between 14 and 15 minutes, whereas the second one appeared in the

chromatogram between 16 and 17 minutes (Fig. 25). With regard to the first fraction, the area under the peak and its height dramatically rose as the incubation proceeded. The same applies for the second fraction, although the relative increase during in vitro peroxidation is smaller. Similar findings were observed in chromatogram obtained when mobile phase consisting of 40-50 % ACN was applied (Fig. 26). Interestingly, in the second fraction there is a small shoulder in front of the main peak, obviously indicating the presence of another fluorescent compound. This co-eluting peak, however, is no more apparent in the 24 h sample. When the same fluorophore was resolved in the samples with 4 mM $ONOO^-$ the fraction 1 was already sizeable at 0 h. Nevertheless, its size became slightly smaller as the incubation with $ONOO^-$ progressed. As for the fraction 2, it was much smaller than the fraction 1. The reverse situation was with 2 mM $ONOO^-$. Furthermore, this fraction was tooth-shaped with two apparent peaks. It grew smaller as the incubation time went on and eventually it almost disappeared. When the other major fluorophores (F355/430 and F360/450) were resolved only one significant fraction was obtained.

The chromatographic methods used for the analysis of lipophilic extracts efficiently resolved the fluorophore mixture into a few fractions. Chromatographic analysis confirmed the spectrofluorimetric results in which 2 mM $ONOO^-$ caused a remarkable increase of fluorescence and 4 mM $ONOO^-$ caused fluorescence attenuation.

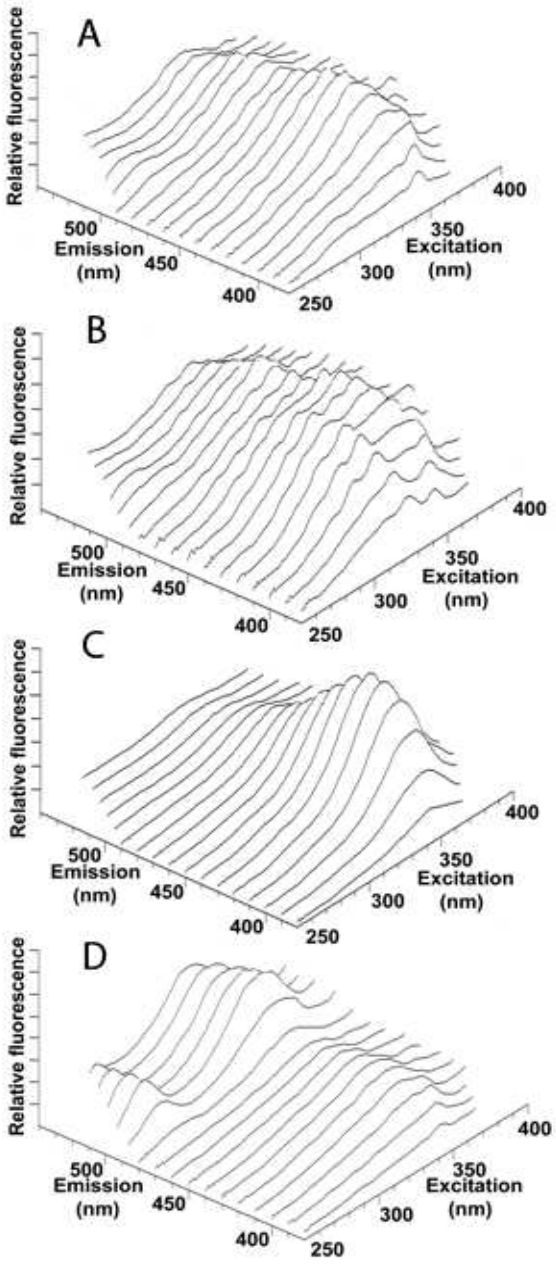

Fig. 21. Tridimensional fluorescence spectral arrays of mitochondrial lipohilic extracts. Mitochondria were incubated in 0.1 M phosphate buffer and spectral arrays show the time 0 h. **A** autooxidation; **B** incubation with 1 mM tert-BuOOH; **C** incubation with 2 mM $ONOO^-$; **D** incubation with 4 mM $ONOO^-$. Fluorescence intensity is expressed in relative fluorescence units.

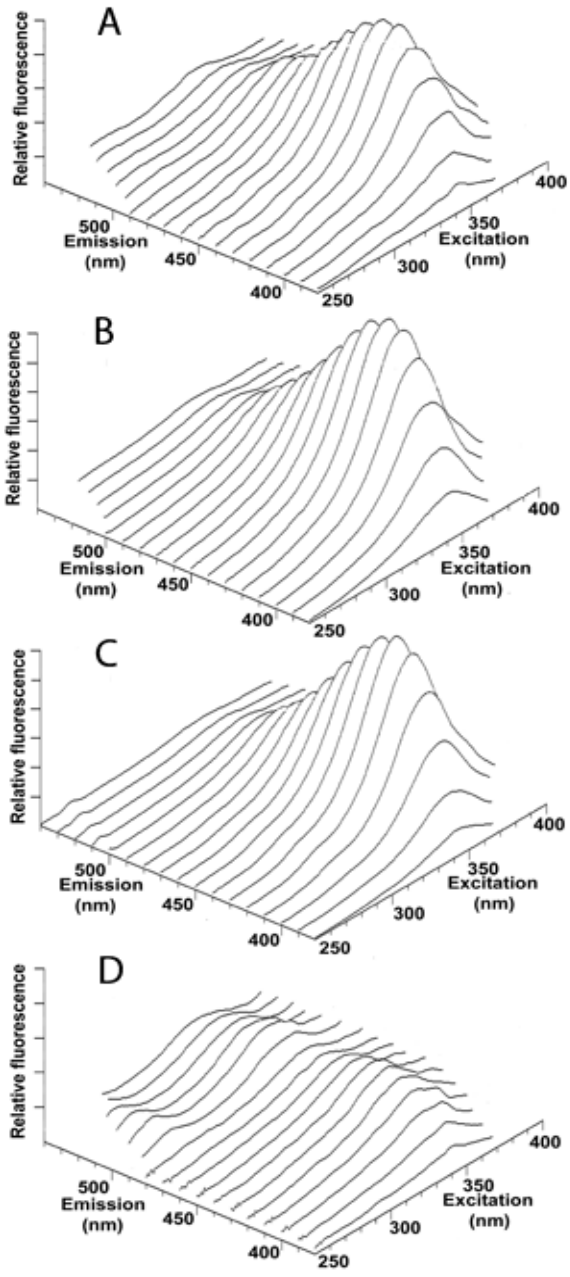

Fig. 22. Tridimensional fluorescence spectral arrays of mitochondrial lipohilic extracts. Mitochondria were incubated in 0.1 M phosphate buffer and spectral arrays show the time 24 h. **A** autooxidation; **B** incubation with 1 mM tert-BuOOH; **C** incubation with 2 mM $ONOO^-$; **D** incubation with 4 mM $ONOO^-$. Fluorescence intensity is expressed in relative fluorescence units.

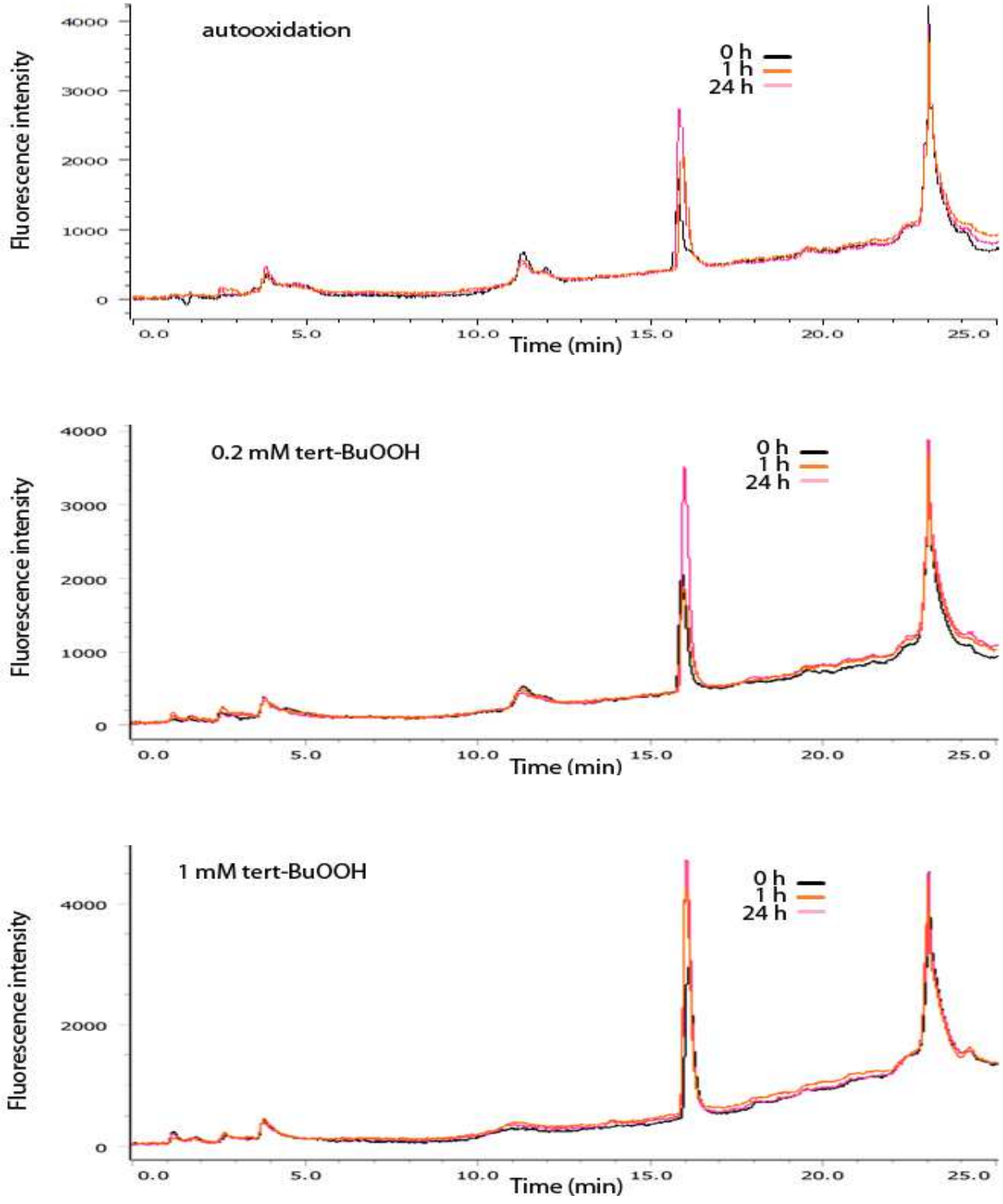

Fig. 23. The chromatograms obtained by HPLC analysis of lipophilic extracts of autooxidized mitochondria and the mitochondria incubated with 200 μM and 1 mM tert-BuOOH. The ordinate indicates fluorescence intensity at 357/440 nm and the abscissa indicates time of chromatographic analysis.

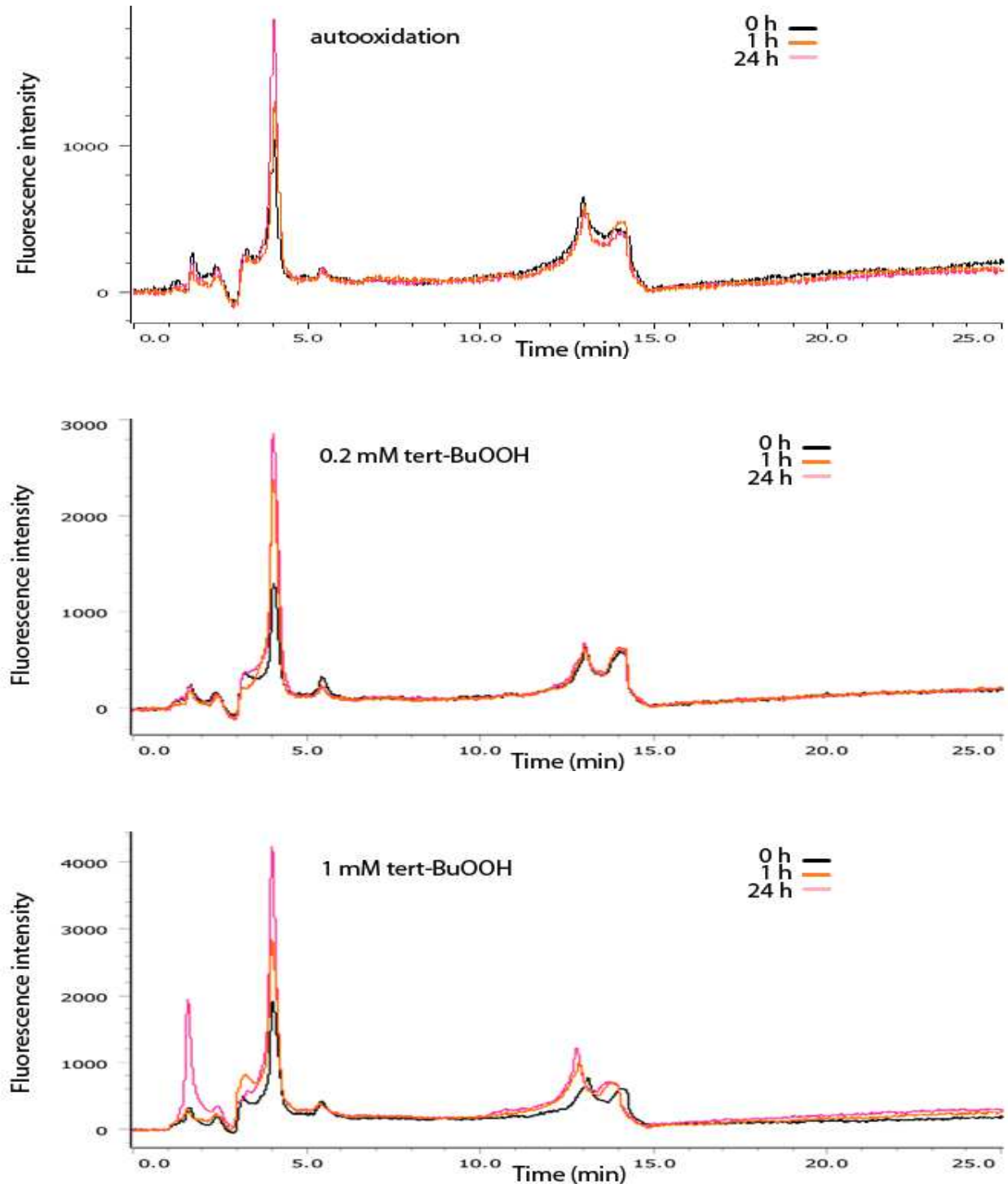

Fig. 24. The chromatograms obtained by HPLC analysis of lipophilic extracts of autooxidized mitochondria and the mitochondria incubated with 200 μM and 1 mM tert-BuOOH. The ordinate indicates fluorescence intensity at 357/440 nm and the abscissa indicates time of chromatographic analysis.

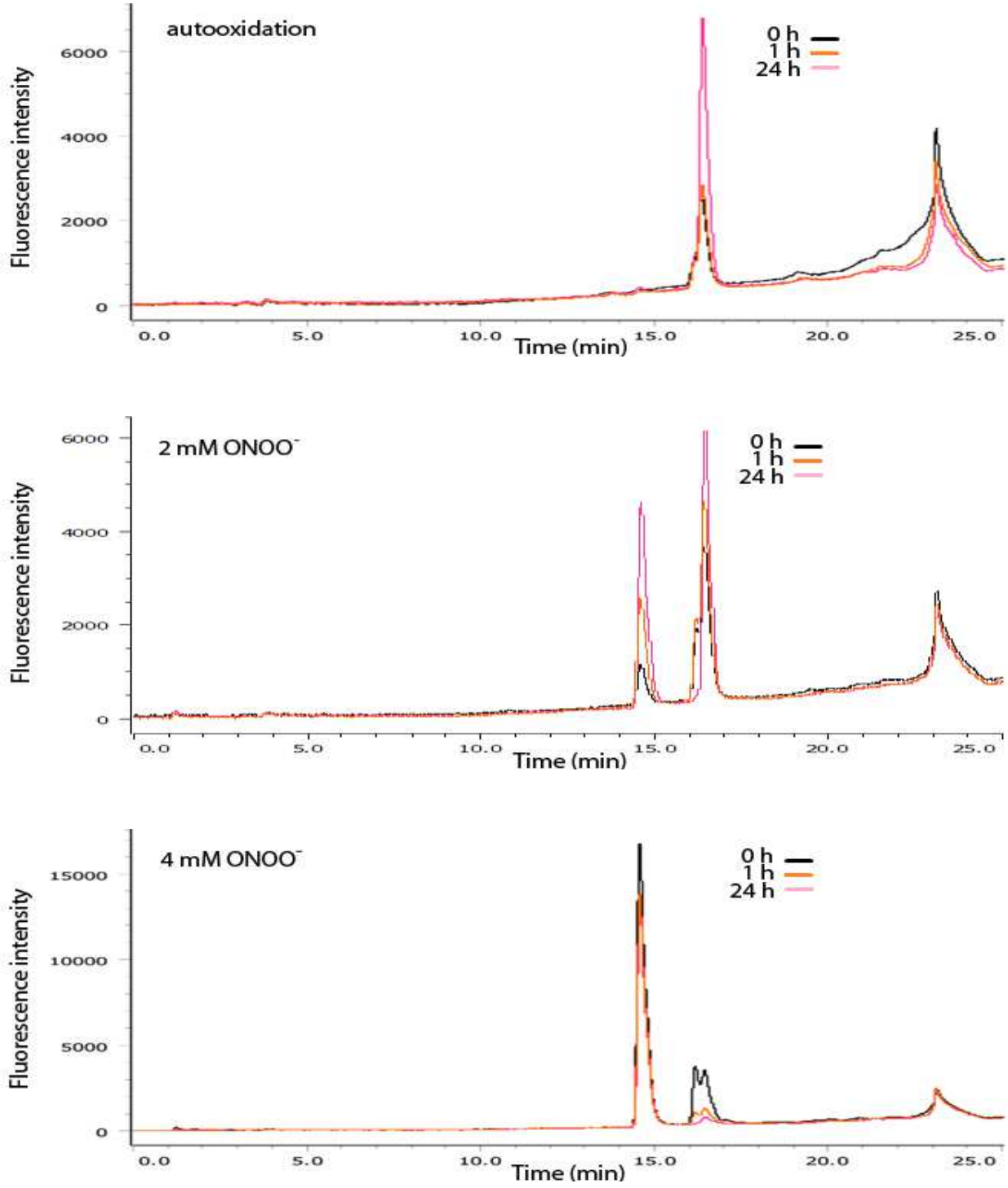

Fig. 25. The chromatograms obtained by HPLC analysis of lipophilic extracts of autooxidized mitochondria and the mitochondria incubated with 2 mM and 4 mM $ONOO^-$. The ordinate indicates fluorescence intensity at 358/500 nm and the abscissa indicates time of chromatographic analysis.

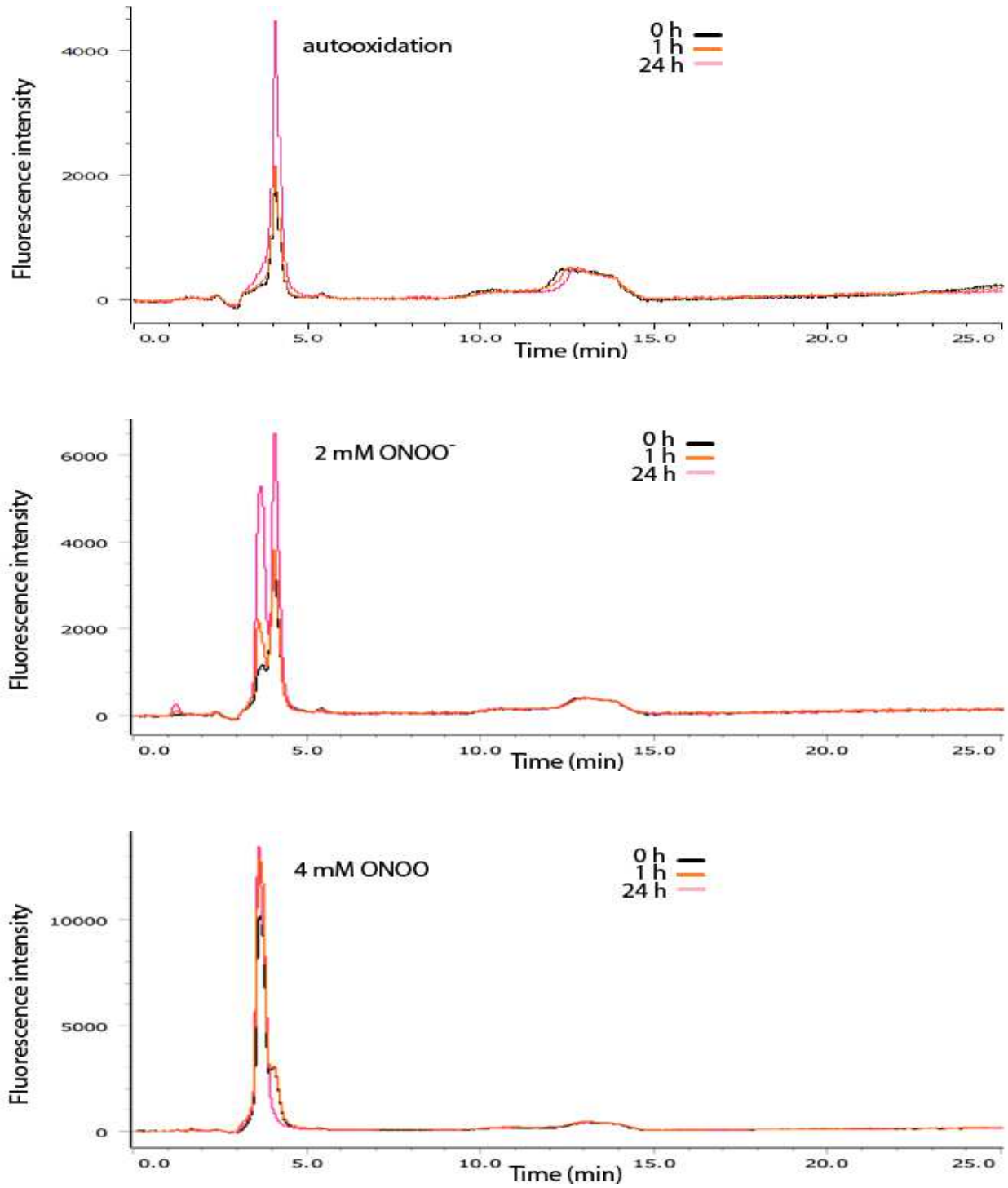

Fig. 26. The chromatograms obtained by HPLC analysis of lipophilic extracts of autooxidized mitochondria and the mitochondria incubated with 2 mM and 4 mM $ONOO^-$. The ordinate indicates fluorescence intensity at 358/500 nm and the abscissa indicates time of chromatographic analysis.

4.4 Oxidative stress during early postnatal development

4.4.1 LFP fluorescence measurements

Lipophilic extracts from rat brains during perinatal and early postnatal development were analysed spectrofluorimetrically by means of tridimensional excitation spectra. The changes in LFP composition and production were studied in order to evaluate the kinetics of their production and the extent of free radical-mediated molecular damage in this period of animal development. LFP were used as markers of such reactions.

Tridimensional fluorescence spectral arrays, which are considered as a fingerprint for a particular mixture of fluorophores, revealed the changes in composition and relative abundance of certain fluorophores in the extracts from rat brains (Fig. 27). There were three major fluorophores, found as fluorescence maxima in 3D spectra: F325/380, F335/410 and F355/440. It was found that the relative amount of all the major fluorophores was the highest in postnatal day 2, after which there was observed a slight decrease. Furthermore, there was an obvious change in 3D spectra shape between postnatal day 90 and the samples from perinatal period. Interestingly, the maximum fluorescence at day 2 was at 335/410 nm, followed by 325/380 nm, while at day 90 it was at 355/440 nm.

Measurements of chloroform extracts from rat brain homogenates, in which LFP were analysed by means of spectrofluorimetry, disclosed that the production of various fluorophores is a dynamic process. LFP measurement can be a reliable tool for assessment of oxidative processes obviously occurring even during early development.

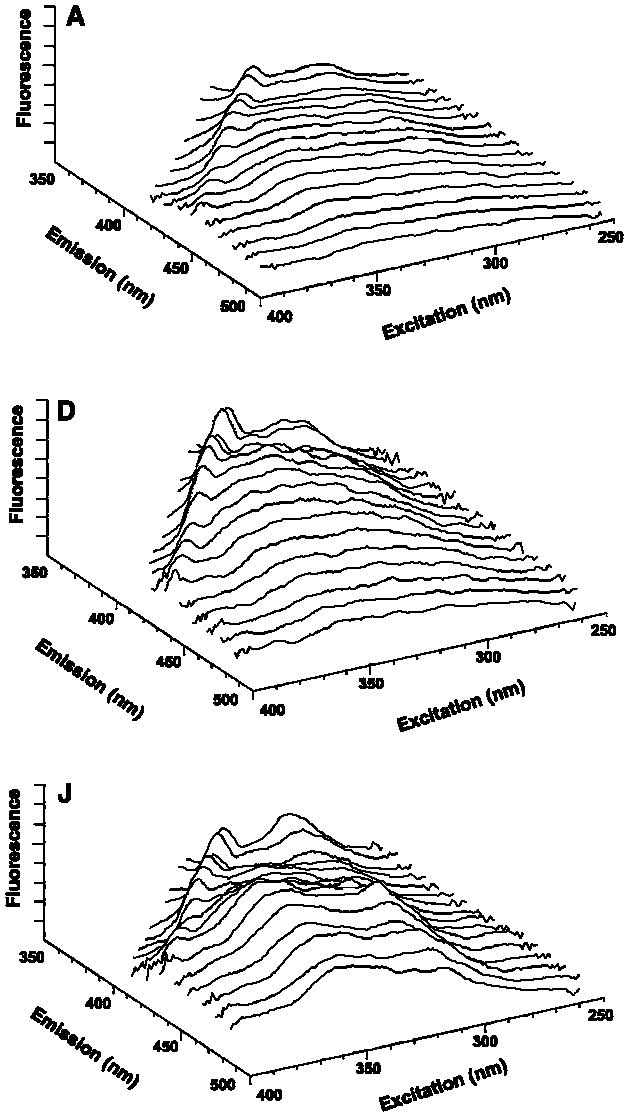

Fig. 27. Examples of 3D fluorescence excitation spectra of brain chloroform extracts. **A** 7 days before birth, **D** postnatal day 2, **J** 3- month-old animals (taken from: Wilhelm J. et al., 2011). Fluorescence intensity is expressed in relative fluorescence units.

4.4.2 Qualitative HPLC analysis

The fluorescent maxima obtained from 3D spectral arrays define the fluorophores with the largest relative concentration in a given sample. Thus as in my previous experiments these fluorophores, being a complex mixture of many different species, were resolved by isocratic HPLC with fluorescence detector adjusted at the wavelengths corresponding to the fluorescence maxima from 3D spectral arrays. Isocratic elution of e.g. F355/410 demonstrated the presence of many fractions, of which some were better separated, while other apparently co-eluted (Fig.28). The chromatograms also reveal, confirming the results of fluorimetric measurements, that the fractionation pattern is different throughout the development indicating changes in the composition of LFP.

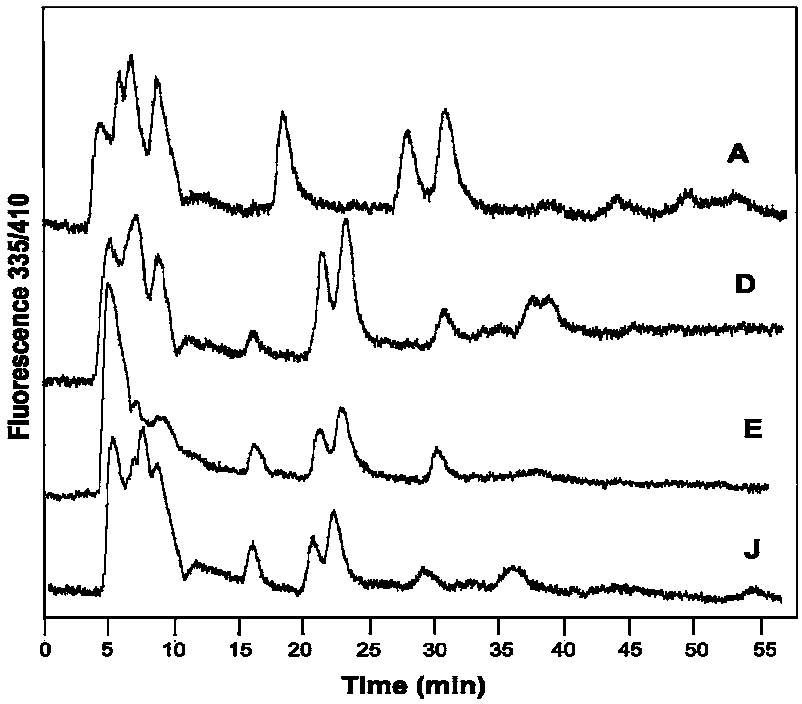

Fig. 28. Examples of the HPLC tracings of the fluorophore F355/410 in brain chloroform extracts of animals of different age: (A) 7 days before birth, (D) postnatal day 2, (E) postnatal day 5, (J) 3-month-old animals. The ordinate indicates fluorescence intensity at 355/410 nm and the abscissa indicates time of analysis (taken from: Wilhelm J. et al., 2011).

4.5. Oxidative stress in erythrocytes from demented subjects

4.5.1 LFP fluorescence measurements

Lipophilic extracts from erythrocytes of patients with cognitive dysfunction linked to "probable Alzheimer's disease" and age-matched controls were analysed spectrofluorimetrically. Fluorophores were characterized by differential synchronous excitation spectra in order to find qualitative differences between two groups within the search for possible biomarkers of Alzheimer's disease in blood.

The maximum difference in fluorescence between group of patients and control group was found at excitation/emission wavelengths 335/360 nm (Fig.29). Hence it must be regarded as quantitative difference, since there is a fluorescence maximum at these wavelengths in control group as well.

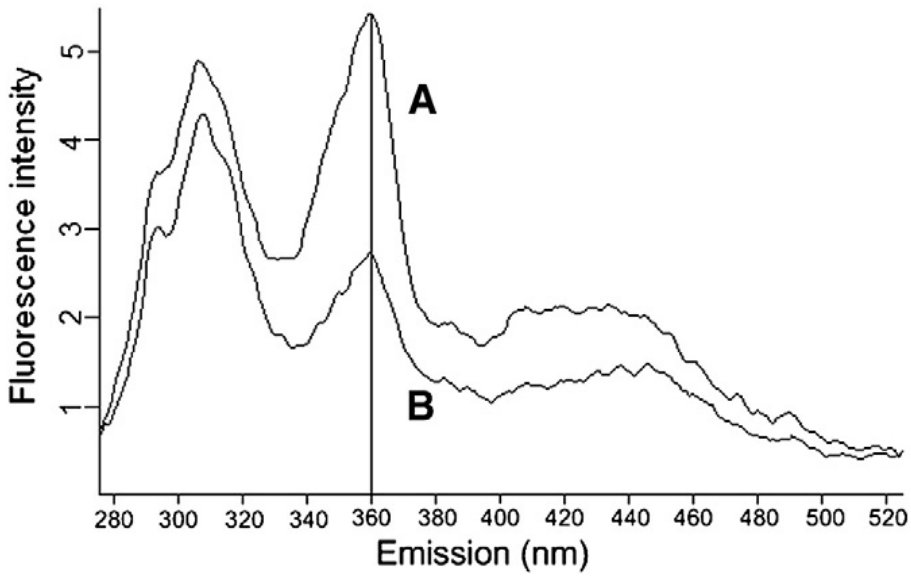

Fig. 29. Synchronous fluorescence spectra of lipophilic extracts from erythrocytes. **A** represents a typical sample from dementia group; **B** represents a typical sample from control group. The ordinate indicates fluorescence intensity in arbitrary units (taken from: Ivica J. et al., 2011). Fluorescence intensity is expressed in relative fluorescence units.

4.5.2 Qualitative HPLC analysis

The fluorophore F335/360, which was found to differ in relative quantity the most between two groups, was analysed by isocratic HPLC method in order to resolve it into different fractions. The major fraction found in dementia group that eluted after 12th minute was virtually not present in control group (Fig. 30).

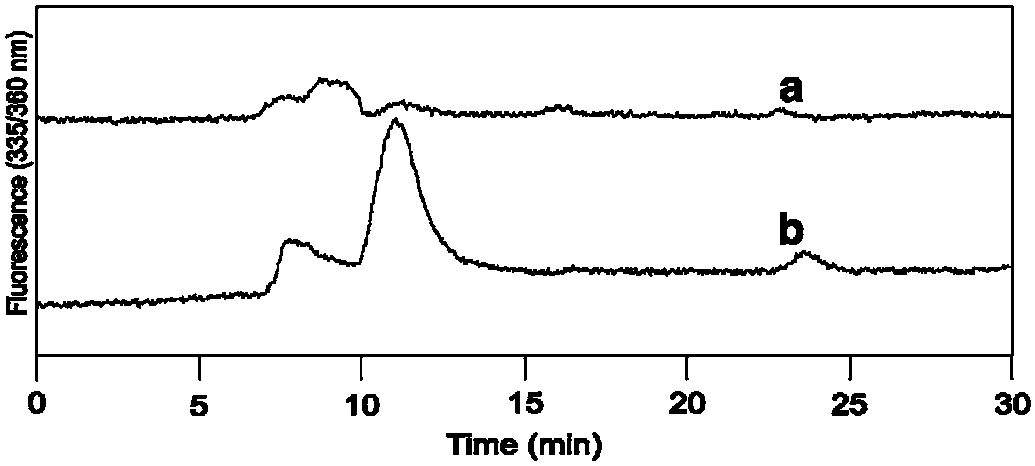

Fig. 30. Example of the chromatograms of fluorophore F335/360 in erythrocytes from: **A** control group, **B** dementia group. The ordinate indicate fluorescence intensity in arbitrary units at 335/360 nm and the abscissa indicates time of analysis (taken from: Ivica J. et al., 2011).

5. DISCUSSION

Fluorescent LFP are established markers of oxidative stress of biological material and their increased production accompanies pathological processes. Lipophilic LFP, in particular, can be reliable and chemically stable indicators of lipid damage in cells. Since LFP are compounds having a fluorophore within their structure, they are most often characterized and analysed by means of spectrofluorimetry. In our experiments lipophilic LFP were measured using their intrinsic fluorescence properties. There are, however, papers describing the measurement of LFP by means of immunochemistry, with specific antibodies developed against certain LFP adducts (Itakura K. et al., 2000; Gu X. et al., 2003).

We measured tridimensional fluorescence spectra along with differential (synchronous) spectra of extracts obtained from isolated mitochondria exposed to in vitro oxidation by various oxidizing agents. Mitochondria are regarded both as source and target of ROS (Anderson E.J. et al., 2012). Their membranes abound with lipids, notably phospholipids, whose peroxidation eventually leads to LFP formation. There are very few studies dealing with the analysis and the characterization of the lipophilic LFP formed in mitochondria as a result of oxidative stress. Mitochondrial LFP were studied either as a consequence of in vivo oxidation of biological material (Wilhelm J and Sonka J., 1981) or after being prepared artificially by in vitro oxidation (Nilsson E and Yin D. Z., 1997). Mitochondrial LFP were primarily analysed in order to acquire more information about these elusive heterogeneous compounds. In the paper by Wilhem and Sonka (1981) the time-course of LFP formation was monitored in rat liver homogenate and mitochondria after the whole body being radiated by gamma rays.

In our work LFP were also artificially prepared by incubating heart mitochondria in vitro with various systems producing free radicals or products that induce chemical changes

leading to LFP formation. For example, mitochondria were incubated in vitro with lipid peroxidation product MDA, a well-known compound participating in fluorescent LFP formation. There are more studies that investigated the formation of fluorescent pigments after MDA was incubated in vitro with, for example, cell membranes (erythrocyte) or vesicles containing different phospholipids. Those studies were undertaken in order to examine the metabolome of various fluorescent pigments generated from MDA. When erythrocytes were incubated with MDA with concentrations similar to the one used in our experiment, maximum fluorescence was found at 360/440 nm (excitation/emission) (Goldstein B. D and McDonagh E. M., 1976). When MDA (1 mM) was incubated for 24 h at 37 °C with artificially made vesicles composed of L-α-phosphatidylethanolamine 1-palmitoyl-2-oleoyl and L-α-phosphatidylethanolamine dioleoyl, LFP fluorophores with maximum fluorescence at 400/470 nm were generated (Wang J. Y. et al., 1996). MDA has been also used in several in vitro studies where it was incubated with some amino-group containing compounds. MDA was incubated with particular compounds in order to elucidate the chemical structure of LFP produced as well as to investigate the spectral properties of the fluorescent end-products. MDA was thus reacted, for example, with an artificially prepared phospholipid containing ethanolamine (Trombly R and Tappel A., 1975). Furthermore, MDA was incubated with very simple compounds such as taurine, GABA, glucosamine or pyridoxamine and the products of all of those reactions were, among others, fluorescent LFP (Kang Z. et al., 2006; Fang C. et al., 2007; Deng Y. et al., 2011 Deng Y. et al., 2012). The concentration of MDA used in the experiments with pyridoxamine and glucosamine was in millimolar range - 5 mM, or even higher - 20 mM when the reactive aldehyde was incubated with lysine-derivative or propylamine (Slatter D.A. et al., 1998; Kang Z. et al., 2006; Fang C. et al., 2007). As for MDA concentration chosen in our experiment, it was micromolar (100 µM) and closer to the levels that can be found in vivo, but still rather high so that it would exert its toxic effect on

biological compounds. pH of the incubation mixture was deliberately set as acidic because MDA at lower pH is mostly present in its keto form and not enolate form. Enolate form is dominant at neutral pH. Keto form of MDA, having two aldehydic groups, is highly reactive and it easily attacks amino-groups of biological compounds (Halliwell B and Gutteridge J. M. C., 2007). In our experiments the focus was actually on studying the kinetics of LFP production in mitochondria incubated with MDA and how this kinetics is affected by incubation temperature. As expected, the higher the temperature the faster LFP production it was. LFP were analysed spectrofluorimetrically and by means of HPLC. The results of spectrofluorimetric measurements, in the form of spectral arrays, confirm that the incubation of mitochondria with MDA leads to fluorescent LFP generation. The emission maxima were in the blue region, which is typical for LFP. In tissues, such blue-emitting pigments arise mainly as a result of ROS overproduction and their rise accompanies pathologies linked to oxidative stress. Specifically, the emission maxima found in our experiment were from 410 – 440 nm, depending on the time of incubation and temperature. As for the excitation maxima, they were in the range 340-365 nm, again depending on the time of incubation and temperature. If LFP formation is accelerated, in our case by increased temperature, there was a tendency of production of fluorophores that emit at around 400 nm when excited at around 300 nm. The similar fluorescence pattern with two maxima was observed in tridimensional spectral arrays of lipophilic extracts of erythrocytes withdrawn from rats exposed for 4 days to hypoxia (Skoumalova A. et al., 2008). Although it is obvious from tridimensional spectra that the incubation of mitochondria with MDA produces a completely new metabolome of fluorescent compounds, we attempted to further analyse individual fluorophores by HPLC. It has been known that particular fluorophores consist of a number of different compounds that can be resolved by using various chromatographic techniques. In our work a new method for qualitative analysis of LFP from mitochondria was developed. Wilhelm and Herget (1999)

described and developed method for isocratic chromatographic analysis of LFP arisen during hypoxia and hypoxia-reoxygenation in rat spleen and erythrocytes. We established also an isocratic method that was used for resolution of fluorophores generated in mitochondria after being incubated with MDA. We succeeded to resolve produced fluorophores into several distinct fractions. From chromatographic data we can see that certain fluorophores consist of several fractions. Individual fractions obtained in our analyses can, however, represent more than one chemical species. Thus fluorescent LFP are indeed a complex mixture of many different compounds. LFP are formed, for example, as a consequence of lipid peroxidation and reactive aldehydes are the main culprit for their production. However, the cascade of the reactions yielding LFP is slow. In attempt for generation a bigger quantity of LFP in vitro and to accelerate the process, we chose to incubate mitochondria MDA at high temperatures. From chromatographic results we see that the incubation of heart mitochondria with MDA after some time gives new peaks belonging to one or more unknown fluorescent compounds or adducts. This can be due to direct reaction of the added reagent with mitochondrial component or perhaps its polymerization, but also there is a possibility of newly synthesized reactive species during incubation process that leads to LFP formation.

Apart from the in vitro incubation of heart mitochondria with lipid peroxidation product MDA, the organelles were exposed to direct in vitro lipid peroxidation by ferrous ions and ascorbic acid or tert-BuOOH. Again we studied in detail the kinetics of LFP production. These two systems have been known as good generators of free radicals involved in lipid peroxidation (Melin A. M. et al., 1997; Micciche F. et al., 2005; Baron C. P. et al., 2006; Petrosillo G. et al., 2009). Furthermore, the mitochondria were exposed to oxidizing and nitrating agent peroxynitrite, which had been used in experiments as prooxidative agent initiating lipid peroxidation before (Kolodziejczyk J. et al., 2011; Singh I. N. et al., 2007).

Lipid peroxidation was assessed by fluorescence measurements of LFP produced during incubation.

Tridimensional as well as synchronous spectra reveal that the fluorescent LFP generated in mitochondria incubated with iron-ascorbate system undergo chemical modifications in the course of incubation. This is deduced if we take a look at the changes of the shape of, in particular, tridimensional spectra of respective samples. In both experiments with iron and ascorbate there were two hilly regions indicating production of LFP with different fluorescence properties, with neither being a dominant one. If we compare the results from two separate papers describing in vitro lipid peroxidation of erythrocyte membranes with iron-ascorbate, we find the same fluorescence maximum of LFP produced, which somewhat differ from our fluorescence maxima found in mitochondrial extracts. Precisely, one was 350/430 nm (Wilhelm J. et al., 2005) and the other 355/430 nm (Skoumalova A. et al., 2008).

When heart mitochondria were exposed to in vitro lipid peroxidation initiated by tert-BuOOH the rate of LFP production was dependent on tert-BuOOH concentration. However, the fluorescence maxima were almost the same in all cases, with the only slight difference in maximum excitation wavelength (350 nm with 100 μM tert-BuOOH and 357 nm with 1 mM tert-BuOOH). The emission was the highest at 440 nm. The spectra obtained after lipid peroxidation with tert-BuOOH show the high similarity with those seen in the experiment with MDA at 37 °C. When erythrocyte membranes were exposed to tert-BuOOH, although in much higher concentration (10 mM), the fluorescence maximum was found to be at 350/420 nm (excitation/emission) (Skoumalova A. et al., 2012).

In the experiments with peroxynitrite LFP were produced immediately upon adding the agent, although when lower concentration was used (2 mM). This implies that peroxynitrite reacts much faster than other oxidants used in our experiments and that it causes

chemical rearrangements that yield LFP very quickly. However, the maximal fluorescence in the samples with 2 mM $ONOO^-$ was similar to the one found in the experiments with tert-BuOOH. The maximum excitation was at 355 nm and the emission at 430 nm. When the concentration of peroxynitrite added to mitochondria was double, tridimensional spectra revealed there was completely different composition of fluorophores present in the extracts. The emission maximum was in another region and it was 500 nm after excitation at 358 nm. If we compare the spectral arrays of lipophilic extracts with both concentrations upon adding peroxynitrite, we can see that sharp increase in fluorescence in the blue region observed with 2 mM $ONOO^-$ is thoroughly missing in the sample where 4 mM $ONOO^-$ had been added into. Furthermore, even after 24 h incubation the fluorescence pattern remained unchanged and there was a decrease in fluorescence in aforementioned region around 500 nm, which saw the emission maximum of the whole spectrum.

As seen in the experiments with MDA, the fluorophores found in spectral arrays with maximum fluorescence, obtained after in vitro lipid peroxidation with tert-BuOOH and peroxynitrite, were analysed by HPLC. Generally, the publications describing the analysis of LFP from biological material using chromatographic techniques are very scarce. Therefore, it was necessary to develop chromatographic method in our laboratory, which will enable separation of various fractions. This is especially essential for LFP from diverse biological samples, where the pigments are usually present in complex mixtures. We first developed method using reverse phase system with isocratic elution and afterwards the methods using gradient system were introduced. Fluorescence detector was used exclusively, for we intended to analyse only fluorescent products of lipid peroxidation. With regard to the analysis of various LFP by HPLC, some pigments prepared by reaction of amine-group containing compounds with the products of lipid peroxidation were reported to have been characterized by this separation method using different detecting tools. Adducts prepared from MDA and

cysteine residues were measured by liquid chromatography-mass spectrometry system (Chowdhury P. K. et al., 2004). Itakura et al. (2000) used isocratic reversed-phase HPLC with fluorescence detector in order to analyse fluorophore derived from lysine-derivative and 4-oxo-2-nonenal. Similarly, the authors from the same laboratory analysed lysine-derived fluorophore generated from oxidized linoleic acid using fluorescence detection (Itakura K and Uchida K., 2003). Furthermore, lipid peroxidation end-products formed in the reaction between MDA and propylamine were analysed by HPLC with photodiode detector, after reactants had been incubated in phosphate buffer for 6 h and 7 days. The incubation over long period (7 days) yielded, as apparent on chromatogram, multiple peaks. (Kang Z. et al., 2006). This is consistent with our findings that lipid peroxidation end-products generated from MDA are diverse compounds, with more products formed as time of incubation increases. However, it must be noted that not all of the end-products are fluorophore-bearing compounds.

Chromatographic analysis of fluorescent LFP formed in mitochondria peroxidized by tert-BuOOH in concentrations up to 1 mM basically gave one fraction, which saw a substantial change during the course of an experiment. This was the case with isocratic and gradient method alike. In our case, the fluorescent species are of unknown structure, i.e. unidentified and therefore chromatographic separation using gradient elution suits better for such samples. By starting with mobile phase composition that has high percentage of water, which cannot remove the fraction of interest from column, and with a subsequent gradual rise of acetonitrile content, we were able to finely resolve the fraction from the interfering peaks.

LFP formed during incubation of mitochondria with $ONOO^-$ were analysed by HPLC using the same methods with gradient as with tert-BuOOH. However, the results were more spectacular, as it was also seen from spectrofluorometric measurements. Thus, in the chromatograms can be seen two dominant fractions, with both increasing in peak area and height as incubation time goes on. The first fraction undoubtedly arose in response to the

exposure of mitochondria to $ONOO^-$, as it was not present in non-peroxidized or autooxidized mitochondria. The second fraction has the same retention time as the one from autooxidation experiments as well as the fraction appearing in the experiments with tert-BuOOH. It was the second fraction that actually disappeared after 24 h incubation of mitochondria with 4 mM $ONOO^-$. On the other hand, the peak regarded as the first fraction was almost 20 times higher with 4 mM $ONOO^-$ at the beginning of the experiment than with 2 mM $ONOO^-$. Nevertheless, after 24 h incubation this peak grew smaller in the sample where 4 mM $ONOO^-$ was added. These analyses, together with afore described spectral measurements, indicate that high concentrations of peroxynitrite destroy LFP species accumulated at lower peroxynitrite concentrations. This is a unique behaviour that was never observed with other free radical generating systems.

Oxidative stress and the damage to biological material are well documented as relevant contributors to pathophysiology of many diseases. Hence the indicators of oxidative damage are usually measured in such subjects to estimate, for example, the extent of damage. Particular compounds can be found in low levels even in normal or disease-free subjects, which is due to continuous ROS production in mitochondria or other sites. In oxidative stress a huge increase in their level is usually observed. Furthermore, during certain pathological process, which is connected to ROS overproduction, completely new products may be formed as consequence.

Indicators of oxidative stress are found early in the pathogenesis of AD (Gustaw-Rothenberg K. et al., 2010). We propose that LFP could be useful biomarkers of this pathological condition. LFP formed in erythrocytes, which can diffuse through circulation into the site of high ROS production in brain, were analysed. The measurement of erythrocyte LFP is very convenient for the cells can be easily isolated after blood has been withdrawn. Spectrofluorimetric measurements revealed the increased level of fluorophore 350/440 nm

(excitation/emission) in subjects with dementia of AD type when compared with age-matched controls. When the fluorophores that showed the biggest difference between the two groups were analysed by HPLC, the most significant results were observed with the fluorophore F335/360. HPLC analysis of this fluorophore showed one remarkable fraction that was present in AD samples and it was barely present in the control samples. This might represent some new fluorescent compound, which is strictly a product of ROS attack involved in pathogenesis of AD. This metabolite might be specific for the processes occurring in AD. Development of separation method is thus a prerequisite for further, a more detailed characterization of such metabolites.

If we compare the results of the qualitative HPLC analysis of fluorescent pigments from the heart mitochondria and erythrocytes, we can observe that in both cases there was just one significant peak that differed between oxidatively altered samples and the control samples.

The increased ROS production is not only linked to pathologies, but also with certain conditions such as normal ageing or during birth. It is to be expected that there is an increased production of ROS after birth due to a sharp rise in oxygen concentration. We measured LFP directly from brain of rats in perinatal period and during early development of the animals. In another study, it was found that during the first few hours after birth DNA from rat liver and kidney was damaged by ROS. The damage was similar to the level of injury found in 24-month-old rats (Randerath E. et al., 1997). Our results indicate a transient accumulation of LFP in neonatal brain. Maximum content of several fluorophores was found on the postnatal day 2, after which the levels were falling down and on the day 10 dropped to prenatal levels. LFP concentration rose significantly again in 3-month-old animals. Rat brain homogenates had three major fluorophores, out of which F335/410 exhibited maximum fluorescence. HPLC analysis of this fluorophore revealed that it can be resolved into several

chromatographically distinct compounds. Again, each fraction seen as a peak might represent more than one chemical species.

For comparison, HPLC analysis of the rat brain homogenates gave much more peaks in the chromatograms than when mitochondria or erythrocytes were used as sample material. This is not surprising since the entire brain tissue was extracted, which gives more sources of LFP than isolated cells or organelles.

Analysis of LFP from rat brain during early postnatal development and from human erythrocytes of patients with dementia of AD type indicates the presence of an entire metabolome of compounds arising as products of free radical reactions. Their chemical structure and biological roles are still unknown and with this regard further studies are required.

6. CONCLUSION

In this work, we developed several chromatographic methods for the separation of fluorescent LFP formed as products of free radical reactions in different biological systems. We applied these methods for the analyses of fluorescent products generated in beef heart mitochondria exposed in vitro to various free radical generators, in erythrocytes membranes, and in developing rat brain.

On analysing LFP from various sources by means of fluorescence spectroscopy and HPLC, we found a whole metabolome of different fluorescent compounds. These compounds are products of oxidative stress and play a significant role in pathophysiology of several pathological processes.

7. SUMMARY

Lipofuscin-like pigments are products of reactions involving free radical attack onto molecules with nucleophilic groups. They can be formed, for example, in the reactions between lipid peroxidation decomposition products, such as aldehydes, and amino-group containing compounds, e.g. phospholipids, peptides. Owing to their intrinsic fluorescent properties LFP can be easily measured. LFP are relatively stable and therefore have been successfully used as robust markers of oxidative damage.

We undertook the metabolomic studies, where fluorescent LFP were first analysed spectrofluorimetrically by using tridimensional and differential fluorescence spectral arrays. After that, certain LFP were analysed by means of high performance liquid chromatography, in order to resolve the mixture of compounds into distinct fractions. For this purpose we used LFP prepared after isolated heart mitochondria had been exposed in vitro to oxidative stress initiated by various triggers. LFP were also analysed during early development in rat brain, which is accompanied by transient increase in oxygen concentration, and in erythrocytes from patients with Alzheimer's disease.

We developed HPLC methods for qualitative analysis of LFP of different origin. This analysis unfolded that LFP indeed consist of many chromatographically different species. By this way we confirmed the existence of a great number of individual fluorescent species involved in pathophysiology of some diseases and conditions.

SOUHRN

Lipofuscinoidní pigmenty (LFP) jsou produkty reakcí, ve kterých volné radikály napadají molekuly s nukleofilními skupinami. LFP vznikají např. v reakcích mezi produkty rozkládaní peroxidů lipidů, což jsou hlavně reaktivní aldehydy, a sloučeninami obsahujícími aminoskupiny (fosfolipidy, peptidy). LFP lze snadno měřit díky jejich vnitřní fluorescenci. Tyto produkty jsou poměrně stabilní, a proto byly úspěšně využívány jako robustní markery oxidačního poškození.

Provedli jsme metabolomické studie, přičemž LFP byly nejprve analyzovány fluorimetricky pomocí trojrozměrných a diferenciálních fluorescenčních spekter. Potom jsme LFP analyzovali pomocí vysokoúčinné kapalinové chromatografie s cílem rozdělit směs látek na jednotlivé frakce. LFP jsme získali z izolovaných mitochondrií vystavených in vitro oxidačnímu stresu zahájenému různými spouštěči. LFP byly rovněž analyzovány v potkaních mozcích během časného rozvoje, což je doprovázeno přechodným zvýšením koncentrace kyslíku, a v erytrocytech z pacientů s Alzheimerovou chorobou.

Vyvinuli jsme HPLC metodu pro kvalitativní analýzu LFP odlišného původu. Tato analýza objevila, že se LFP opravdu skládají z mnoha chromatograficky odlišných látek. Tímto způsobem jsme potvrdili jsoucnost velkého počtu jednotlivých fluorescenčních látek, jež se účastní patofyziologie některých chorob a stavů.

8. REFERENCES

1. Adam-Vizi, V., Starkov, A. A. (2010) Calcium and mitochondrial reactive oxygen species generation: how to read the facts. *J Alzheimers Dis,* 20 Suppl 2**,** S413-26.
2. Anderson, E. J., Katunga, L. A., Willis, M. S. (2012) Mitochondria as a source and target of lipid peroxidation products in healthy and diseased heart. *Clin Exp Pharmacol Physiol,* 39**,** 179-93.
3. Armstrong, D., Wilhelm, J., Smid, F., Elleder, M. (1992) Chromatography and spectrofluorometry of brain fluorophores in neuronal ceroid lipofuscinosis (NCL). *Mech Ageing Dev,* 64**,** 293-302.
4. Balazy, M., Nigam, S. (2003) Aging, lipid modifications and phospholipases--new concepts. *Ageing Res Rev,* 2**,** 191-209.
5. Baron, C. P., Refsgaard, H. H., Skibsted, L. H., Andersen, M. L. (2006) Oxidation of bovine serum albumin initiated by the Fenton reaction--effect of EDTA, tert-butylhydroperoxide and tetrahydrofuran. *Free Radic Res,* 40**,** 409-17.
6. Bates, T. E., Loesch, A., Burnstock, G., Clark, J. B. (1995) Immunocytochemical evidence for a mitochondrially located nitric oxide synthase in brain and liver. *Biochem Biophys Res Commun,* 213**,** 896-900.
7. Bergendi, L., Benes, L., Durackova, Z., Ferencik, M. (1999) Chemistry, physiology and pathology of free radicals. *Life Sci,* 65**,** 1865-74.
8. Boveris, A., Cadenas, E. (2000) Mitochondrial production of hydrogen peroxide regulation by nitric oxide and the role of ubisemiquinone. *IUBMB Life,* 50**,** 245-50.
9. Boveris, A., Chance, B. (1973) The mitochondrial generation of hydrogen peroxide. General properties and effect of hyperbaric oxygen. *Biochem J,* 134**,** 707-16.

10. Brand, M. D. (2010) The sites and topology of mitochondrial superoxide production. *Exp Gerontol,* 45**,** 466-72.
11. Buettner, G. R., Ng, C. F., Wang, M., Rodgers, V. G., Schafer, F. Q. (2006) A new paradigm: manganese superoxide dismutase influences the production of H2O2 in cells and thereby their biological state. *Free Radic Biol Med,* 41**,** 1338-50.
12. Cadenas, E., Davies, K. J. (2000) Mitochondrial free radical generation, oxidative stress, and aging. *Free Radic Biol Med,* 29**,** 222-30.
13. Cardoso, A. R., Chausse, B., Da Cunha, F. M., Luevano-Martinez, L. A., Marazzi, T. B., Pessoa, P. S., Queliconi, B. B. & Kowaltowski, A. J. (2012) Mitochondrial compartmentalization of redox processes. *Free Radic Biol Med*.
14. Castro, L., Demicheli, V., Tortora, V., Radi, R. (2011) Mitochondrial protein tyrosine nitration. *Free Radic Res,* 45**,** 37-52.
15. Catala, A. (2009) Lipid peroxidation of membrane phospholipids generates hydroxy-alkenals and oxidized phospholipids active in physiological and/or pathological conditions. *Chem Phys Lipids,* 157**,** 1-11.
16. Catala, A. (2010) A synopsis of the process of lipid peroxidation since the discovery of the essential fatty acids. *Biochem Biophys Res Commun,* 399**,** 318-23.
17. Cleeter, M. W., Cooper, J. M., Derley-Usmar, V. M., Moncada, S., Schapira, A. H. (1994) Reversible inhibition of cytochrome c oxidase, the terminal enzyme of the mitochondrial respiratory chain, by nitric oxide. Implications for neurodegenerative diseases. *FEBS Lett,* 345**,** 50-4.
18. Davydov, V. V., Shvets, V. N. (2001) Lipid peroxidation in the heart of adult and old rats during immobilization stress. *Exp Gerontol,* 36**,** 1155-60.

19. Davis, C. W., Hawkins, B. J., Ramasamy, S., Irrinki, K. M., Cameron, B. A., Islam, K., Daswani, V. P., Doonan, P. J., Manevich, Y., Madesh, M. (2010) Nitration of the mitochondrial complex I subunit NDUFB8 elicits RIP1- and RIP3-mediated necrosis. *Free Radic Biol Med,* 48**,** 306-17.
20. De Grey, A. D. (2002) HO2*: the forgotten radical. *DNA Cell Biol,* 21**,** 251-7.
21. Del Rio, L. A. (2011) Peroxisomes as a cellular source of reactive nitrogen species signal molecules. *Arch Biochem Biophys,* 506**,** 1-11.
22. Del Rio, D., Stewart, A. J., Pellegrini, N. (2005) A review of recent studies on malondialdehyde as toxic molecule and biological marker of oxidative stress. *Nutr Metab Cardiovasc Dis,* 15**,** 316-28.
23. Deng, Y., He, N. Y., Xu, L. J., Li, X. L., Li, S., Li, Z. Y., Liu, H. N. (2011) A Rapid Scavenger of the Lipid Peroxidation Product Malondialdehyde: New Perspective of Taurine. *Advanced Science Letters,* 4**,** 442-448.
24. Deng, Y., Xu, L., Zeng, X., Li, Z., Qin, B., He, N. (2012) New perspective of GABA as an inhibitor of formation of advanced lipoxidation end-products: it's interaction with malondiadehyde. *J Biomed Nanotechnol,* 6**,** 318-24.
25. Dikalov, S. (2011) Cross talk between mitochondria and NADPH oxidases. *Free Radic Biol Med,* 51**,** 1289-301.
26. Drahota, Z., Chowdhury, S. K., Floryk, D., Mracek, T., Wilhelm, J., Rauchova, H., Lenaz, G., Houstek, J. (2002) Glycerophosphate-dependent hydrogen peroxide production by brown adipose tissue mitochondria and its activation by ferricyanide. *J Bioenerg Biomembr,* 34**,** 105-13.
27. Drechsel, D. A., Patel, M. (2010) Respiration-dependent H2O2 removal in brain mitochondria via the thioredoxin/peroxiredoxin system. *J Biol Chem,* 285**,** 27850-8.

28. Droge, W. (2002) Free radicals in the physiological control of cell function. *Physiol Rev,* 82**,** 47-95.

29. Dukhande, V. V., Isaac, A. O., Chatterji, T., Lai, J. C. (2009) Reduced glutathione regenerating enzymes undergo developmental decline and sexual dimorphism in the rat cerebral cortex. *Brain Res,* 1286**,** 19-24.

30. Esterbauer, H., Dieber-Rotheneder, M., Waeg, G., Striegl, G., Jurgens, G. (1990) Biochemical, structural, and functional properties of oxidized low-density lipoprotein. *Chem Res Toxicol,* 3**,** 77-92.

31. Esterbauer, H., Koller, E., Slee, R. G., Koster, J. F. (1986) Possible involvement of the lipid-peroxidation product 4-hydroxynonenal in the formation of fluorescent chromolipids. *Biochem J,* 239**,** 405-9.

32. Esterbauer, H., Schaur, R. J., Zollner, H. (1991) Chemistry and biochemistry of 4-hydroxynonenal, malonaldehyde and related aldehydes. *Free Radic Biol Med,* 11**,** 81-128.

33. Esworthy, R. S., Ho, Y. S., Chu, F. F. (1997) The Gpx1 gene encodes mitochondrial glutathione peroxidase in the mouse liver. *Arch Biochem Biophys,* 340**,** 59-63.

34. Fang, C., Peng, M., Li, G., Tian, J., Yin, D. (2007) New functions of glucosamine as a scavenger of the lipid peroxidation product malondialdehyde. *Chem Res Toxicol,* 20**,** 947-53.

35. Folstein, M. F., Folstein, S. E., McHugh, P. R. (1975) "Mini-mental state". A practical method for grading the cognitive state of patients for the clinician. *J Psychiatr Res,* 12**,** 189-98.

36. Forstermann, U., Sessa, W. C. (2012) Nitric oxide synthases: regulation and function. *Eur Heart J,* 33**,** 829-37, 837a-837d.

37. Freinbichler, W., Colivicchi, M. A., Stefanini, C., Bianchi, L., Ballini, C., Misini, B., Weinberger, P., Linert, W., Vareslija, D., Tipton, K. F., Della Corte, L. Highly reactive oxygen species: detection, formation, and possible functions. (2011) *Cell Mol Life Sci,* 68**,** 2067-79.
38. Fridovich, I. (1995) Superoxide radical and superoxide dismutases. *Annu Rev Biochem,* 64**,** 97-112.
39. Fukuzawa, K., Kishikawa, K., Tokumura, A., Tsukatani, H., Shibuya, M. (1985) Fluorescent pigments by covalent binding of lipid peroxidation by-products to protein and amino acids. *Lipids,* 20**,** 854-61.
40. Gazaryan, I. G., Krasnikov, B. F., Ashby, G. A., Thorneley, R. N., Kristal, B. S., Brown, A. M. (2002) Zinc is a potent inhibitor of thiol oxidoreductase activity and stimulates reactive oxygen species production by lipoamide dehydrogenase. *J Biol Chem,* 277**,** 10064-72.
41. Giorgio, M., Trinei, M., Migliaccio, E., Pelicci, P. G. (2007) Hydrogen peroxide: a metabolic by-product or a common mediator of ageing signals? *Nat Rev Mol Cell Biol,* 8**,** 722-8
42. Girotti, A. W. (1985) Mechanisms of lipid peroxidation. *J Free Radic Biol Med,* 1**,** 87-95.
43. Goldstein, B. D., McDonagh, E. M. (1976) Spectrofluorescent detection of in vivo red cell lipid peroxidation in patients treated with diaminodiphenylsulfone. *J Clin Invest,* 57**,** 1302-7.
44. Gonzalvez, F., Gottlieb, E. (2007) Cardiolipin: setting the beat of apoptosis. *Apoptosis,* 12**,** 877-85.
45. Greco, T., Shafer, J., FIiskum, G. Sulforaphane inhibits mitochondrial permeability transition and oxidative stress. *Free Radic Biol Med,* 51**,** 2164-71.

46. Grivennikova, V. G., Vinogradov, A. D. (2006) Generation of superoxide by the mitochondrial Complex I. *Biochim Biophys Acta,* 1757**,** 553-61.

47. Gu, X., Meer, S. G., Miyagi, M., Rayborn, M. E., Hollyfield, J. G., Crabb, J. W., Salomon, R. G. (2003) Carboxyethylpyrrole protein adducts and autoantibodies, biomarkers for age-related macular degeneration. *J Biol Chem,* 278**,** 42027-35.

48. Gustaw-Rothenberg, K., Lerner, A., Bonda, D. J., Lee, H. G., Zhu, X., Perry, G., Smith, M. A. (2010) Biomarkers in Alzheimer's disease: past, present and future. *Biomark Med,* 4**,** 15-26.

49. Haas, D. W., Elliottt, W. B. (1963) Oxidative phosphorylation and respiratory control in digitonin fragments of beef heart mitochondria. *J Biol Chem,* 238**,** 1132-6.

50. Habib, S., Ali, A. (2011) Biochemistry of nitric oxide. *Indian J Clin Biochem,* 26**,** 3-17.

51. Halliwell, B. (1997) Antioxidants: the basics--what they are and how to evaluate them. *Adv Pharmacol,* 38**,** 3-20.

52. Halliwell, B., Gutteridge, J. M. (1984) Oxygen toxicity, oxygen radicals, transition metals and disease. *Biochem J,* 219**,** 1-14.

53. Halliwell, B., Gutteridge, J. M. (2007) Free Radicals in Biology and Medicine. 4th edition, Oxford University Press; Oxford.

54. Han, D., Antunes, F., Canali, R., Rettori, D., Cadenas, E. (2003) Voltage-dependent anion channels control the release of the superoxide anion from mitochondria to cytosol. *J Biol Chem,* 278**,** 5557-63.

55. Herrero, E., De La Torre-Ruiz, M. A. (2007) Monothiol glutaredoxins: a common domain for multiple functions. *Cell Mol Life Sci,* 64**,** 1518-30.

56. Holley, A. K., Dhar, S. K., St Clair, D. K. (2010) Manganese superoxide dismutase vs. p53: regulation of mitochondrial ROS. *Mitochondrion,* 10**,** 649-61.

57. Howden, P. J., Faux, S. P. (1996) Fibre-induced lipid peroxidation leads to DNA adduct formation in Salmonella typhimurium TA104 and rat lung fibroblasts. *Carcinogenesis,* 17**,** 413-419.

58. Chandel, N. S., Budinger, G. R. (2007) The cellular basis for diverse responses to oxygen. *Free Radic Biol Med,* 42**,** 165-74.

59. Chen, Y. R., Chen, C. L., Zhang, L., Green-Church, K. B., Zweier, J. L. (2005) Superoxide generation from mitochondrial NADH dehydrogenase induces self-inactivation with specific protein radical formation. *J Biol Chem,* 280**,** 37339-48.

60. Chio, K. S., Reiss, U., Fletcher, B., Tappel, A. L. (1969) Peroxidation of subcellular organelles: formation of lipofuscinlike fluorescent pigments. *Science,* 166**,** 1535-6.

61. Chio, K. S., Tappel, A. L. (1969) Synthesis and characterization of the fluorescent products derived from malonaldehyde and amino acids. *Biochemistry,* 8**,** 2821-6.

62. Chowdhury, P. K., Halder, M., Choudhury, P. K., Kraus, G. A., Desai, M. J., Armstrong, D. W., Casey, T. A., Rasmussen, M. A., Petrich, J. W. (2004) Generation of fluorescent adducts of malondialdehyde and amino acids: toward an understanding of lipofuscin. *Photochem Photobiol,* 79**,** 21-5.

63. Itakura, K., Oya-Ito, T., Osawa, T., Yamada, S., Toyokuni, S., Shibata, N., Kobayashi, M., Uchida, K. (2000) Detection of lipofuscin-like fluorophore in oxidized human low-density lipoprotein. 4-hydroxy-2-nonenal as a potential source of fluorescent chromophore. *FEBS Lett,* 473**,** 249-53.

64. Itakura, K., Uchida, K. (2001) Evidence that malondialdehyde-derived aminoenimine is not a fluorescent age pigment. *Chem Res Toxicol,* 14**,** 473-5.

65. Itakura, K., Uchida, K. (2003) Lysine-derived fluorophores formed by autoxidation of linoleic acid. *Chem Phys Lipids,* 123**,** 187-91.

66. Ivica, J., Skoumalova, A., Topinkova, E., Wilhelm, J. (2011) HPLC Separation of Fluorescent Products of Lipid Peroxidation in Erythrocytes and Mitochondria. *Chromatographia,* 73**,** S67-S73.

67. Jezek, P., Hlavata, L. (2005) Mitochondria in homeostasis of reactive oxygen species in cell, tissues, and organism. *Int J Biochem Cell Biol,* 37**,** 2478-503.

68. Judge, S., Leeuwenburgh, C. (2007) Cardiac mitochondrial bioenergetics, oxidative stress, and aging. *Am J Physiol Cell Physiol,* 292**,** C1983-92.

69. Kanai, A. J., Pearce, L. L., Clemens, P. R., Birder, L. A., Vanbibber, M. M., Choi, S. Y., De Groat, W. C., Peterson, J. (2001) Identification of a neuronal nitric oxide synthase in isolated cardiac mitochondria using electrochemical detection. *Proc Natl Acad Sci U S A,* 98**,** 14126-31.

70. Kang, Z., Li, H., Li, G., Yin, D. (2006) Reaction of pyridoxamine with malondialdehyde: Mechanism of inhibition of formation of advanced lipoxidation end-products. *Amino Acids,* 30**,** 55-61.

71. Kikugawa, K., Machida, Y., Kida, M., Kurechi, T. (1981) Studies on Peroxidized Lipids .3. Fluorescent Pigments Derived from the Reaction of Malonaldehyde and Amino-Acids. *Chemical & Pharmaceutical Bulletin,* 29**,** 3003-3011.

72. Kirsch, M., De Groot, H. (2001) NAD(P)H, a directly operating antioxidant? *FASEB J,* 15**,** 1569-74.

73. Klaunig, J. E., Kamendulis, L. M., Hocevar, B. A. Oxidative stress and oxidative damage in carcinogenesis. *Toxicol Pathol,* 38**,** 96-109.

74. Koch, M., Mostert, J., Arutjunyan, A. V., Stepanov, M., Teelken, A., Heersema, D., De Keyser, J. (2007) Plasma lipid peroxidation and progression of disability in multiple sclerosis. *Eur J Neurol,* 14**,** 529-33.

75. Kolodziejczyk, J., Saluk-Juszczak, J., Wachowicz, B. (2011) In vitro study of the antioxidative properties of the glucose derivatives against oxidation of plasma components. *J Physiol Biochem,* 67**,** 175-83.
76. Koster, J. F., Slee, R. G. (1980) Lipid peroxidation of rat liver microsomes. *Biochim Biophys Acta,* 620**,** 489-99.
77. Koster, J. F., Slee, R. G., Van Berkel, T. J. (1982) On the lipid peroxidation of rat liver hepatocytes, the formation of fluorescent chromolipids and high molecular weight protein. *Biochim Biophys Acta,* 710**,** 230-5.
78. Kowattowski, A. J., De Souza-Pinto, N. C., Castilho, R. F., Vercesi, A. E. (2009) Mitochondria and reactive oxygen species. *Free Radic Biol Med,* 47**,** 333-43.
79. Kudin, A. P., Augustynek, B., Lehmann, A. K., Kovacs, R., Kunz, W. S. (2012) The contribution of thioredoxin-2 reductase and glutathione peroxidase to H(2)O(2) detoxification of rat brain mitochondria. *Biochim Biophys Acta*.
80. Kussmaul, L., Hirst, J. (2006) The mechanism of superoxide production by NADH:ubiquinone oxidoreductase (complex I) from bovine heart mitochondria. *Proc Natl Acad Sci U S A,* 103**,** 7607-12.
81. Lancaster, J. R., Jr. (2006) Nitroxidative, nitrosative, and nitrative stress: kinetic predictions of reactive nitrogen species chemistry under biological conditions. *Chem Res Toxicol,* 19**,** 1160-74.
82. Lassmann, H. (2011) Mechanisms of neurodegeneration shared between multiple sclerosis and Alzheimer's disease. *J Neural Transm,* 118**,** 747-52.
83. Lauridsen, C., Jensen, S. K. (2012) alpha-Tocopherol incorporation in mitochondria and microsomes upon supranutritional vitamin E supplementation. *Genes Nutr*.

84. Lee, S., Tak, E., Lee, J., Rashid, M. A., Murphy, M. P., Ha, J., Kim, S. S. (2011) Mitochondrial H2O2 generated from electron transport chain complex I stimulates muscle differentiation. *Cell Res,* 21**,** 817-34.

85. Lenaz, G. (2001) The mitochondrial production of reactive oxygen species: mechanisms and implications in human pathology. *IUBMB Life,* 52**,** 159-64.

86. Limon-Pacheco, J., Gonsebatt, M. E. (2009) The role of antioxidants and antioxidant-related enzymes in protective responses to environmentally induced oxidative stress. *Mutat Res,* 674**,** 137-47.

87. Liu, Y., Fiskum, G., Schubert, D. (2002) Generation of reactive oxygen species by the mitochondrial electron transport chain. *J Neurochem,* 80**,** 780-7.

88. Lowes, D. A., Galley, H. F. (2011) Mitochondrial protection by the thioredoxin-2 and glutathione systems in an in vitro endothelial model of sepsis. *Biochem J,* 436**,** 123-32.

89. Lowry, O. H., Rosebrough, N. J., Farr, A. L., Randall, R. J. (1951) Protein measurement with the Folin phenol reagent. *J Biol Chem,* 193**,** 265-75.

90. Madamanchi, N. R., Runge, M. S. (2007) Mitochondrial dysfunction in atherosclerosis. *Circ Res,* 100**,** 460-73.

91. Maiorino, M., Scapin, M., Ursini, F., Biasolo, M., Bosello, V., Flohe, L. (2003) Distinct promoters determine alternative transcription of gpx-4 into phospholipid-hydroperoxide glutathione peroxidase variants. *J Biol Chem,* 278**,** 34286-90.

92. Mari, M., Morales, A., Colell, A., Garcia-Ruiz, C., Fernandez-Checa, J. C. (2009) Mitochondrial glutathione, a key survival antioxidant. *Antioxid Redox Signal,* 11**,** 2685-700.

93. Mather, O. C., Singh, A., Van Boxel, G. I., White, S. A., Jackson, J. B. (2004) Active-site conformational changes associated with hydride transfer in proton-translocating transhydrogenase. *Biochemistry,* 43**,** 10952-64.

94. McGrath, L. T., McGleenon, B. M., Brennan, S., McColl, D., Mc, I. S., Passamore, A. P. (2001) Increased oxidative stress in Alzheimer's disease as assessed with 4-hydroxynonenal but not malondialdehyde. *Qjm,* 94**,** 485-90.

95. McKhann, G., Drachman, D., Filstein, M., Katzman, R., Price, D., Stadlan, E. M. (1984) Clinical diagnosis of Alzheimer's disease: report of the NINCDS-ADRDA Work Group under the auspices of Department of Health and Human Services Task Force on Alzheimer's Disease. *Neurology,* 34**,** 939-44.

96. Melin, A. M., Peuchant, E., Perromat, A., Clerc, M. (1997) In vitro influence of ascorbate on lipid peroxidation in rat testis and heart microsomes. *Mol Cell Biochem,* 169**,** 171-6.

97. Micciche, F., Van Haveren, J., Oostveen, E., Laven, J., Ming, W., Okanoyman, Z., Van Der Linde, R. (2005) Oxidation of methyl linoleate in micellar solutions induced by the combination of iron (II)/ascorbic acid and iron(II)/H2O2. *Arch Biochem Biophys,* 443**,** 45-52.

98. Montfoort, A., Bezstarosti, K., Groh, M. M., Koster, J. F. (1987) The influence of the chain length of aldehydes on the fluorescence of chromolipids. *FEBS Lett,* 226**,** 101-4.

99. Montine, T. J., Beal, M. F., Cudkowicz, M. E., O'Donnell, H., Margolin, R. A., McFarland, L., Bachrach, A. F., Zackert, W. E., Roberts, L. J., Morrow, J. D. (1999) Increased CSF F2-isoprostane concentration in probable AD. *Neurology,* 52**,** 562-5.

100. Miwa, S., St-Pierre, J., Partridge, L., Brand, M. D. (2003) Superoxide and hydrogen peroxide production by Drosophila mitochondria. *Free Radic Biol Med,* 35**,** 938-48.

101. Miyamoto, S., Martinez, G. R., Medeiros, M. H., Di Mascio, P. (2003) Singlet molecular oxygen generated from lipid hydroperoxides by the russell mechanism: studies using 18(O)-labeled linoleic acid hydroperoxide and monomol light emission measurements. *J Am Chem Soc,* 125**,** 6172-9.

102. Mozaffarian, D., Wu, J. H. (2011) Omega-3 fatty acids and cardiovascular disease: effects on risk factors, molecular pathways, and clinical events. *J Am Coll Cardiol*, 58**,** 2047-67.

103. Munkres, K. D., Rana, R. S. (1978) Aging of Neurospora-Crassa .7. Accumulation of Fluorescent Pigment (Lipofuscin) and Inhibition of Accumulation by Nordihydroguaiaretic Acid. *Mechanisms of Ageing and Development*, 7**,** 399-406.

104. Niki, E. (2009) Lipid peroxidation: physiological levels and dual biological effects. *Free Radic Biol Med*, 47**,** 469-84.

105. Nilsson, E., Yin, D. (1997) Preparation of artificial ceroid/lipofuscin by UV-oxidation of subcellular organelles. *Mech Ageing Dev*, 99**,** 61-78.

106. Nulton-Persson, A. C., Szweda, L. I. (2001) Modulation of mitochondrial function by hydrogen peroxide. *J Biol Chem*, 276**,** 23357-61.

107. Okado-Matsumoto, A., Fridovich, I. (2001) Subcellular distribution of superoxide dismutases (SOD) in rat liver: Cu,Zn-SOD in mitochondria. *J Biol Chem*, 276**,** 38388-93.

108. Ostadalova, I., Vobecky, M., Chvojkova, Z., Mikova, D., Hampl, V., Wilhelm, J., Ostadal, B. (2007) Selenium protects the immature rat heart against ischemia/reperfusion injury. *Mol Cell Biochem*, 300**,** 259-67.

109. Panfili, E., Sandri, G., Ernster, L. (1991) Distribution of glutathione peroxidases and glutathione reductase in rat brain mitochondria. *FEBS Lett*, 290**,** 35-7.

110. Paradies, G., Petrosillo, G., Pistolese, M., Ruggiero, F. M. (2002) Reactive oxygen species affect mitochondrial electron transport complex I activity through oxidative cardiolipin damage. *Gene*, 286**,** 135-41.

111. Patenaude, A., Ven Murthy, M. R., Mirault, M. E. (2004) Mitochondrial thioredoxin system: effects of TrxR2 overexpression on redox balance, cell growth, and apoptosis. *J Biol Chem,* 279**,** 27302-14.

112. Patkova, J., Vojtisek, M., Tuma, J., Vozeh, F., Knotkova, J., Santorova, P., Wilhelm, J. (2012) Evaluation of lipofuscin-like pigments as an index of lead-induced oxidative damage in the brain. *Exp Toxicol Pathol,* 64**,** 51-6.

113. Petrat, F., Pindiur, S., Kirsch, M., De Groot, H. (2003) NAD(P)H, a primary target of 1O2 in mitochondria of intact cells. *J Biol Chem,* 278**,** 3298-307.

114. Petrosillo, G., Moro, N., Ruggiero, F. M., Paradies, G. (2009) Melatonin inhibits cardiolipin peroxidation in mitochondria and prevents the mitochondrial permeability transition and cytochrome c release. *Free Radic Biol Med,* 47**,** 969-74.

115. Pryor, W. A. (1986) Oxy-radicals and related species: their formation, lifetimes, and reactions. *Annu Rev Physiol,* 48**,** 657-67.

116. Puddu, P., Pudu, G. M., Cravero, E., De Pascalis, S., Muscari, A. (2009) The emerging role of cardiovascular risk factor-induced mitochondrial dysfunction in atherogenesis. *J Biomed Sci,* 16**,** 112.

117. Quinlan, C. L., Gerencser, A. A., Treberg, J. R., Brand, M. D. (2011) The mechanism of superoxide production by the antimycin-inhibited mitochondrial Q-cycle. *J Biol Chem,* 286**,** 31361-72.

118. Radi, R., Turrens, J. F., Chang, L. Y., Bush, K. M., Crapo, J. D., Freeman, B. A. (1991) Detection of catalase in rat heart mitochondria. *J Biol Chem,* 266**,** 22028-34.

119. Randerath, E., Zhou, G. D., Randerath, K. (1997) Organ-specific oxidative DNA damage associated with normal birth in rats. *Carcinogenesis,* 18**,** 859-66.

120. Rao, V., Kiran, R. (2011) Evaluation of correlation between oxidative stress and abnormal lipid profile in coronary artery disease. *J Cardiovasc Dis Res,* 2**,** 57-60.

121. Reed, T. T. (2011) Lipid peroxidation and neurodegenerative disease. *Free Radic Biol Med,* 51**,** 1302-19.

122. Rejholcova, M., Wilhelm, J. (1986) Relationship between lipofuscin-like pigments formation and lipolysis in gamma irradiated rats. *Agressologie,* 27**,** 475-6.

123. Rejholcova, M., Wilhelm, J. (1989) Time course of lipolytic activity and lipid peroxidation after whole-body gamma irradiation of rats. *Radiat Res,* 117**,** 21-5.

124. REJHOLCOVA, M. & WILHELM, J. (1989) Lipid peroxidation and lipolysis during fasting. *Acta Univ Carol Med (Praha),* 35**,** 43-61.

125. Riazy, M., Lougheed, M., Adomat, H. H., Guns, E. S., Eigendorf, G. K., Duronio, V., Steinbrecher, U. P. (2011) Fluorescent adducts formed by reaction of oxidized unsaturated fatty acids with amines increase macrophage viability. *Free Radic Biol Med,* 51**,** 1926-36.

126. Robinson, M. A., Baumgardner, J. E., Otto, C. M. (2011) Oxygen-dependent regulation of nitric oxide production by inducible nitric oxide synthase. *Free Radic Biol Med,* 51**,** 1952-65.

127. Russo, G. L. (2009) Dietary n-6 and n-3 polyunsaturated fatty acids: from biochemistry to clinical implications in cardiovascular prevention. *Biochem Pharmacol,* 77**,** 937-46.

128. Rydstrom, J. (2006) Mitochondrial NADPH, transhydrogenase and disease. *Biochim Biophys Acta,* 1757**,** 721-6.

129. Salvi, M., Battaglia, V., Brunati, A. M., La Rocca, N., Tibaldi, E., Pietrangeli, P., Marcocci, L., Mondovi, B., Rossi, C. A., Toninello, A. (2007) Catalase takes part in rat liver mitochondria oxidative stress defense. *J Biol Chem,* 282**,** 24407-15.

130. Seehafer, S. S., Pearce, D. A. (2006) You say lipofuscin, we say ceroid: defining autofluorescent storage material. *Neurobiol Aging,* 27**,** 576-88.

131. Sen, T., Sen, N., Jana, S., Khan, F. H., Chatterjee, U., Chakrabarti, S. (2007) Depolarization and cardiolipin depletion in aged rat brain mitochondria: relationship with oxidative stress and electron transport chain activity. *Neurochem Int,* 50**,** 719-25.

132. Shigenaga, M. K., Hagen, T. M., Ames, B. N. (1994) Oxidative damage and mitochondrial decay in aging. *Proc Natl Acad Sci U S A,* 91**,** 10771-8.

133. Shimasaki, H., Maeba, R., Tachibana, R., Ueta, N. (1995) Lipid peroxidation and ceroid accumulation in macrophages cultured with oxidized low density lipoprotein. *Gerontology,* 41 Suppl 2**,** 39-51.

134. Schapira, A. H. (1995) Oxidative stress in Parkinson's disease. *Neuropathol Appl Neurobiol,* 21**,** 3-9.

135. Silkstone, R. S., Mason, M. G., Nicholls, P., Cooper, C. E. (2012) Nitrogen dioxide oxidizes mitochondrial cytochrome c. *Free Radic Biol Med,* 52**,** 80-7.

136. Singh, I. N., Sullivan, P. G., Hall, E. D. (2007) Peroxynitrite-mediated oxidative damage to brain mitochondria: Protective effects of peroxynitrite scavengers. *J Neurosci Res,* 85**,** 2216-23.

137. Siskova, A., Wilhelm, J. (2001) The effects of hyperoxia, hypoxia, and ischemia/reperfusion on the activity of cytochrome oxidase from the rat retina. *Physiol Res,* 50**,** 267-73.

138. Skoumalova, A., Herget, J., Wilhelm, J. (2008) Hypercapnia protects erythrocytes against free radical damage induced by hypoxia in exposed rats. *Cell Biochem Funct,* 26**,** 801-7.

139. Skoumalova, A., Ivica, J., Santorova, P., Topinkova, E., Wilhelm, J. (2011) The lipid peroxidation products as possible markers of Alzheimer's disease in blood. *Exp Gerontol,* 46**,** 38-42.

140. Skoumalova, A., Madlova, P., Topinkova, E. (2012) End products of lipid peroxidation in erythrocyte membranes in Alzheimer's disease. *Cell Biochem Funct*.

141. Skoumalova, A., Rofina, J., Schwippelova, Z., Gruys, E., Wilhelm, J. (2003) The role of free radicals in canine counterpart of senile dementia of the Alzheimer type. *Exp Gerontol,* 38**,** 711-9.

142. Slatter, D. A., Bolton, C. H., Bailey, A. J. (2000) The importance of lipid-derived malondialdehyde in diabetes mellitus. *Diabetologia,* 43**,** 550-7.

143. Slatter, D. A., Murray, M., Bailey, A. J. (1998) Formation of a dihydropyridine derivative as a potential cross-link derived from malondialdehyde in physiological systems. *FEBS Lett,* 421**,** 180-4.

144. Stanley, B. A., Sivakumaran, V., Shi, S., McDonald, I., Lloyd, D., Watson, W. H., Aon, M. A., Paolocci, N. (2011) Thioredoxin reductase-2 is essential for keeping low levels of H(2)O(2) emission from isolated heart mitochondria. *J Biol Chem,* 286**,** 33669-77.

145. Starkov, A. A., Fiskum, G., Chinopoulos, C., Lorenzo, B. J., Browne, S. E., Patel, M. S., Beal, M. F. (2004) Mitochondrial alpha-ketoglutarate dehydrogenase complex generates reactive oxygen species. *J Neurosci,* 24**,** 7779-88.

146. St-Pierre, J., Buckingham, J. A., Roebuck, S. J., Brand, M. D. (2002) Topology of superoxide production from different sites in the mitochondrial electron transport chain. *J Biol Chem,* 277**,** 44784-90.

147. Sugamura, K., Keaney, J. F., Jr. (2011) Reactive oxygen species in cardiovascular disease. *Free Radic Biol Med,* 51**,** 978-92.

148. Tertov, V. V., Kaplun, V. V., Mikhailova, I. A., Suprun, I. V., Orekhov, A. N. (2001) The content of lipoperoxidation products in normal and atherosclerotic human aorta. *Mol Cell Biochem,* 225**,** 21-8.

149. Tretter, L., Adam-Vizi, V. (2004) Generation of reactive oxygen species in the reaction catalyzed by alpha-ketoglutarate dehydrogenase. *J Neurosci,* 24**,** 7771-8.

150. Trombly, R., Tappel, A. (1975) Fractionation and analysis of fluorescent products of lipid peroxidation. *Lipids,* 10**,** 441-7.

151. Trombly, R., Tappel, A. L., Coniglio, J. G., Grogan, W. M., Jr., Rhamy, R. K. (1975) Fluorescent products and polyunsaturated fatty acids of human testes. *Lipids,* 10**,** 591-6.

152. Turrens, J. F. (2003) Mitochondrial formation of reactive oxygen species. *J Physiol,* 552**,** 335-44.

153. Vaca, C. E., Wilhelm, J., Harmsringdahl, M. (1988) Studies on Lipid-Peroxidation in Rat-Liver Nuclei and Isolated Nuclear-Membranes. *Biochimica Et Biophysica Acta,* 958**,** 375-387.

154. Van Kuijk, F. J., Dratz, E. A. (1987) Detection of phospholipid peroxides in biological samples. *Free Radic Biol Med,* 3**,** 349-54.

155. Van Kuijk, F. J., Holte, L. L., Dratz, E. A. (1990) 4-Hydroxyhexenal: a lipid peroxidation product derived from oxidized docosahexaenoic acid. *Biochim Biophys Acta,* 1043**,** 116-8.

156. Vasankari, T., Kujala, U., Heinonen, O., Kapanen, J., Ahotupa, M. (1995) Measurement of serum lipid peroxidation during exercise using three different methods: diene conjugation, thiobarbituric acid reactive material and fluorescent chromolipids. *Clin Chim Acta,* 234**,** 63-9.

157. Vazquez-Memije, M. E., Capin, R., Tolosa, A. & El-Hafidi, M. (2008) Analysis of age-associated changes in mitochondrial free radical generation by rat testis. *Mol Cell Biochem,* 307**,** 23-30.

158. Victor, V. M., Rocha, M., Herance, R., Hernandez-Mijares, A. (2011) Oxidative stress and mitochondrial dysfunction in type 2 diabetes. *Curr Pharm Des,* 17**,** 3947-58.

159. Wang, J. Y., Suzuki, K., Miyazawa, T., Ueki, T., Kouyama, T. (1996) Fluorescence polarization study on the dynamics and location of peroxidized fluorescent phospholipids in liposomes. *Arch Biochem Biophys,* 330**,** 387-94.

160. Wang, X., Liao, Y., Li, G., Yin, D., Sheng, S. (2008) A comparative study of artificial ceroid/lipofuscin from different tissue materials of rats. *Exp Aging Res,* 34**,** 282-95.

161. Wang, Y., Peng, F., Tong, W., Sun, H., Xu, N., Liu, S. (2010) The nitrated proteome in heart mitochondria of the db/db mouse model: characterization of nitrated tyrosine residues in SCOT. *J Proteome Res,* 9**,** 4254-63.

162. Weisiger, R. A., Fridovich, I. (1973) Mitochondrial superoxide simutase. Site of synthesis and intramitochondrial localization. *J Biol Chem,* 248**,** 4793-6.

163. Weisiger, R. A., Fridovich, I. (1973) Superoxide dismutase. Organelle specificity. *J Biol Chem,* 248**,** 3582-92.

164. Wihlmark, U., Wrigstad, A., Roberg, K., Brunk, U. T., Nilsson, S. E. (1996) Lipofuscin formation in cultured retinal pigment epithelial cells exposed to photoreceptor outer segment material under different oxygen concentrations. *Apmis,* 104**,** 265-71.

165. Wilhelm, J. (1983) Thyroxine deiodination during in vitro lipid peroxidation of rat liver inner membrane particles. *Endocrinol Exp,* 17**,** 17-22.

166. Wilhelm, J., Brzak, P., Rejholcova, M. (1989) Changes of lipofuscin-like pigments in erythrocytes and spleen after whole-body gamma irradiation of rats. *Radiat Res,* 120**,** 227-33.

167. Wilhelm, J., Fuksova, H., Schwippelova, Z., Vytasek, R., Pichova, A. (2006) The effects of reactive oxygen and nitrogen species during yeast replicative ageing. *Biofactors,* 27**,** 185-193.

168. Wilhelm, J., Herget, J. (1999) Hypoxia induces free radical damage to rat erythrocytes and spleen: analysis of the fluorescent end-products of lipid peroxidation. *Int J Biochem Cell Biol,* 31**,** 671-81.

169. Wilhelm, J., Ivica, J., Kagan, D., Svoboda, P. Early postnatal development of rat brain is accompanied by generation of lipofuscin-like pigments. *Mol Cell Biochem,* 347**,** 157-62.

170. Wilhelm, J., Skoumalova, A., Vytasek, R., Fisarkova, B., Hitka, P., Vajnek, L. (2005) Erythrocyte membranes inhibit respiratory burst and protein nitration during phagocytosis by macrophages. *Physiol Res,* 54**,** 533-9.

171. Wilhelm, J., Sonka, J. (1980) Effects of Sublethal Gamma-Irradiation and Exercise on Succinate Oxidase and Metabolites of Lipid Peroxides .2. Rat Skeletal-Muscle. *Agressologie,* 21**,** 87-91.

172. Wilhelm, J., Sonka, J. (1980) Effect of Sublethal Gamma-Irradiation and Exercise on Succinate Oxidase and Metabolites of Lipid Peroxides .1. Rat-Liver. *Agressologie,* 21**,** 81-86.

173. Wilhelm, J., Sonka, J. (1981) Modulation of Invivo Metabolic Effects of Gamma-Irradiation by Thyroid Status Manipulations. *Strahlentherapie,* 157**,** 762-765.

174. Wilhelm, J., Sonka, J. (1981) Time-course of changes in lipofuscin-like pigments in rat liver homogenate and mitochondria after whole body gamma irradiation. *Experientia,* 37**,** 573-4.

175. Wilhelm, J., Sonka, J. (1982) Ionizing irradiation and fasting in the rat. II. Effect on energy metabolism. *Agressologie,* 23**,** 79-81.

176. Wilhelmova, N., Domingues, P. M. D. N., Srbova, M., Fuksova, H., Wilhelm, J. (2006) Changes in nonpolar aldehydes in bean cotyledons during ageing. *Biologia Plantarum,* 50**,** 559-564.

177. Wilhelmova, N., Prochazkova, D., Machackova, I., Vagner, M., Srbova, M., Wilhelm, J. (2004) The role of cytokinins and ethylene in bean cotyledon senescence. The effect of free radicals. *Biologia Plantarum,* 48**,** 523-529.

178. Wu, T., Rifai, N., Willett, W. C., Rimm, E. B. (2007) Plasma fluorescent oxidation products: independent predictors of coronary heart disease in men. *Am J Epidemiol,* 166**,** 544-51.

179. Wu, T., Willett, W. C., Rifai, N., Rimm, E. B. (2007) Plasma fluorescent oxidation products as potential markers of oxidative stress for epidemiologic studies. *Am J Epidemiol,* 166**,** 552-60.

180. Yin, D. (1995) Studies on age pigments evolving into a new theory of biological aging. *Gerontology,* 41 Suppl 2**,** 159-72.

181. Yin, D. (1996) Biochemical basis of lipofuscin, ceroid, and age pigment-like fluorophores. *Free Radic Biol Med,* 21**,** 871-88.

182. Yu, W., Dittenhafer-Reed, K. E., Denu, J. M. (2012) SIRT3 Protein Deacetylates Isocitrate Dehydrogenase 2 (IDH2) and Regulates Mitochondrial Redox Status. *J Biol Chem,* 287**,** 14078-86.

183. Zhu, X., Castellani, R. J., Moreira, P. I., Aliev, G., Shenk, J. C., Siedlak, S. L., Harris, P. L., Fujioka, H., Sayre, L. M., Szweda, P. A., Szweda, L. I., Smith, M. A., Perry, G. (2012) Hydroxynonenal-generated crosslinking fluorophore accumulation in Alzheimer disease reveals a dichotomy of protein turnover. *Free Radic Biol Med,* 52**,** 699-704.